Sensory Ecology

of Electromagnetic Radiation Perception

in Subterranean Mole-Rats

(*Fukomys anselli & Fukomys kafuensis*)

Inaugural-Dissertation

zur Erlangung des Doktorgrades Dr. rer. nat.

des Fachbereiches Biologie und Geographie
an der Universität Duisburg-Essen

Vorgelegt von

Regina E. Moritz

aus Bottrop

Januar 2007

Die der vorliegenden Arbeit zugrunde liegenden Experimente wurden in der Abteilung Allgemeine Zoologie der Universität Duisburg-Essen, Campus Essen, in der Abteilung Physiologie und Ökologie des Verhaltens und in der Dr. Senckenbergischen Anatomie der Johann Wolfgang Goethe-Universität, Frankfurt/Main durchgeführt.

1. GUTACHTER:
Prof. Dr. Hynek Burda

2. GUTACHTER:
Prof. Dr. Leo Peichl

3. GUTACHTER:
Prof. Dr. Bernd Sures

VORSITZENDER DES PRÜFUNGSAUSSCHUSSES:
Prof. Dr. Martin Heil

Tag der mündlichen Prüfung:
07. Mai 2007

Non quia difficilia sunt audemus,
sed quia non audemus difficilia sunt.

Lucius Annaeus Seneca

in memoriam

Dr. Mathias Kawalika (1962-2006)

LIST OF CONTENTS

I SUMMARY

Subterranean living animals must handle orientation in their habitat with limited cues, among which is light scarcity. Zambian mole-rats belong to the rodent genus *Fukomys* and spend the majority of their lifetime underground in extensive burrow systems. These mole-rats have generally been considered as functionally blind, but recent morphological findings have suggested that their visual capabilities must have been underestimated. The odds of cue scarcity underground have also apparently led to the use of a sensory system for orientation quite uncommon in mammals: magnetoreception.

This thesis deals with new findings on both the visual and the magnetic sense in small Zambian mole-rat species of the Genus *Fukomys* – two senses coupled to the minuscule, inconspicuous eye. While the retina provides the basis for light perception, the cornea is probably the site where magnetic perception takes place.

Firstly, I show in part A that the formerly thought 'blind' *Fukomys* mole-rats can distinguish between light and dark even until at least a light intensity of 0.6 μmol $\text{photons} \cdot \text{m}^{-2} \cdot \text{s}^{-1}$ (approximately 33 lux). This thesis has also undergone the first approach to measure wavelength propagation in a tunnel, showing that long wavelengths (600-700 nm) travel, as expected, furthest in a horizontal tunnel, and that photons in this spectral range can still be detected, though at a very low (scotopic) level, at 70 cm apart from a tunnel opening illuminated with a light intensity resembling that on a clear day.

Secondly, in part B, I also show that the hitherto poorly understood transduction mechanism of the magnetic sense in mole-rats is based on magnetite rather than on biochemical processes. The site of the respective magnetite-harbouring receptors can be confined to the ocular region, more specifically the cornea, where ferrous inclusions with magnetic properties might be coupled with the receptors for mediating magnetic information. The magnetic sense is not lateralised. This thesis also contributes to a further understanding of the neuronal processing of magnetic information in mammals, finding that hippocampal structures, e.g. structures coordinating spatial memories, are also involved in magnetic orientation. Magnetic cues might supply the animal with both directional compass and map information.

II ZUSAMMENFASSUNG

Subterran lebende Tiere müssen bei der Orientierung in ihrem Habitat mit limitierten Informationen auskommen; zu diesen zählt auch Lichtknappheit. Sambische Graumulle gehören zur Nagergattung *Fukomys* und verbringen den größten Teil ihres Lebens unterirdisch in ausgedehnten Gangsystemen. Diese Graumulle wurden bislang stets als blind bezeichnet; jedoch haben neuere morphologische Studien gezeigt, dass die visuellen Möglichkeiten dieser Tiere anscheinend stark unterschätzt wurden. Die Gegebenheiten der unterirdischen Reizarmut haben auch dazu geführt, dass Graumulle ein Sinnessystem zur Orientierung nutzen, das unter Säugern recht selten vorkommt: die Magnetwahrnehmung.

Diese Arbeit beschäftigt sich mit neuen Ergebnissen zu dem visuellen und dem magnetischen Sinn in zwei Graumullarten aus Sambia (*Fukomys anselli* und *Fukomys kafuensis*) – zwei Sinne, deren Rezeptorebenen im winzigen, unscheinbaren Auge verortet sind. Während in der Retina die Lichtwahrnehmung stattfindet, stellt die Cornea wahrscheinlich den Ort der Magnetrezeption.

Teil A meiner Arbeit zeigt, dass die früher als ‚blind' bezeichneten Graumulle sehr wohl zwischen Hell und Dunkel bis zu einem niedrigen Schwellenwert von mindestens 0.6 µmol $\text{Photonen} \cdot \text{m}^{-2} \cdot \text{s}^{-1}$ wahrnehmen (ca. 33 Lux). Darüber hinaus habe ich den ersten Versuch unternommen, Wellenlängenweiterleitung in einem Tunnel zu bestimmen; wie erwartet konnte gezeigt werden, dass lange Wellenlängen (600-700 nm) in einem horizontalen Tunnel am weitesten getragen werden, und dass Photonen in diesem Spektralbereich auch in 70 cm Entfernung von der Tunnelöffnung bei einer einem hellen Tag ähnelnden Beleuchtung immer noch gemessen werden können, wenn auch in einem sehr niedrigen (skotopischen) Bereich.

Zweitens zeigt Teil B dieser Arbeit, dass der bislang nur schlecht verstandene Übertragungsmechanismus des Magnetsinns auf Magnetit beruht, und nicht auf biochemischen Prozessen. Der Ort der entsprechenden Magnetit-basierten Rezeptoren kann auf die Augenregion beschränkt werden, genauer auf die Cornea, in der eisenhaltige Inklusionen mit möglichen magnetischen Eigenschaften die Rezeptoren für die Übertragung magnetischer Information darstellen könnten. Der Magnetsinn ist nicht lateralisiert. Diese Arbeit trägt auch zu einem besseren Verständnis der neuronalen Verarbeitung magnetischer Information in Säugern bei, da sie Ergebnisse zur hippocampalen Aktivität unter magnetischen Stimuli vorstellt, also einer Hirnstruktur, die räumliche Erinnerungen koordiniert. Magnetische Signale könnten das Tier mit Richtungsinformation für den Kompass und mit Karteninformation versorgen.

III GENERAL INTRODUCTION

The term "orientation" refers to an animal's ability to orient in space and time, to maintain a specific spatial position, or to create new spatial relationships with its environment (Merkel 1980; Zwahr 1993). Finding the way is a necessity for securing territory, food and reproduction; orientation thus represents a life characteristic and explains the variety of orientation organs and systems to be found across the animal kingdom (Merkel 1980). How an organism perceives its environment and how it orients within it, depends on its sensory organs, which transduce different cues depending on whether they are optical, mechanical, electrical, olfactory, or other chemical stimuli (Merkel 1980). Stimulus-evoked information must be 1) localised in space and 2) identified (Ewert 1973); though orientation is based mainly on these various information types, imprinting, memory or learning also vitally support the orientation process (Merkel 1980; Zwahr 2003).

Living above ground provides an animal with diverse cues for spatial orientation, but the underground picture is less colourful: besides darkness, subterranean rodents face restriction in useful orientation cues such as odours or sounds (Burda et al. 1990a). Targets and landmarks are not directly perceptible and, as a consequence, distant orientation is heavily impeded. Subterranean mammals need to solve several major tasks relevant to spatial orientation: 1) they have to orient quickly and efficiently in their burrow system, in order to access nest, food chambers, latrines, and harvesting grounds. 2) They must maintain their course direction when digging longer foraging and dispersing tunnels. Straight tunnelling conserves energy because the animals do not search in the same area twice. 3) They need to restore and interconnect damaged burrows, effectively bypass obstacles, etc. 4) Animals temporarily leaving their burrows while foraging or searching for mates above ground need to find their way back home. Subterranean living mammals thus need to make use of efficient orientation capabilities, which are specialized towards this peculiar habitat.

III.1 Subterranean *Fukomys* Mole-Rats

Mole-rats of the genus *Fukomys*, formerly denominated as *Cryptomys* (Kock et al. 2006), are strictly subterranean rodents of the family Bathyergidae that occur in Africa south of the Sahara. To our current knowledge, the bathyergid family comprises six genera: *Bathyergus*, *Cryptomys, Fukomys, Georychus, Heliophobius,* and *Heterocephalus* (Faulkes et al. 2004; Ingram et al. 2004; Kock et al. 2006; van Daele et al. 2004). While the genus *Cryptomys* is distributed across South Africa, its sister genus *Fukomys* is widely distributed across South-central and West Africa (Ingram et al. 2004).

Fukomys mole-rats occur mainly in grassland or savanna (fig. 1). Like other bathyergids, they spend most of their lifetime in sealed extensive burrow systems, where they forage for geophyte bulbs and roots. Most species show a specialized organization of their underground systems with diverse tunnels, and designated nesting, food and latrine chambers (cf., Brett 1991; Scharff & Grütjen 1997; Nevo 1999; Scharff et al. 2001).

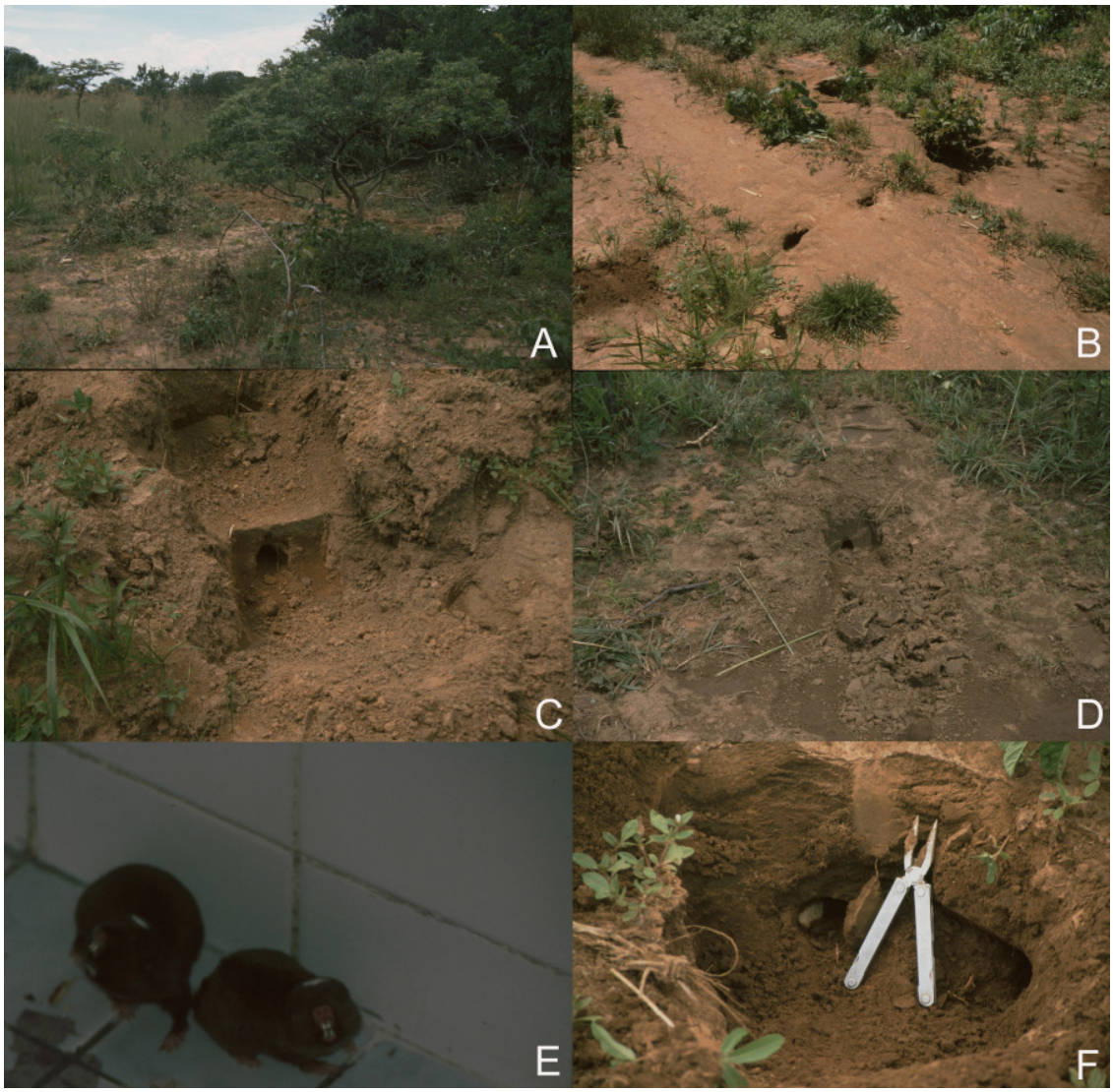

Fig. 1 The mole-rats' Zambian habitat. (A) shows a typical field site where mole-rat burrow systems can be found beneath a dry savanna landscape in the Southwest of Zambia. (B) shows a burrow subterraneously bridging the footpath separating two adjacent maniok fields, creating a nourishing interconnection. In (C) and (D), tunnel entrances of a burrow system are presented after having been opened by native mole-rat hunters. After such a wildlife capture, mole-rats are sitting in a bathtub (E). (F) shows the rare field find of two adjacent tunnel entrances, probably a bend or crossing, with a piece of bait (maniok) plugged into the left entrance hole.

Fukomys mole-rats show a social system that is rare in mammals: eusociality. The animals live in large colonies that consist of the breeding pair and their non-reproductive offspring of several generations; most offspring show a lifelong philopatry (Burda 1989, 1990; Burda et al. 2000).

III.2 Orientation in the Subterranean Habitat

Subterranean *Fukomys* mole-rats show sporadic aboveground activity (Scharff & Grütjen 1997), but they presumably spend the majority of their life in their constantly dark subterranean habitat (cf., Burda 1990; Nevo 1999). For orientation within a familiar burrow system or for short-distance tasks, landmark-independent navigation is likely to be used. This kind of true navigation is described by an animal's ability to return to a place without using landmarks or cues from its destination and its outward journey (Boles & Lohmann 2003). In one type of true navigation, path integration (also called dead reckoning), an animal uses idiothetic cues, i.e. internal movement cues based on proprioceptive and vestibular information from sensory flow, or efferent copies of movement commands. However, depending exclusively on self-generated signals, path integration is severely constrained by the rapid accumulation of errors (Etienne et al. 1988; Benhamou et al. 1990). Therefore, an external directional reference is inevitable for navigation over longer tracks. For successful navigation within the complex burrow maze, a subterranean rodent thus requires, besides idiothetic cues, a compass sense and also a mental representation of its environment, i.e. a cognitive map that can be used for spatial navigation and spatial memory (reviewed in Etienne & Jeffery 2004).

The subterranean ecotope is, on the one hand, simply structured and stable, and, on the other hand, highly specialized and peculiar. Its physical properties differ markedly from the above ground biosphere, particularly in its monotony and scarcity of stimuli (reviewed in Burda et al. 1990a; Burda & Begall 2002; Burda et al. 2007). Subterranean rodents have thus evolved some (sometimes extreme) sensory adaptations in response to these conditions. A first review on the sensory ecology of these underground mammals was given by Burda et al. (1990a) and recently updated (Francescoli 2000; Begall et al. 2007a).

III.3 Sensory Adaptations in *Fukomys*

The phylogenetically oldest basic sense, olfaction, has been shown to be extensively used by subterranean rodents. It helps them e.g. in odour-guided foraging by means of kairomones or during their important social interactions (reviewed in Heth & Todrank 2007). Hearing in these underground mammals is shifted to the low-frequency range: both hearing apparatus and vocalizations are tuned to these sounds in accordance with the acoustical properties of the subterranean habitat (reviewed in Begall et al. 2007b). Regarding the tactile sense, subterranean rodents may well be regarded as touch specialists, in reaction to life in the tight, complex burrow systems (reviewed in Park et al. 2007), and also the perception of substrate vibrations is not unusual (cf., Narins et al. 1997; Rado et al. 1998; Mason & Narins 2001).

Former studies on vision in subterranean mammals had proposed a convergent evolution towards degenerate eyes, but recent findings have unravelled a diversity of visual systems, including unusual photoreceptor properties in blind mole-rats, *Spalax ehrenbergi*, (David-Gray et al. 2002) and in Ansell's mole-rats, *Fukomys anselli* (Peichl et al. 2004). In most subterranean species, vision can, however, not serve for spatial orientation purposes (reviewed in Němec et al. 2007).

The Earth's magnetic field provides a relatively constant and reliable source of directional, and perhaps also positional, information that can be used for orientation. Hence, it may not be surprising that the first evidence for a mammalian magnetic compass came from a subterranean rodent, Ansell's mole-rat (*Fukomys anselli*) (Burda et al. 1990b). The exact use of this magnetic sense and its role in orientation has hitherto been unclear, but it is plausible that they control e.g. their digging direction by magnetic information (Burda & Begall 2002). Some other (subterranean) rodents have been demonstrated to either show spontaneous or learned use of magnetic field information.

III.4 Electromagnetic Radiation

Electromagnetic (EM) radiation is evoked by moving charges (cf., Lipton et al. 1997). It can be classified into types due to variations in wavelength or frequency (i.e. oscillation rate). Frequency and wavelength are related inversely: higher frequencies have shorter wavelengths, and lower frequencies have longer wavelengths. Their relationship is defined, like all wave motions, through the wave's velocity (cf., Pedrotti & Pedrotti 1993; Hecht 2001).

The classification into wavelength types is summarized in the electromagnetic spectrum. The spectrum is defined by the properties of electromagnetic disturbances propagating through space: these disturbances can be monochromatic (characterized by a single wavelength) or

polychromatic (characterized by many wavelengths). The term 'wavelength' denominates the distance between two adjacent crests of the wave's successive troughs and crests. The term 'spectrum' of the radiation denominates the distribution of energy among the various constituent waves (cf., Pedrotti & Pedrotti 1993). The radiation types include, following their frequency and differences in the way they are produced or detected: radio waves, microwaves, infrared radiation, visible light, ultraviolet radiation, X-rays and gamma rays (cf., Hecht 2001; Tipler 2004). The visible part of the electromagnetic spectrum (fig. A1) implies just a narrow range of electromagnetic waves, i.e. from approximately 380 to 770 nm.

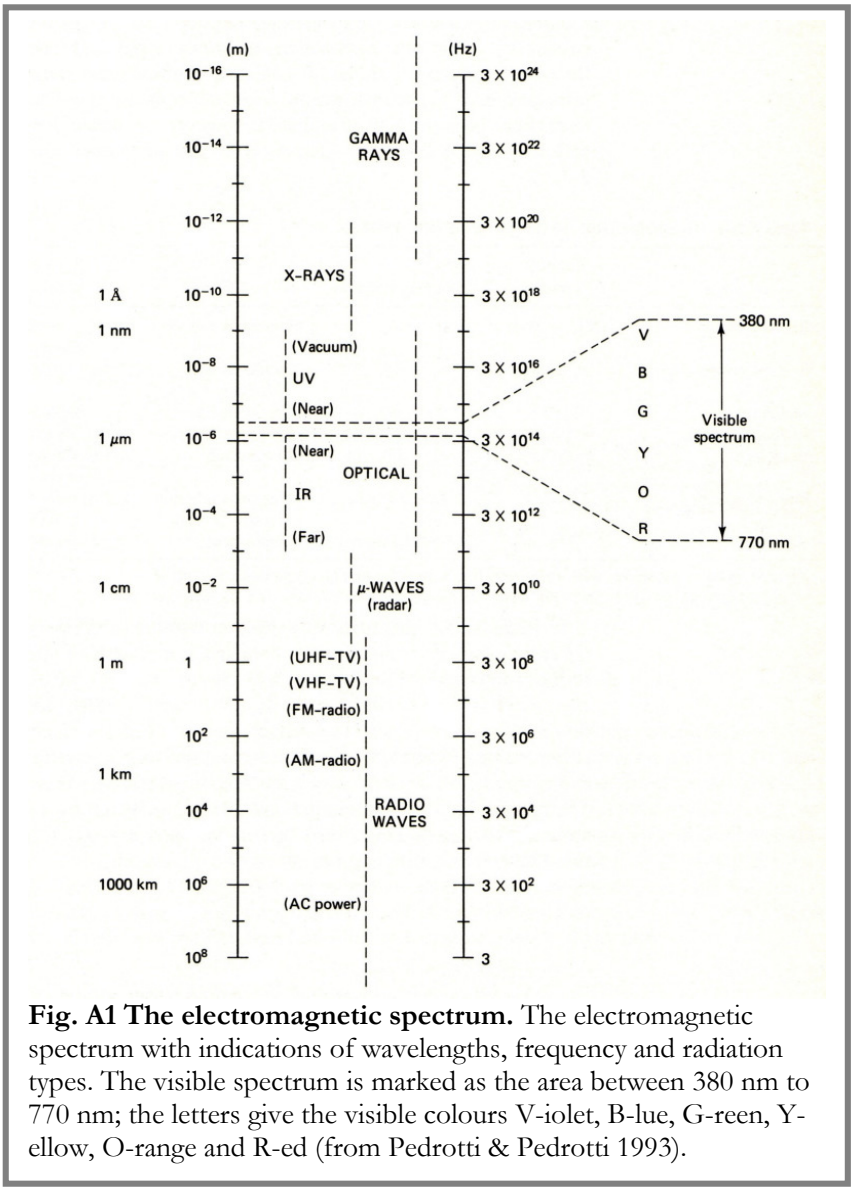

Fig. A1 The electromagnetic spectrum. The electromagnetic spectrum with indications of wavelengths, frequency and radiation types. The visible spectrum is marked as the area between 380 nm to 770 nm; the letters give the visible colours V-iolet, B-lue, G-reen, Y-ellow, O-range and R-ed (from Pedrotti & Pedrotti 1993).

These waves are capable of producing visual sensation in the human eye; thus they are referred to as 'light'. The visible spectrum includes the range of colours from red (long-wavelength end) to violet (short-wavelength end) and is neighboured by the infrared and the ultraviolet region, respectively. These three regions (visible light, infrared and ultraviolet) together form the 'optic spectrum' (cf., Pedrotti & Pedrotti 1993). Fig. A2 gives the

electromagnetic spectrum in terms of both wavelength and frequency and the visible part of the spectrum.

Electromagnetic waves of much lower frequency than visible light were first predicted by James Clerk Maxwell and later discovered by Heinrich Hertz. Maxwell established four simple equations connecting the properties of electric and magnetic fields, and he already foresaw the resulting wavelike nature of these fields, as well as their symmetry. According to these equations, a time-varying (i.e. oscillating) electric field generates a magnetic field and *vice versa*. The oscillating fields form together an electromagnetic wave (cf., Lipton et al. 1997; Pedrotti & Pedrotti 1993). This wave is self-propagating in space; its electric and magnetic components oscillate at right angles to each other and to the direction of propagation (cf., Tipler 2004). From Maxwell on, light has been regarded a particular region of the electromagnetic radiation spectrum (cf., Lipton et al. 1997; Pedrotti & Pedrotti 1993).

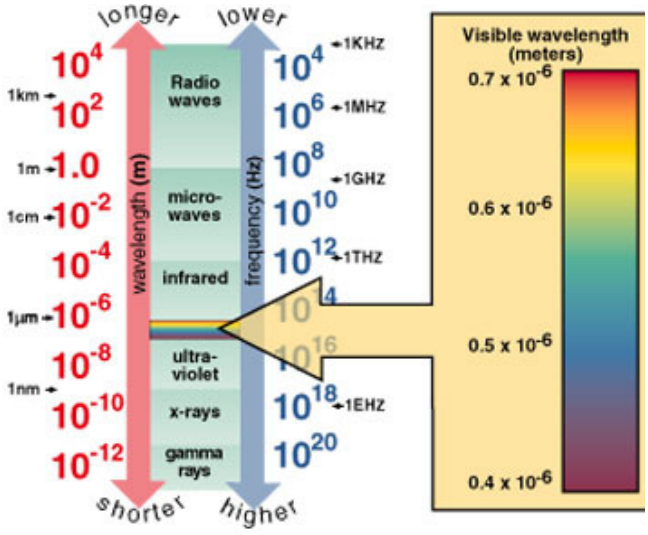

Fig. A2 Visible wavelengths in the electromagnetic spectrum. The left part of the figure shows the inversely proportional dependency of wavelengths and frequencies and the radiation types. Between IR and UV radiation, the visible spectrum is shown in detail with the transition between visible colours (from: http://extension.missouri.edu/explore/images/eq0453spectrum.jpg).

III.5 Contribution of this thesis to *Fukomys* sensory research

My dissertation thesis deals with two of the above mentioned sensory aspects that are connected to the eye: the visual and the magnetic sense in *Fukomys* mole-rats. Both senses deal with incoming electromagnetic radiation signals. My thesis should fundamentally contribute to 1) a more detailed understanding of the use of the specialized visual settings of subterranean *Fukomys* mole-rats and to 2) a step forward in identification, characterization and particularly location of a light-independent magnetoreceptor in this mammal.

»And if you see a long tunnel, stay away from the light!« (*Donkey from 'Shrek'*)

A LIGHT PERCEPTION

1 INTRODUCTION

Orientation towards and with help of the light is phylogenetically old and thus widely spread in the animal kingdom (Merkel 1980). The visual system is a very complex, but also very well investigated sensory system. Large parts of the cortex and several subcortical systems are involved in its numerous functions, including perception and localisation of objects, controlling the eye movements, and visual control during spatial movements (Zeki 1994). The eye itself represents the entry gate to the visual system; the information available to the visual brain centers depends on the eye's features (cf., Němec et al. 2007).

The physical precondition to vision, light, has been, in the history of science, described either as particles or as waves (light waves are made up by photons, which are nothing else but discrete packets of energy or quanta). These two descriptions, however, are not compatible, and the twentieth century made it clear that "somehow light was both wave and particle, yet it was precisely neither". This paradoxon (the "wave-particle duality") was finally explained by quantum electrodynamics (cf., Pedrotti & Pedrotti 1993; Tipler 2004).

During the light perception process, a photon is absorbed by an atom; it subsequently excites an electron and elevates it to a higher energy level. If the energy is great enough, the electron may escape the positive pull of the nucleus and jump to an energy level high enough to liberate it from the atom. On the other hand, when an electron descends to a lower energy level in an atom, it emits a photon of light equal to the bridged energy difference (cf., Hecht 2001; Tipler 2004).

Though the physical principles of light perception are the same across the animal kingdom, visual capabilities and underlying structures and mechanisms differ starkly. Light sensitivity, i.e. the excitation possibility through light is in most cases bound to specific light sensory organs, eyes, with at least one visual pigment. The respective vertebrate sensory organ is the lens eye, a dioptrical apparatus that follows physical optics and creates a sharp and light intensive picture on the eye's background; this type of eye with the light perceiving structures being turned away from the light source is called *inverse* (Czihak et al. 1990). The vertebrate eye

probably represents a composite structure, that integrates distinct light-sensitive cell types with independent evolutionary histories (Arendt et al. 2004), or, in other words, the eye results from evolutionarily conserved genes and nevertheless highly divergent morphological features (Oakley 2003).

1.1 Visual Capabilities in *Fukomys*

Eyes of subterranean rodents show a high variability in size (Němec et al. 2007). The subterranean African mole-rats have minuscule eyes with an eyeball diameter of about 2 mm (Peichl et al. 2004). As eye size determines the retinal image size and thus image quality and visual acuity (Němec et al. 2007), they have hitherto been generally thought to lack a functional visual system and have been regarded as blind, this view being supported by their constantly dark habitat and the displayed microphthalmia. Also, they do not show any immediate behavioural response to light or other visual signals such as object movement (Eloff 1958; Burda et al. 1990a).

However, the eyes of Zambian mole-rats are located superficially and are not covered by a skin layer as is the case in the blind mole-rat, *Spalax ehrenbergi* (cf., Sanyal et al. 1990), so that they can be directly reached by light. It is well observable that *Fukomys* mole-rats blink their eyes regularly, that their eyes are in some individuals more protruded than in others, and that they might use their eyes for orientation (personal laboratory observations).

It should be noted that already Poduschka (1978) doubted that mole-rats are fully unsusceptible to light. It then lasted more than twenty years until morphological and immunocytochemical studies indicated that vision in Zambian Ansell's mole-rats, *Fukomys anselli,* might be functional: despite their tiny eyes and also a quantitatively reduced visual system (Němec et al. 2004), adult Ansell's mole-rats reveal a qualitatively normal dioptric apparatus and retina (fig. A3), plus a high cone share of about 10% (8-15,000/mm^2) (Oelschläger et al. 2000; Cernuda-Cernuda et al. 2003; Němec et al. 2004; Peichl et al. 2004).

Cones are the photoreceptors serving photopic 'daylight' vision and colour vision, in contrast to the rods that serve scotophic 'night' vision. The high proportion of these 'daylight' or colour photoreceptors is rather unusual among mammals and unexpectedly high for a subterranean animal if compared to nocturnal above ground living mammals like rats with 0.5-3% cones (reviewed in Peichl 2005). Next to the cone proportion in the retina, which appears unusually high particularly as the rod density is unusually low (110,000-150,000/mm^2), a second peculiarity can be observed in the Ansell's mole-rat's retina: the opsin characteristics.

In the normal mammalian retina, two spectral cone types, i.e. two visual pigments, can be found: L-cones with the pigment L-opsin sensitive to middle to long wavelengths; and S-cones with the pigment S-opsin sensitive to short wavelengths (reviewed in Jacobs 1993). Twenty percent of the cones found in the Ansell's mole rat's eye are exclusively sensitive to short wavelengths, 10% exclusively to long wavelengths, and 70% of the cones are potential dual-pigment photoreceptors sensitive for both short and long wavelengths, but with the short-wave-sensitive pigment dominating markedly (Peichl et al. 2004). Calculating the percentages together, 90% of the cones in the *Fukomys anselli* retina are sensitive to short wave light and stand in contrast to the cone situation in the blind mole-rat's retina with no short wave sensitive cones at all (cf., Sanyal et al. 1990; Cernuda-Cernuda et al. 2002). *Fukomys anselli* thus could theoretically possess dichromatic colour vision, assumed that the postreceptoral circuitry is given (Peichl et al. 2004).

However, it is difficult to exactly determine which wavelength precisely is absorbed by the visual pigments present in single photoreceptors. Though the opsin-specific antibodies identified the opsin family (S and L), Peichl and colleagues (2004) could not yield information on the photoreceptor's exact spectral tuning, as the applied antibodies recognize blue as well as UV-sensitive S-opsins (cf., Szél et al. 2000). Though most mammalian S-opsins are sensitive to blue light, it is not improbable that the S-cones in the *Fukomys* retina react to UV-light, as is the case in some rodents (Jacobs et al. 1991).

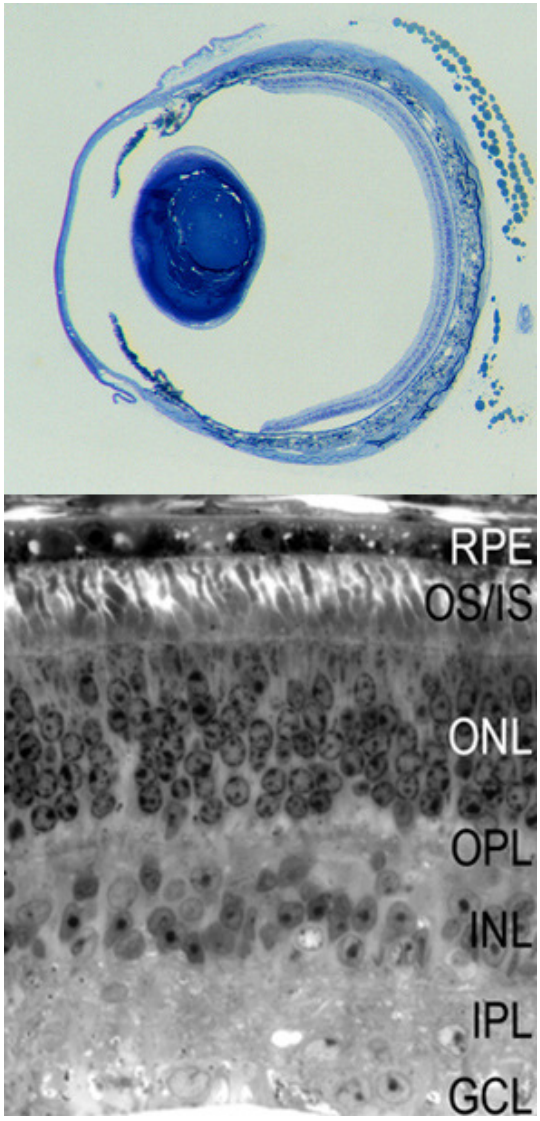

Fig. A3 The mole-rat eye. The upper part of the panel shows a sagittal section of the Ansell's mole-rat eye; the diameter is approximately 2 mm. Picture with kind permission by L. Peichl. The lower part of the panel shows a vertical section through the retina, which shows a normal layer arrangement and no indications of gross regression. RPE Retinal Pigment Epithelium, OS/IS Outer segment/inner segment, ONL Outer Nuclear Layer, OPL Outer Plexiform Layer, INL Inner Nuclear Layer, IPL Inner Plexiform Layer, GCL Ganglion Cell Layer (from Peichl et al. 2004).

The method of choice to examine the spectral tuning of the short wave sensitive cones is Micro-Spectro-Photometry (MSP) on single cells (also called *single cell recording*), involving measurements of absorption spectra of individual retinal rods or cones by passing a fine light beam through the receptor which is positioned on the stage of a microscope. This method appeared unsuccessful in *Fukomys* mole-rats, though. Despite the relatively high number of cones in the mole-rat retina (Peichl et al. 2004), and despite the successful labelling of cones with PNA (*peanut agglutinin*) prior to the MSP, all cells that could be isolated out of the retinas of four animals, turned out to be common rods with absorbance peaks not unusual for rodents (J. Bowmaker & R. Cernuda-Cernuda, personal communication).

Regarding the neuronal level of vision in Ansell's mole-rats, both olivary pretectal nucleus and ventral lateral geniculate nucleus are rather well developed, i.e. brain structures involved in brightness discrimination. A comparable quality can also be found in their pupillary light reflex, and sleep orchestrating and circadian responses to light (Oelschläger et al. 2000; Němec et al. 2004). In addition, light exposure elicits expression of the immediate early gene c-fos in the retrosplenial cortex indicating that *F. anselli* is well attentive to visual stimuli (Oelschläger et al. 2000).

On the other hand, a marked reduction of visual input to the superior colliculus clearly hints at just a little importance of light stimuli for Ansell's mole-rats (Němec et al. 2004), and the authors suggest that the apparent behavioural blindness of these animals might be caused by the fact that they are unable to generate spatially appropriate orientation responses, particularly as those midbrain structures are also reduced, in which coordination of visuo-motor reflexes takes place.

All in all, these preceding findings suggest that the *Fukomys* mole-rats under study do distinguish light intensities and that light may affect their behaviour.

1.2 Arising questions

The recent morphological and immunocytochemical findings of a mosaic of rather well developed or conserved eye structures and visual centres combined with reduction signs called for a thorough behavioural examination of visual capacities of these mole-rats. Amid this evolutionary and ecological discrepancy of no apparent need for vision in a dark underground world and a theoretically functional visual framework, it is wondrous that no detailed behavioural study on the visual performance of bathyergid mole-rats had been undertaken so far. We thus aimed at investigating the influence of light on the spontaneous preferential nest building behaviour in two Zambian *Fukomys* species. Secondly, using enucleated animals from

other studies (B2.3), we wanted to examine retinal involvement by examining their light perception performance. Thirdly, the light perception threshold was to be determined.

It has remained unstudied to date how wavelengths are propagated underground e.g. through an open tunnel entrance. To better understand the visual performance of the subterranean mole-rats regarding their habitat, we aimed at examining wavelength propagation in a tunnel.

2 MATERIAL AND METHODS

2.1 Study Animals

We tested adult pairs of different age of the two closely related *Fukomys*-species *F. anselli* and *F. kafuensis* as well as their hybrids. The mole-rats were housed at ambient room temperature and under a natural daylight depending light regime in glass cages of different sizes (minimum: L60 x W35 x H35 cm) filled with a layer of horticultural peat in the mole-rat housing facilities of the laboratories of the Department of General Zoology, University of Duisburg-Essen. They were fed *ad libitum* with carrots, potatoes, lettuce and apples and had sufficient supplies of nesting and enrichment material (e.g. small plastic boxes, tissue paper, paper rolls, plastic rolls, plastic boxes and wooden boxes). The animals were either born in captivity or had been captured in the field and kept under laboratory conditions for at least 18 months prior to experiments.

Most pairs used in this study consisted of a male and a female breeder, and occasionally of sibling pairs. We took care to test each mole-rat only once per experimental set-up, which was ensured by the use of tissue compatible transponders (bio-capsules, 12 x 2.1 mm, ISO-standard 11784) with unique number codes (ALVIC-transponder, ALVETRA GmbH, Neumünster, Germany), that had been injected subcutaneously with a cannula (32 x 2.6 mm) under aseptic conditions into a skin fold on the animals' back. The mole-rats had been carrying the transponders for a couple of months prior to the experiments and did not show any adverse effects towards them.

2.2 Demonstrating Light Perception

2.2.1 Study rationale

We predicted that the animals would prefer dark chambers over light ones to build their nests (scotophilia) and would try to avoid lighted chambers (heliophobia), if they were able to perceive light. Spontaneous reactions to light were tested through preferential nesting behaviour under strong artificial light versus darkness as well as under much lower natural daylight intensities versus darkness to examine whether the animals prefer dark or light boxes to build their nests.

We further tested the involvement of retinal photoreceptors in the here shown visual performance of Zambian mole-rats. To this end, we used the enucleated mole-rats of our magnetoreception studies (B2.3) and examined their visual performance. Should the animals not be able to distinguish between light and dark anymore under this condition, the retina could be regarded as the seat of the receptors mediating photic signals in Zambian mole-rats.

2.2.2 Study procedure

In the first study of this chapter, altogether 70 adult pairs of mole-rats were tested in two different experiments: experiment 1 comprised the exposure to strong halogen light in a two-armed maze, and experiment 2 comprised exposure to natural daylight intensities in an eight-armed maze. The experiments are separately listed in the following.

2.2.2.1 Halogen light

We examined mole-rats in a two-armed maze under strong halogen light. The two-choice test chamber was located in a small windowless room separated from the animal housing room (fig. A4). The apparatus was made from light-impervious plastic (0.5 cm thick) and consisted of a circular centre and two opposite arms (L15 x W9 x H9 cm) that terminated in nesting boxes (L20 x W20 x H20 cm). The nesting boxes could be closed with a lid made from the same plastic material. In the middle of each lid was a space (5 x 5 cm), in which an opaque plate could be inserted to shade the respective box.

We used self-made halogen lamps (illuminant: 100 W) enlightening the nesting boxes on both sides from 20 cm above. Both lamps were switched on in each trial to ensure an even distribution of the lamp-generated noise. Above each of the square lid spaces, we placed glass dishes (6 cm high, diameter 9.5 cm) filled with cold water in order to absorb the heat radiation generated by the halogen lamps and to balance the temperature regime within the maze. We additionally measured temperature in the running system without animals inside and sensors

fixed in the middle of both nesting boxes at about 10 cm height. We recorded temperature every ten minutes during eight runs of minimal 30 minutes (Eltek 1000 Series, Squirrel Meter/Logger; Eltek Ltd., Cambridge, UK).

Fig. A4 Mazes for light perception studies. Two-armed maze with halogen light switched on (A) and eight-armed maze with translucent lids on the nesting boxes (B). In our study, four opaque and four translucent lids were used, being randomly distributed.

In the halogen-lighted box, white light intensity was ~60 μmol $\text{photons} \cdot \text{m}^{-2} \cdot \text{s}^{-1}$ (LI-250 Light Meter; LI-COR Biosciences, Lincoln, NE, U.S.A.) while in the shaded box, it was totally dark (<0.01 μmol $\text{photons} \cdot \text{m}^{-2} \cdot \text{s}^{-1}$). The tunnels and the circular starting box were hardly reached by light (<0.5 μmol $\text{photons} \cdot \text{m}^{-2} \cdot \text{s}^{-1}$). Within the starting box (height 30 cm, diameter 25 cm), there was a metallic cylinder, which was inserted tightly to the plastic wall and could be partly rotated (±10 cm) by a thin bar from outside. By rotating the inner cylinder, the entrances into the two arms could be opened. In the middle of the inner cylinder, we placed a smaller solid cylinder (height 25 cm, diameter 10 cm) to prevent the animals from building the nest in this part of the maze.

We placed one mole-rat pair on the bottom of the centre cylinder with the doors closed and provided it with carrot pieces and stripes of tissue paper (38 x 7 cm). The starting box was tightly closed with a lid. Both terminal boxes were covered tightly with one of them randomly being opaquely shaded (square lid space with inserted plate) and the other one being translucent (square lid space open). The water filled dishes were placed over the square lid spaces, and the white light sources were switched on. Then the inner cylinder was rotated so that the mole-rats could enter and explore both sides of the binary choice apparatus. During the tests, the room's ceiling lighting was switched off.

We checked for a built nest after 30 minutes and most nests were finished by then. We supplied animals that had not yet finished their nest with more sheets of tissue paper and

checked again after another 30 minutes. A choice was counted as made as soon as the provided tissue paper was collected in one box or if animals nested (= slept) in one of the tunnels.

We also performed control tests with two opaque lids and with two transparent lids, respectively, to test for random distribution under control conditions.

2.2.2.2 Natural daylight

After the first positive results from the binary choice apparatus indicating a strong light avoiding behaviour, we tested pairs of mole-rats for this heliophobic behaviour also under much weaker natural daylight conditions in an eight-armed maze (fig. A4). The radial construction offered us the advantage of eight boxes with four randomly distributed dark and four translucent lids, providing the mole-rats with a greater choice. This design enabled us to test preferential behaviour as well as possible systematic, light-independent directional preferences. The radial maze was placed on a table in the mole-rat housing room. From a central cylinder, eight radial arrayed tunnels protruded (representing the directions 45°, 90°, 135°, 180°, 225°, 270°, 315°, 360°), ending in nesting boxes with removable lids either made from translucent or from opaque plastic material. Except for these lids, which had no square openings, measurements and modus operandi were exactly the same as in the binary choice apparatus. Tests were conducted under ambient room temperature and during daytime in (German) winter with low daylight intensities and no additional room ceiling lighting. Light intensities in the boxes with translucent lids ranged between 5 and 10 μmol $\text{photons} \cdot \text{m}^{-2} \cdot \text{s}^{-1}$ (LI-250 Light Meter; LI-COR Biosciences, Lincoln, NE, U.S.A.).

After each trial in both experimental set-ups, we placed the animals back into their home colony. Between trials, we washed the apparatus thoroughly with a mild detergent and acetic acid (3%) to remove any odorous traces.

2.2.2.3 Retinal involvement

We tested five adult pairs of enucleated Ansell's mole-rats (cf., B2.3) for nesting preferences in a two-armed maze with the choice between strong halogen light and darkness. For enucleation details see B2.4. Each pair was tested between four and seven times depending on the animals' motivation in order to gather enough data for analysis, as the number of enucleated animals was restricted. The study set-up followed the one described in A2.2.2.1 for the halogen light experiment.

2.3 The Light Perception Threshold

2.3.1 Study rationale

Now that we knew the mole-rats could perceive light, and that even at low daylight intensities, we wanted to narrow down their perception threshold of white light. As conditional training based on a strong white light stimulus connected to a food reward was unsuccessful (R. Wegner & P. Dammann, unpublished data), we tested spontaneous reactions to several graded intensities of white light in a T-maze to find out down to which light intensity Zambian mole-rats can learn (i.e. perceive) the location of a light source in order to find a food reward. Preceding the threshold study, we trained the same animals to find a food reward in front of a white light stimulus in a different set-up than the unsuccessful one to confirm the mole-rats' ability to perceive light and to create a basis of well-learned intensities for the threshold examination procedure.

2.3.2 Study procedure

Five mole-rats of the species *Fukomys kafuensis* (4 females, 1 male) were tested in the preceding light learning experiment and three individuals of this group (3 females) were consecutively tested in the light perception threshold study.

In the preceding learning experiment, the mole-rats were trained to reach a food reward connected to a light stimulus in a maze (for details, see fig. A5) using operant conditioning. The maze was made from thick, light-impervious plastic material with a non-reflective, black inner side. Two coldlight lamps (KL 150B, Schott, Mainz; light source Xenophot 15V 150W) were inserted into both terminal tunnels of the T-shaped maze and both were switched on to prevent unilateral auditory, lamp-generated cues. The illuminated side, that the animals were trained to, was determined in a randomized pattern for each run of the experimental series. A food reward (sunflower seeds) was placed at the end of the iluminated tunnel. On the dark side, light was blocked by an inserted metal plate; sunflower seeds were also placed on this side, behind the metal plate, to exclude that the animals were guided by the odour of the reward rather than by the light stimulus. As the metal plate was not tight regarding the food smell, placing seeds on both sides ensured that the animals chose the illuminated side to reach their reward. Olfactory orientation would have resulted in a random choice independent of the illuminated side.

The learning experiments comprised eight learning series with eight different light intensities, beginning with a light intensity that was assumed to be definitely perceivable by the mole-rats and then by reducing the intensity gradually down in the following learning series in

order to reach a good starting intensity for the threshold study. The eight light intensities were regulated by the lamps' switch that allowed to adjust 10 intensities in total. Light intensity was measured with a LI-250 Light Meter (LI-COR Biosciences, Lincoln, NE, U.S.A.). The order of the tested animals was randomized daily to avoid any dependency of the individuals' performance to certain daytimes.

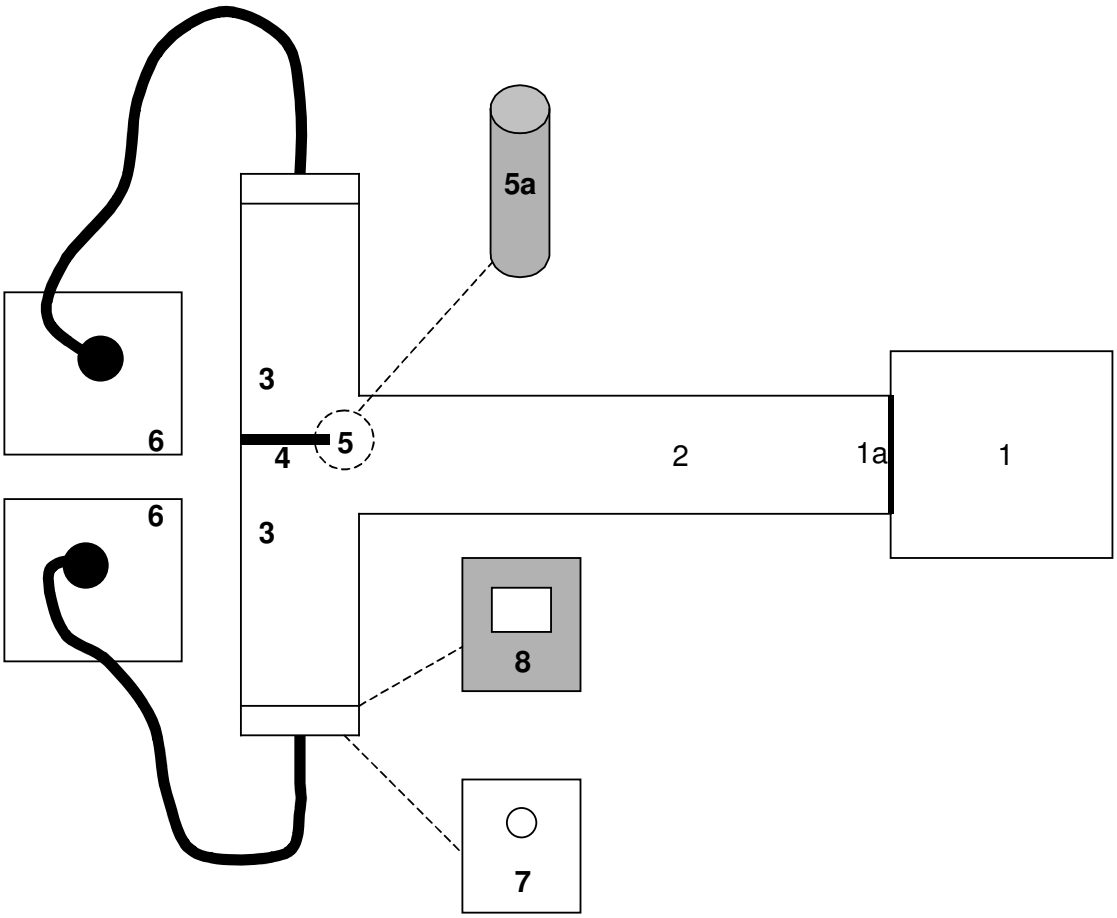

Fig. A5 T-maze for the study of light perception thresholds in mole-rats (top view). The maze contained a starting box (1) that was connected to a starting tunnel (2) by a metal slider (1a). The starting tunnel diverged into two tunnel ends (3), which were separated by an opaque plastic wall (4) at the decision point (5). The tunnel roof opened at the decision point into a small peep hole, onto which a telescope tube (5a) was inserted for observation. The tunnel ends were illuminated by cold light lamps (6), whose point lights were inserted into opaque plastic end plates with appropriate notches (7). Behind these end plates, metal plates (8) with square openings (5 x 5 cm) were inserted, which served either as a light blocker (inserted with the opening directed downwards) or as frames (inserted with the opening directed upwards) for the paper filters used in the threshold study. These paper filters were slid into the gap between end plates (7) and metal plates (8); into this gap, the sunflower seeds were placed in the dark tunnel, whereas in the illuminated tunnel, the seeds were placed directly in front of the metal plate. Size of the starting box: 16 x 16 x 16 cm; height of tunnels: 8 cm; width of tunnels: 9 cm; total length of the transverse tunnel element: 42 cm; length of starting tunnel element until junction: 38 cm. Figure modified after a draft by T. Pletz.

Learning series consisted of one to two trials per day on consecutive days. Each trial comprised five runs. The total number of runs of one learning series depended strongly on the mole-rats' motivation and thus varied heavily. The tested animal was placed in the starting box. The starting box was opened after one to two minutes of habituation by gently pulling up the slide that separated the box from the long tunnel element. The animal in most cases quickly left the starting box and ran along the long tunnel. The telescope tube allowed watching the animal's decision at the decision point. The choices (light or dark) were then recorded. After each run, the maze was cleaned with a mild detergent and carefully wiped dry. The animal was placed back in the closed starting box and, after the five trials had been completed, in the family cage.

Learning performance was recorded as the share of the total number of correct runs performed so far compared to the total number of runs performed so far. Learning success was defined as a constant percental share of more than 50% (random) correct choices.

In the threshold study, the lowest of the learned eight light intensities was used as a base line for quick determination of the lowest measurable light intensity the animals could be trained to. Due to massive motivational problems in two of the mole-rats and due to their relative bad performance in the learning experiments, only three animals (all females) were tested in the threshold study. These animals had proven to yield reliable results in the preceding runs.

The experimental procedure followed the one of the learning experiment with the difference that light intensity was changed within a trial (five runs) in the following way: the first run started with a light intensity that the animal had already shown as learned. If the run was correctly performed, i.e. when the animal chose the illuminated side, light intensity was reduced in the next run. This happened as long as the animal was successfully performing. When the animal made a mistake, i.e. chose the dark side, this intensity was repeated in the following run of the trial with maximally three repetitions. In case of three negative repetitions, light intensity was increased again. The next trial was in any case started with an intensity that had been learned with certainty (more than 50%). Light intensities were regulated by inserting paper filters into the terminal tunnels (see legend fig. A5). It is important to note that the test series was ended by technical limitations, i.e. it was impossible to create (and test perception of) light intensities lower than 0.6 μmol $\text{photons} \cdot \text{m}^{-2} \cdot \text{s}^{-1}$.

Both lamps were switched on during the threshold experiments to generate equal conditions on both sides of the maze due to the lamp-generated noise. Light was blocked from the dark tunnel by turning the metal plates upside down and by inserting a layer of thick, opaque felt. To make sure that the lamps did not heat up the maze and influenced

performance within or between trials or between animals, that were tested later on a testing day, mean temperature of measures made every third second was recorded every minute during ten runs of five to ten minutes (Eltek 1000 Series, Squirrel Meter/Logger; Eltek Ltd., Cambridge, UK). Temperature was measured at the two decision points of the two tunnel terminals.

We also performed control tests with both sides illuminated to test for random choices under equal conditions.

2.4 Light spectrum in a tunnel

2.4.1 Study rationale

In order to integrate the hitherto results on vision in Zambian mole-rats, we examined the spectral characteristics of white light before and during penetration in a tunnel system. It has been just recently shown that vascular tissue in the stem and in the roots of woody plants can conduct light (Sun et al. 2003). The authors demonstrated that light can even reach the outside of these plant structures by leaking out of structures such as vessels, tracheids or fibres. While light from the visible spectrum and from the ultraviolet range is apparently badly conducted, the far-red and near infra-red region (i.e. beyond 720 nm) seems to be conducted the most efficiently. This effect certainly comes with the long wavelength character of these regions, as longer wavelengths are generally propagated better than shorter ones due to the few contact points of their broader waves with the outer substrate and thus due to the smaller attenuation that they undergo.

Subterranean burrow systems are a vastly unknown territory, and the possibility of hitherto not discovered ways of conductance of certain wavelengths - such as the above mentioned findings (Sun et al. 2003) - of sunlight into the earth show the importance of examining wavelength properties underground.

2.4.2 Study procedure

The experiments were conducted on a winter afternoon in a room without ceiling lights to avoid photic contamination. Light intensity within the room was approximately 2.6 µmol $\text{photons} \cdot \text{m}^{-2} \cdot \text{s}^{-1}$, thus below low daylight intensities. Wavelength propagation/attenuation was measured in a T-maze (fig. A6). The main tunnel was filled with horticultural peat, attempting to create a soil-surrounded tunnel within the plastic maze.

The maze was tightly closed against light except of the T-shaped maze part where the light was positioned (fig. A6). Here, an area of about 5 cm x 5 cm was being left open, imitating the opening of a tunnel roof (e.g. as happens when a tunnel is damaged or broken from above by a predator or by mole-rat hunters). Light intensity under this hole was 0.06 $\mu mol\ photons \cdot m^{-2} \cdot s^{-1}$ under natural light conditions. The sides of this maze part adjacent to the opening were covered with thick, black, light impervious paper sheets. White light was produced by a halogen lamp. This lamp was positioned above the tunnel opening at different heights (80, 60, 40, 20 and 10 cm) to create diverse light intensities from daylight to sunlight.

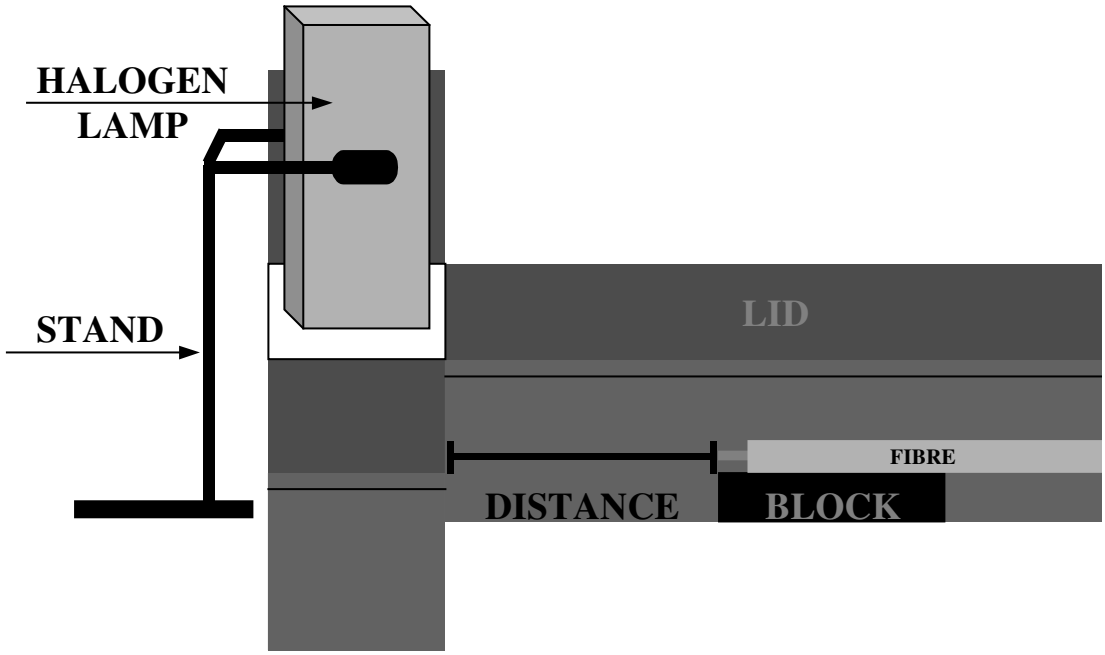

Fig. A6 T-maze for measurements of light propagation in a tunnel. All maze tunnel parts were 9 x 9 cm in height and width. The main tunnel was 100 cm long, the T-shaped tunnel 120 cm. The tunnels were closed. The white light source, a halogen lamp, was positioned at different heights over the opening in the T-shaped tunnel's middle by moving it vertically on a stand. During these measures, the spectrometer fibre was positioned directly under the lamp. With the lamp positioned at 10 cm above the tunnel opening, the spectrometer was positioned at different distances from the junction in the main tunnel, fixated on a block.

Wavelengths were measured with a HR4000 High-Resolution Spectrometer and analyzed with SpectraSuite Spectrometer Operating Software (both Ocean Optics Inc., Dunedin, FL). The collection area of the fibre was 0.12 cm^2; calibration was performed on the same halogen lamp used. We firstly performed a spectral analysis directly below the halogen light positioned at different heights to examine the arriving spectral distribution at diverse light intensities. Additionally, we performed measurements at 5, 10, 20, 30, 50, 60, 65, 67.5, and 70 cm from the light entrance into the tunnel opening by injecting the fibre from the end of the main tunnel and fixating it on a wooden block at a height of about five centimetres; this was done to examine maximal wavelength propagation/attenuation in a tunnel with white light infiltrating this tunnel perpendicular from above, with the light source positioned at 10 cm height.

2.5 Statistical analysis

In the two-armed and the eight-armed maze preference tests, and in the controls of the learning/threshold experiment, we analyzed the data for a preferential choice using Chi-square tests.

In the eight-armed maze condition, we checked for any possible distinct directional preference additionally with a circular statistics test (Rayleigh test of uniformity; ORIANA 2.02, Kovach Computing Services, Anglesey, UK).

In the two-armed maze, mean temperatures (given as $X \pm$ SD) measured in both boxes were compared using a paired two-tailed *t*-test. The same test was applied in the T-maze of the threshold study for comparing mean temperatures at the two measure points (given as $X \pm$ SD).

Results from the learning and threshold experiments were not statistically analyzed. A learning effect was considered as significant, i.e. not random, when the number of correct choices constantly summed up to a cumulated percentage of more than 50% of all runs. Learning success in the learning experiments is demonstrated by two representative learning curves (for the strongest and the second lowest light intensity) in the respective figures with the random threshold being indicated.

Except for the circular statistics (ORIANA 2.02), all analyses were conducted with SPSS® 12.0.

3 RESULTS

3.1 Demonstrating Light Perception

In the two-choice test chamber, the mole-rats showed clear heliophobic behaviour towards the halogen light stimulus and significantly preferred the dark box (= scotophilia) for nesting (fig. A7; $N = 20$, Chi-square test: $X^2_1 = 9.8$, $P = 0.002$).

In the controls, the mole-rats did also nest in the circular centre around the inserted smaller cylinder, designed actually to prevent them from nesting during the experiments. However, animals showed a random choice between these three nesting possibilities both in the dark/dark controls ($N = 16$, Chi-square test: $X^2_2 = 3.5$, $P = 0.17$) and in the white light/white light controls ($N = 16$, Chi-square test: $X^2_2 = 1.625$, $P = 0.44$).

Mean temperatures did not differ between the lighted (23.83±0.76 °C, $N = 8$) and the dark box (23.95±0.66 °C, $N = 8$; Paired *t*-test: $t_7 = -0.63$, $P = 0.548$).

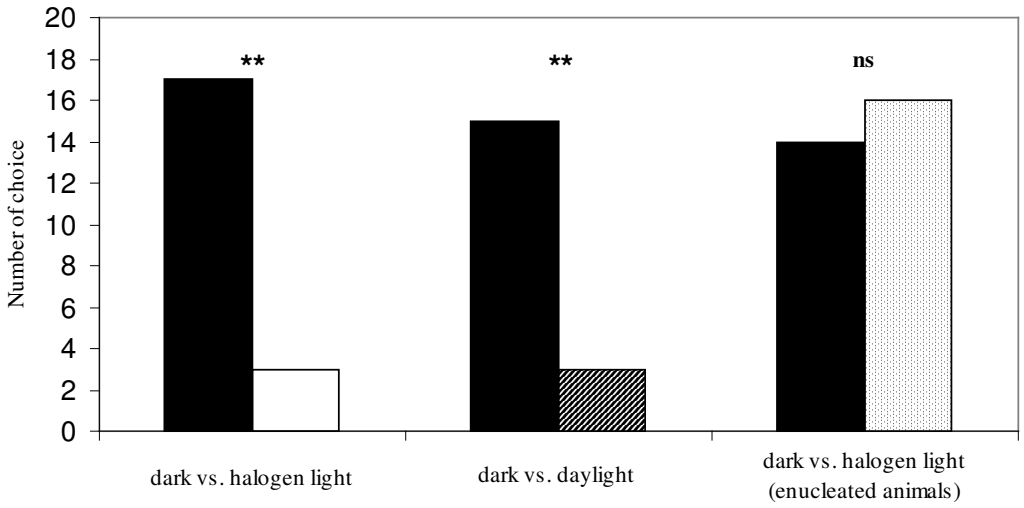

Fig. A7 Nesting choices of sighted and enucleated mole-rats under different light regimes. Number of choices for nesting chambers that mole-rat pairs made in preference tests. Tests were performed with sighted animals under darkness versus a halogen white light regime in a two-armed maze (black/white) and under darkness versus natural daylight conditions in an eight-armed maze(black/bold hatching); and with enucleated animals under darkness versus halogen light in a two-armed maze (black/polka dots). Significance is indicated with two asterisks indicating a *P*-value below 0.01.

The mole-rats displayed significant heliophobic behaviour also under weak daylight conditions in the radial eight-armed maze with four randomly distributed translucent lids (fig. A7; N = 18, Chi-square test: X^2_1 = 8, P = 0.005). Animals did not show any preference for nesting in a specific direction (N = 18, Mean vector α = 325°, Length of mean vector r = 0.19, Rayleigh test: P = 0.52).

With the eyes ectomized, the mole-rats could not distinguish between light and dark anymore (fig. A7; N = 30, Chi-square test: X^2_1 = 0.133, P = 0.72). When regarding the mole-rat pairs' singular preferences, the picture was inconsistent, but still insignificant regarding any preference (fig. A8), except one pair that chose darkness in four out of four trials (N = 4, Chi-square test: X^2 could not be calculated due to the constant variable N, P = 0.045) and one pair that chose light more often than darkness in a nearly significant manner (P3, N = 7, Chi-square test: X^2_1 = 3.57, P = 0.06). Statistical values for the other four tested pairs (P1, P2, P4) are: P1 & P2, N = 6, Chi-square test: X^2_1 = 0.667, P = 0.41; P4, N = 7, Chi-square test: X^2_1 = 1.29, P = 0.26.

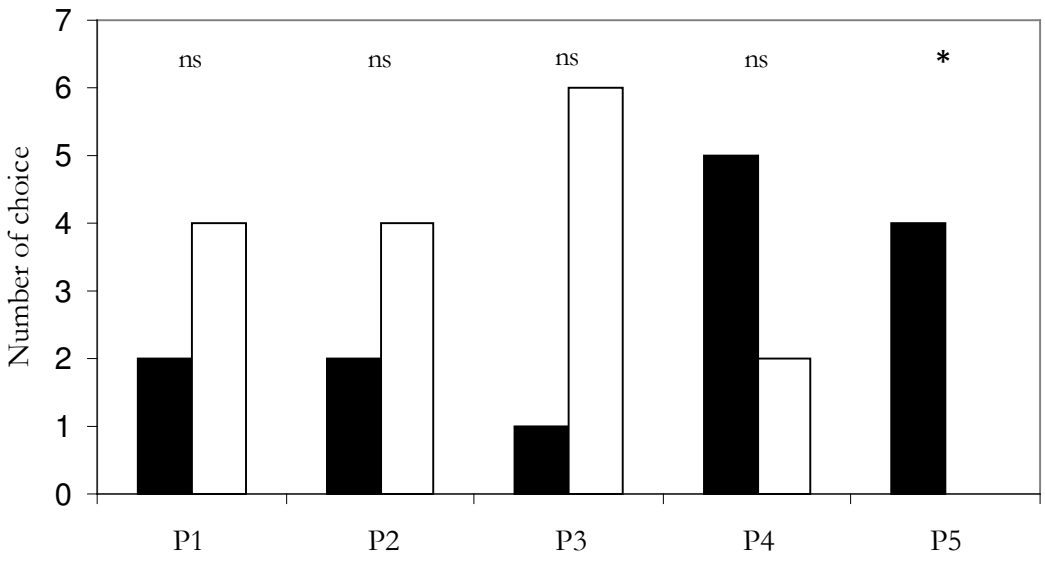

Fig. A8 Single nesting choices of enucleated mole-rat pairs between darkness and white light. Number of choices that enucleated mole-rats made in preference tests under darkness versus a halogen white light regime (black/white) in a two-armed maze with "ns" indicating not significant differences, and * indicating the probability of error $P < 0.05$. P1-P5 represent the tested pairs.

3.2 The Light Perception Threshold

In the learning experiment, the mole-rats showed learning success in all eight applied light intensities, with correct choices of the illuminated tunnel in far more than 50% of all performed runs (tab. A1, see next page). Only animal 4 showed difficulties during learning series of three intensities (32, 13, and 11 µmol $\text{photons} \cdot \text{m}^{-2} \cdot \text{s}^{-1}$, respectively) with correct choices lower than the random probability. The individual learning gain over trials is demonstrated in the two representative learning curves of the learning performance in the strongest and the second lowest light intensity (figs. A9 and A10, see second next page). Note that the three intensities 13, 10, and 11 µmol $\text{photons} \cdot \text{m}^{-2} \cdot \text{s}^{-1}$, representing very close photon flux rates, yielded no differences in learning performances. The similar values resulted from technical problems with the lamps that were recognized not till after the study. These problems were overcome before starting the threshold experiments.

The three tested animals in the threshold study showed high learning rates including the last tested light intensity of 0.6 µmol $\text{photons} \cdot \text{m}^{-2} \cdot \text{s}^{-1}$ with constant correct choices in more than 50% of the cases, mostly with much more than 60% correct choices and with more than 65% correctness (cumulated percentage value) at the lowest tested intensity (tab. A2, see next page). No learning curve could be created here, as tests were not consecutively conducted with increasing light intensities and did not aim at visualizing a learning gain.

In the controls, the animals showed a random choice between the two illuminated tunnel endings, indicating no lateral preference (N = 26, Chi-square test: X^2_2 = 1.385, P = 0.24).

Mean temperatures did not differ between the two measure points at the lighted decision point (22.33±0.22 °C, N = 10) and the dark decision point (22.31±0.17 °C, N = 10) (Paired t-test: t_9 = -0.629, P = 0.545).

Table A1 Light perception learning experiments. The table gives the final percentages of correct runs in learning series with eight different light intensities (i.e. the share of all correct runs in all performed runs). Maze runs were performed under operant conditioning to white light; correct decisions were choices of the illuminated side. Light intensities are given in μmol $\text{photons} \cdot \text{m}^{-2} \cdot \text{s}^{-1}$. The number of performed runs for each light intensity series is also given; all animals performed the same number of runs. Note that the similar values of the fourth, fifth, and sixth series resulted from unrecognized technical lamp problems.

Intensity	32	23	18	13	10	11	7	5
Animal	%	%	%	%	%	%	%	%
1	71	58	76	70	80	76	71	80
2	62	53	76	57	70	76	74	53
3	62	54	56	53	65	80	79	53
4	44	61	60	45	50	48	56	53
5	62	54	58	61	80	64	63	47
no. runs	45	100	50	30	45	45	25	15

Table A2 Light perception threshold experiments. The table gives the numbers of all runs and all correct runs as well as the percentage of the correct decisions. Maze runs were performed under operant conditioning to white light; correct decisions were choices of the illuminated side. Light intensities are given in μmol $\text{photons} \cdot \text{m}^{-2} \cdot \text{s}^{-1}$.

			Light intensity						
Animal	Runs	Σ	7	5	4	3	2	1	0.6
1	Sum	178	4	24	23	44	45	29	9
	Correct	128	3	20	19	32	29	19	6
	Correct %	72	75	83	83	73	64	66	67
2	Sum	176	3	25	34	44	33	21	16
	Correct	122	2	17	25	30	19	17	12
	Correct %	69	67	68	74	68	58	81	75
3	Sum	173	4	31	40	45	31	13	9
	Correct	113	2	25	25	24	20	11	6
	Correct %	65	50	81	63	53	65	85	67

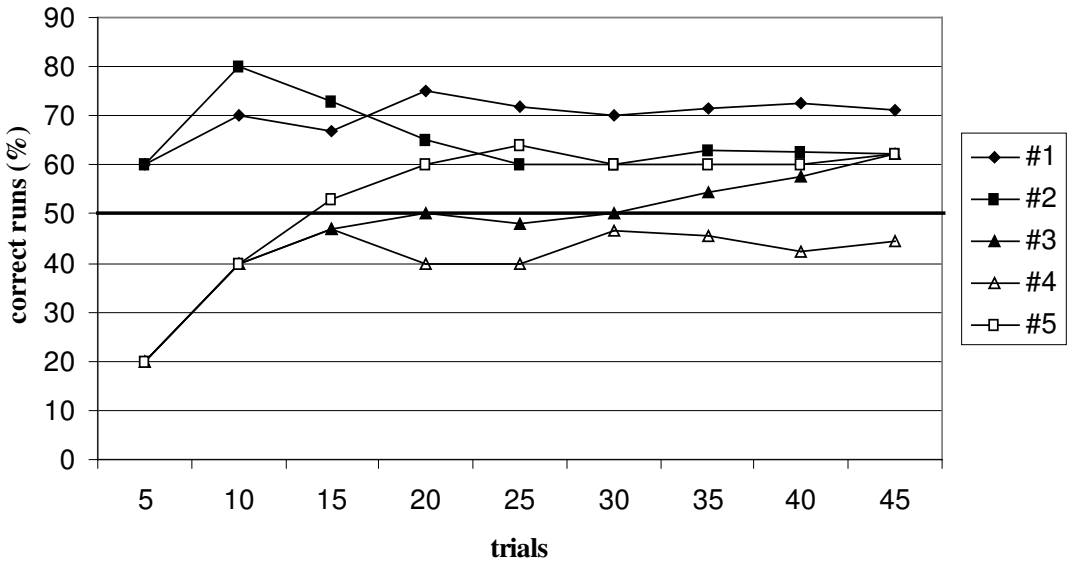

Fig. A9 Learning curves of five mole-rats trained to a white light stimulus with a strong intensity of 23 µmol photons $\cdot m^{-2} \cdot s^{-1}$. The random threshold of 50% is indicated by a bold black bar. Four of five animals (except for animal #4) showed a learning gain during the learning series and yielded more than 50% correct choices. Animals #1 and #2 displayed constant performances above 60% during the whole series. Animals #3 and #5 showed classical learning curves during the series, with animal #5 overcoming the 50% threshold after 15, and with animal #3 after 35 trials.

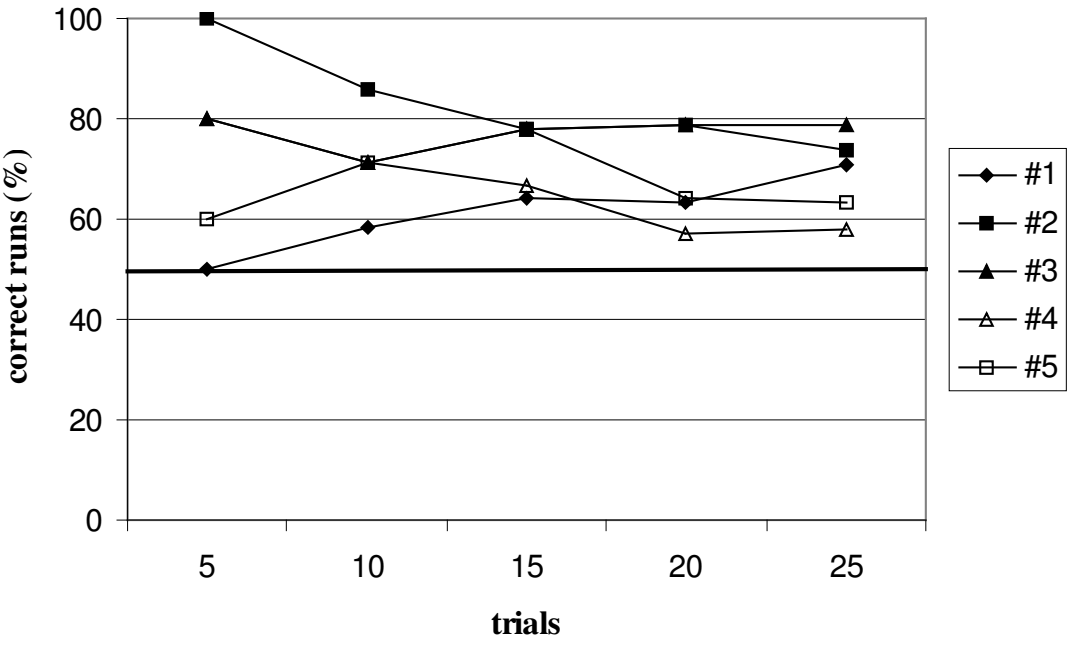

Fig. A10 Learning curves of five mole-rats trained to a white light stimulus with a low intensity of 7 µmol photons $\cdot m^{-2} \cdot s^{-1}$**.** The random threshold of 50% is indicated by a bold black bar. All five animals reached a learning performance with more than 50% correct choices; except for animal #4, the mole-rats even were successful in more than 60% of all runs. Animal #1 shows a classical learning curve. This animal seemed to be particularly motivated throughout the whole study.

3.3 Light spectrum in a tunnel

Spectral analysis of halogen white light of different intensities deriving from a lamp positioned at different heights, showed that, as was to be expected, absolute irradiance (photon flux density) increased with increasing intensity, i.e. with decreasing lamp height (tab. A3). Thermal radiation (noise) of the light source was always detected in the spectral range beyond 900/950 nm.

Table A3 Light intensity measurements. Light intensity was measured in an artificial tunnel opening with the probe of a spectrometer positioned directly in the lightpath of a halogen white light source at different lamp heights (LH). The total light intensity of the light source as measured by the LI-COR in µmol $\text{photons} \cdot \text{m}^{-2} \cdot \text{s}^{-1}$ is given (measured total intensity, MTI). Light intensities of the three wavelength areas blue, green and red as indicated by the nm spectra are given in µWatt/cm² (W) as measured by the spectrometer, and converted into µmol $\text{photons} \cdot \text{m}^{-2} \cdot \text{s}^{-1}$ (phot). Diverse circumstances result in a deviation between the measured total light intensity and the calculated photon sum of the three measured wavelengths; these circumstances are discussed in the text. The share of each wavelength area within the total photon catch, i.e. the contribution of the wavelengths to the spectrum, is given in % based on the mean of the measured total light intensity and the sum of the single wavelength' intensities (mean total intensity, mTI); these values do not exactly add up to 100%.

LH		400-500 nm	500-600 nm	600-700 nm	sum	MTI	mTI
80	W	20.87	115.07	122.52	258.46		
	phot	0.96	5.29	5.64	11.89	15	13.44
	%	7.14	39.36	41.96			100
60	W	35.08	158.44	220.42	413.94		
	phot	1.61	7.29	10.14	19.04	24.3	21.67
	%	7.43	33.64	46.79			100
40	W	146.31	464.57	517.59	1,128.47		
	phot	6.73	21.37	23.81	51.91	55.7	53.8
	%	12.51	39.72	44.26			100
20	W	646.97	2,093	2,456.3	5,196.27		
	phot	29.76	96.28	112.99	239.03	304.4	271.71
	%	10.95	35.43	41.58			100
10	W	2,185.6	7,254.5	9,600.7	19,040.8		
	phot	100.54	333.71	441.63	875.88	604.5	740.19
	%	13.58	45.08	59.66			100

At 80 cm height (with an intensity of 15 µmol $\text{photons} \cdot \text{m}^{-2} \cdot \text{s}^{-1}$), irradiance was generally low and showed peaks at 600 nm and 900 nm, i.e. in the transition between green and red and in the infrared region (beyond approximately 800 nm). At 60 cm height (with an intensity of 24.3 µmol $\text{photons} \cdot \text{m}^{-2} \cdot \text{s}^{-1}$), irradiance was markedly increased, and the peak in the infrared region could not be detcted anymore; wavelengths were obviously blocked below 450 nm. At 40 cm height (with an intensity of 55.7 µmol $\text{photons} \cdot \text{m}^{-2} \cdot \text{s}^{-1}$), irradiance again increased, and also the peak in the infrared spectral area occurred again. From this height (intensity) on, wavelengths were also propagated beyond 400 nm. At 20 cm height (with an intensity of 304.4 µmol $\text{photons} \cdot \text{m}^{-2} \cdot \text{s}^{-1}$), irradiance was increased by five times compared to the value from the 40 cm height measurement; thermal noise from beyond approximately 850 nm increased markedly. With the lamp positioned at 10 cm height above the fibre (with an intensity of 604.5 µmol $\text{photons} \cdot \text{m}^{-2} \cdot \text{s}^{-1}$), irradiance increased again markedly. A distinct peak could only be detected at 600 nm; thermal noise already occurred at 850 nm. The share of photons in the blue spectral range (400-500 nm) lay between 7 and 14 %, in the green range (500-600 nm) between 34 and 45%, and the red spectral range (600-700 nm) displayed the highest spectral proportion with 42 to 60%. The white light spectra produced by the lamp being positioned in 80 cm and in 10 cm height are given representatively in fig. A11 on the following page. All other spectra can be found in the Appendix (AD).

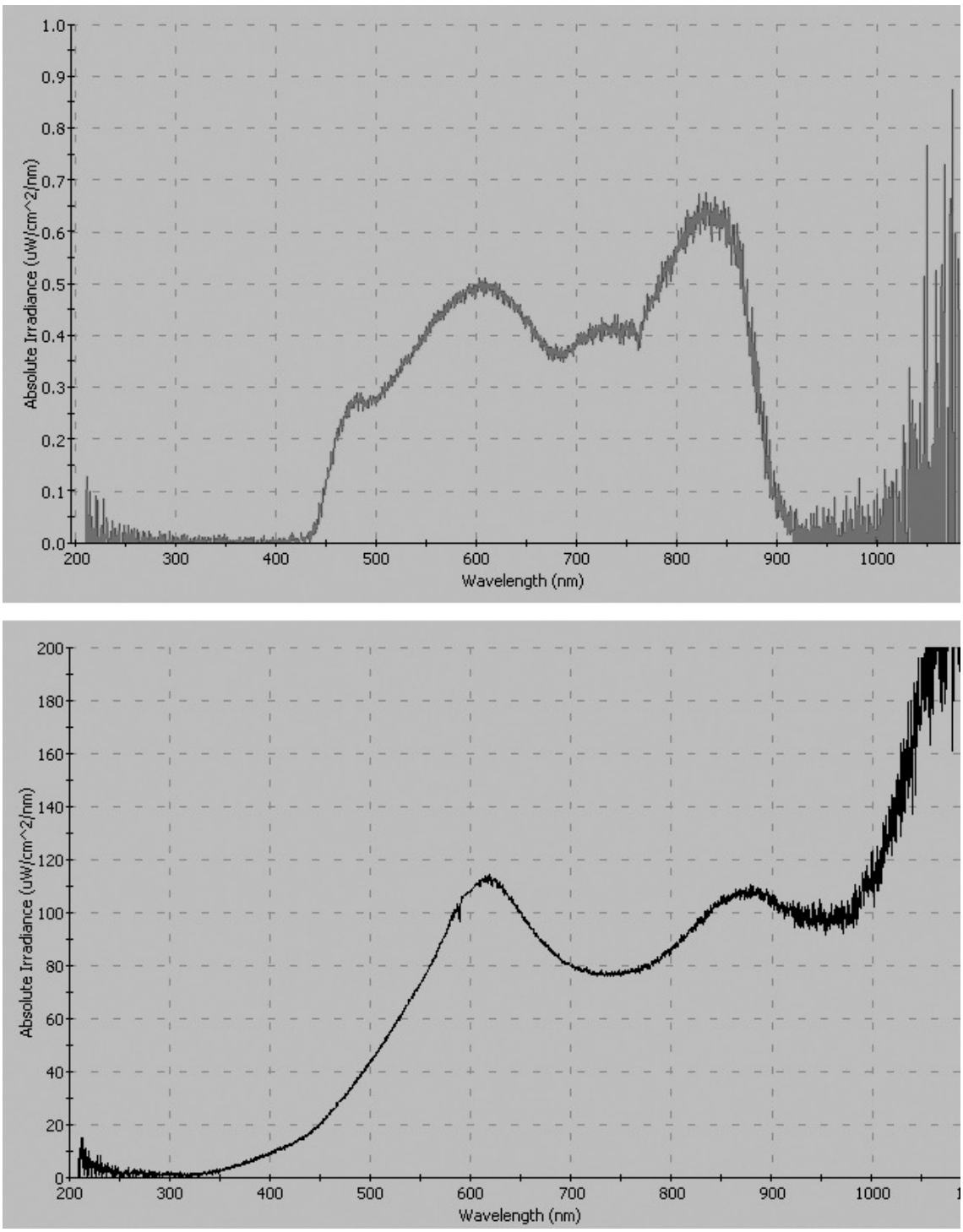

Fig. A11 Wavelength spectra of white light in a tunnel opening under low and strong illumination. Spectra were measured under a halogen white light source being placed above the spectrometer fibre in different heights to create diverse light intensities. This figure shows the wavelength shares of white light with an intensity of 15 µmol $\text{photons} \cdot \text{m}^{-2} \cdot \text{s}^{-1}$ in the tunnel opening produced by a lamp height of 80 cm above the hole (upper part of the panel) and the wavelength shares of white light with an intensity of 605 µmol $\text{photons} \cdot \text{m}^{-2} \cdot \text{s}^{-1}$ with the lamp positioned 10 cm above the tunnel opening (lower part of the panel). In this and the following spectral figures, the wavelength is indicated at the x-axis in nm; absolute irradiance (i.e. photon flux density per time and area) is given as µWatt/cm²/nm at the y-axis. Note the different scale of irradiance, indicating a significant increase when the lamp is close. Also note the thermal noise on the right side of the spectrum, which is produced by the lamp's warmth and increasing with the lamp coming closer to the fibre.

Measuring attenuation of wavelengths in a tunnel at different distances from the illuminated tunnel opening, it became clear that the spectral range between 400 and 500 nm (blue) was already not, or not well, propagated anymore at a distance of 5 cm from the light source. Wavelengths from 500 nm to 700 nm (green and red) were still detectably propagated until a distance of 60 cm. Even at 65 cm distance, there were still some measurable photons in the red range (600 to 700 nm). At 67.5 cm distance and at 70 cm distance, the fibre hardly, but still detected photons in this spectral range; the number of these photons, i.e. the intensity level still lay, however, above the scotopic range (< $9 * 10^{-5}$ µmol $\text{photons} \cdot \text{m}^{-2} \cdot \text{s}^{-1}$ or <0.005 lux; Kelber & Gross 2006). For all attenuation measurements, see tab. A4. For the attenuation measurements of the representative distances 5 cm, 30 cm, and 67.5 cm, refer to fig. A12 on the next page. All other attenuation spectra can be found in the Appendix (AD).

In all distances, the red spectral range made up for the largest proportion within the total spectrum (max. 0.16% of the total incoming photons). Second best propagated were the green wavelengths (max. 0.07%, i.e. less than half as much as in the red range), and the blue wavelengths were attenuated strongest (max. 0.01%).

Table A4 Light propagation measurements. Irradiance of three wavelengths was measured in different distances from the opening of an artificial tunnel with a halogen white light source positioned in 10 cm height above the opening. The distance of the fibre's collection area from the junction is given as DIST (see fig. A6). Light intensities of the three wavelength areas (λ) blue, green and red are given in µWatt/cm² (W) as measured by the spectrometer, and converted into µmol $\text{photons} \cdot \text{m}^{-2} \cdot \text{s}^{-1}$ (phot). The share of each wavelength within the total photon catch, i.e. the contribution of the wavelength area to the spectrum, is given in % based on the same calculation as in tab. A3.

λ (nm)	DIST	5	10	20	30	50	60	65	67.5	70
400-500 (blue)	W	2.05	0.92	0.42	0.29	0.08	0.05	0.06	0.12	0.01
	phot	0.09	0.04	0.02	0.01	0.004	0.002	0.003	0.005	0.0005
	%	0.01	0.01	0.003	0.002	0.0005	0.0003	0.0003	0.0007	0.0001
500-600 (green)	W	10.57	4.33	1.90	1.24	0.3	0.2	0.17	0.12	0.02
	phot	0.49	0.2	0.09	0.06	0.014	0.009	0.008	0.005	0.001
	%	0.07	0.03	0.01	0.01	0.002	0.001	0.001	0.0007	0.0001
600-700 (red)	W	25.15	9.8	3.95	2.42	0.59	0.4	0.32	0.14	0.04
	phot	1.16	0.45	0.18	0.11	0.027	0.018	0.015	0.006	0.0018
	%	0.16	0.06	0.02	0.02	0.004	0.002	0.002	0.0009	0.0002

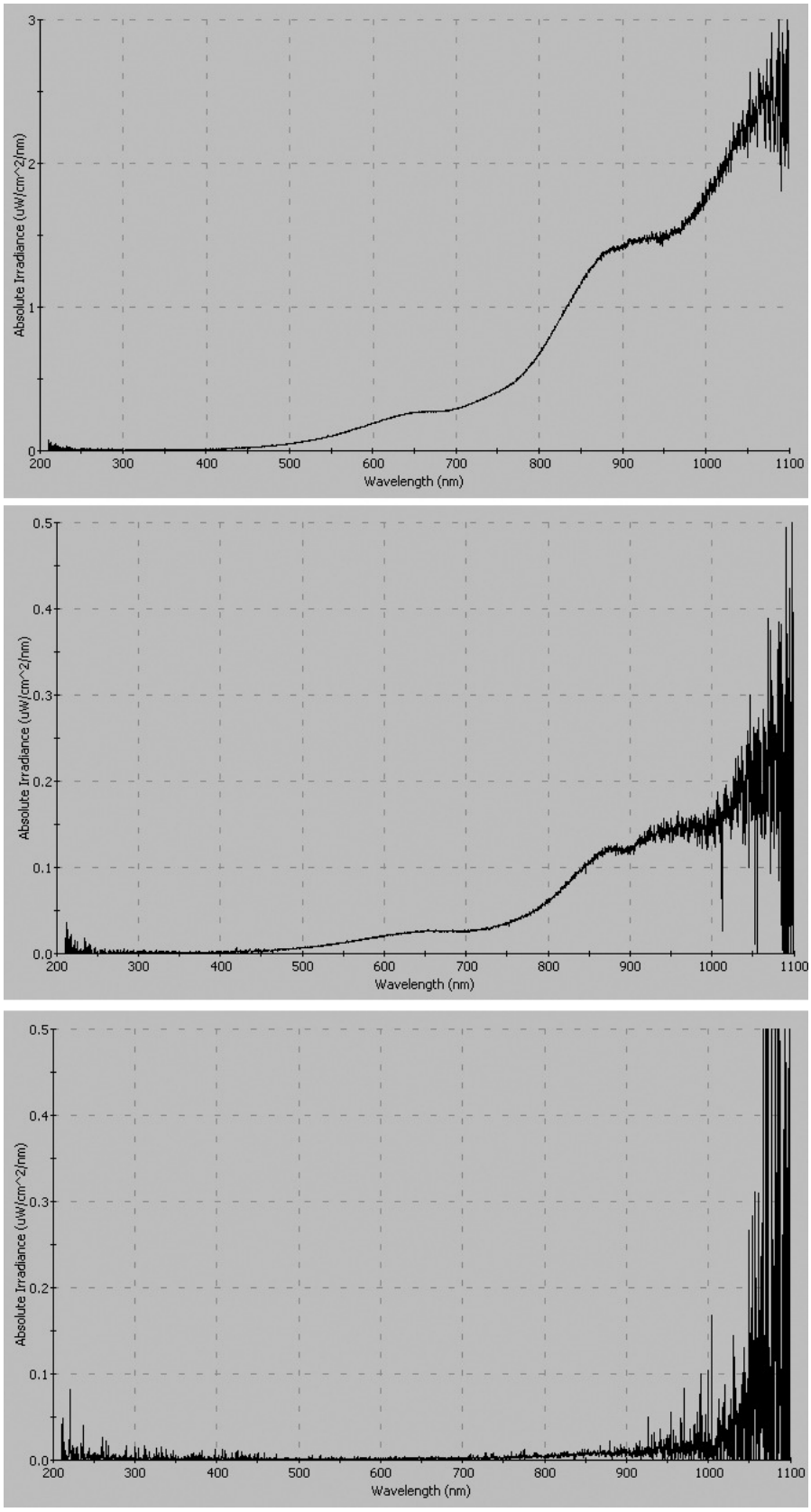

Fig. A12 Spectral attenuation of white light in a tunnel. The figure gives the wavelength shares of white light of an intensity of 604.5 µmol $\text{photons} \cdot \text{m}^{-2} \cdot \text{s}^{-1}$ projected into the tunnel opening by a lamp in 10 cm height. Irradiance measurements are given conducted in 5 cm distance from the tunnel opening (upper panel part), in 30 cm distance (middle panel part), and in 67.5 cm distance (lower panel part). Note the changing irradiance scale. Note also the thermal radiation on the right side of the figure.

4 DISCUSSION

The first part of this thesis has presented new results on the visual behaviour of Zambian *Fukomys* mole-rats, which show that the eye has seemingly taken over specialized functions in these underground 'blind' rodents. Ethological studies of mole-rat vision, combined here with a technical study of the optical conditions in a model tunnel, open wide discussion possibilities in the following.

Demonstrating Light Perception

Our first study gives ethological support for the assumption made on the basis of the recent morphological findings (Oelschläger et al. 2000; Cernuda-Cernuda et al. 2003; Němec et al. 2004; Peichl et al. 2004) that *Fukomys* mole-rats are capable to perceive light, that the retina receives photic cues, and that this light-encoded information can be used to make a meaningful decision. However, the real adaptive meaning of this ability is far from being clear. For sure, *Fukomys* mole-rats do not flee away from light in panic (own observation). Under our housing conditions, they sleep uncovered on the surface, though they would have the possibility to transport the substrate to one corner of their cage and hide under it - a behaviour blind mole-rats (*Spalax*) or moles (*Talpa*) would always exhibit (H. Burda, personal communication). In the field, Zambian mole-rats appear quite rarely above ground (Scharff & Grütjen 1997), probably e.g. when dispersing, foraging, or during flooding, and they do so also in the daytime, demonstrating that their surface activity is not strictly nocturnal. They also do not show any efforts to hide or look for shaded or dark objects (M. Kawalika, personal communication). Surely these mole-rats do not need light information to know which direction they should dig in order to hide. Both their vestibular organ and somatosensory perception provide fast and reliable information on the directional matter as well as on whether the animal is above ground or fully or only partly in a tunnel. Based on these considerations, we speculate that the adaptive biological meaning of the observed capacity to perceive light may lie rather in attentiveness to light than in perceiving and searching darkness. This approach explains better the paradoxon between the visual system unsuited for above-ground orientation (or: designed for underground orientation) and the photoreceptor mosaic adapted to the perception of daylight intensities rather than to a dark environment (Němec et al. 2007).

In many cases, incidence of light may well indicate a tunnel being opened by predators and may thus warn the animal not to approach the opening too closely but to instead plug it (own field observations). This plugging of illuminated tunnels was elicited also under laboratory conditions in the pocket gopher (*Thomomys* spp.) (Werner et al. 2005). Note that

opening of a tunnel does not lead to air currents within burrow systems (H. Burda; field measurements). However, first attempts in the course of this study to trigger plugging behaviour in illuminated tunnels were unsuccessful. The maze used (length of the main tunnel: 1 m; length of the illuminated terminal tunnels: 60 cm) was probably too short, so that the mole-rats did not accept the maze as a tunnel system (A. Schinkoeth, personal communication). We suggest repeating these experiments in a maze system with the sizes similar to those used by Werner et al. (2005) (main tunnel 10 m long; side tunnels 1 m long). This system would have a size enlarged by the factor ten, enabling the animals to move freely over longer distances in the maze. A complementary explanation has been suggested by Němec et al. (2007): light influx may indicate an accidental burrow collapse and induce its maintenance.

Differentiation between light and dark can help subterranean mammals to entrain either daily and/or annual cycles just as sighted, surface-dwelling mammals do. However, clearly photoperiodic Eurasian blind mole-rats (*Spalax*) with their minuscule degenerated and subcutaneous eyes provide the best evidence that photoperception and vision (sight) can be decoupled (Cooper et al. 1993; reviewed in Nevo 1999). Among bathyergids, the naked mole-rat (*Heterocephalus glaber*) from East Africa and also the Mashona mole-rat (*Fukomys darlingi*) from southern Africa show the capability of entraining circadian rhythms to light as a zeitgeber (Riccio & Goldman 2000a, b; Vasicek et al. 2005). However, only few unpublished studies (Fleissner & Fleissner; Daan & Everts; Fritzsche & Gattermann) have examined circadian rhythms in *F. anselli*. All results strongly indicate that the animals display free-running activity rhythms with individual-specific spontaneous periods. For seasonal entrainment, light in the nearly constant 12:12 LD-rhythm of the habitat so close to the equator would be hardly of use as a zeitgeber. Accordingly, Zambian *Fukomys* species do not undergo a seasonal reproduction cycle (Burda 1989, 1990; Scharff et al. 2001).

The Light Perception Threshold

Our study of learning demonstrates one thing above all: that learning tasks are a challenge in mole-rats, as performance on each day as well as over the whole study period depends extremely on individual motivation, a mole-rat character heavily influenced by the strong exploration drive that decreases rapidly if the task remains unchanged. It becomes also clear that, maybe due to lacking motivation, learning in two-choice experiments is time-consuming and does not yield as convincing results in Zambian mole-rats as is the case e.g. in two-choice learning experiments with European moles (*Talpa europaea*), that showed 90% correct responses over only 30 to 45 trials (Johannesson-Gross 1988). Even more interesting is the fact that only three animals could be used in the threshold study – due to lacking motivation

of the other two, which lingered in the maze very long before making a decision at all. These two were the reproductive pair, both being wild-captured. Hence the question arises whether it was really lacking motivation that made them perform so reluctantly or whether their visual capabilities were worse than those of their offspring reared in a lighted laboratory, and whether they thus needed more time for preferential decisions. It would be thinkable that the eye, or better the neuronal pathways of vision, degenerate after birth if not constantly excited by light cues. A loss of possible function during development has been already shown in *Spalax ehrenbergi*, where the lense starts to degenerate soon after ocular development onset (Sanyal et al. 1990); however, this degenerative process is phylogenetically pre-determined and independent of later light exposure. The process of neuronal plasticity would explain the use of vision in the light-reared offspring better: neuronal plasticity refers to changes that occur in brain organization, particularly to changes in the location of specific information processing functions. These changes derive from learning and also from experience. As the concept of plasticity can be applied to environmental events (Schwartz & Begley 2003), the unusual event of constant light exposure might re-activate the usually rarely used visual brain-centers.

Our study showed that mole-rats can at least discriminate a difference between light and dark in the intensity order of 0.6 μmol $\text{photons} \cdot \text{m}^{-2} \cdot \text{s}^{-1}$. This value seems small, and indeed the light intensity appeared low, but 0.6 μmol $\text{photons} \cdot \text{m}^{-2} \cdot \text{s}^{-1}$ equal 33 lux, and 33 lux belongs to the photopic range of vision (>5 lux; Kelber & Gross 2006). However, subterranean European moles (*Talpa europaea*) have been shown to discriminate light at much higher light intensities (350 lux), and to be unable to perceive light at an intensity of 60 lux (Johannesson-Gross 1988) – the Zambian mole-rats have yet, in our study, shown a performance about twice as good as the European mole.

It is nevertheless a pity that both the light sources and the light measuring instrument did not allow to test visual performance under presence of lower light intensities, even down to scotopic levels ($<9*10^{-5}$ μmol $\text{photons} \cdot \text{m}^{-2} \cdot \text{s}^{-1}$ or <0.005 lux). Tests examining light perception abilities in the scotopic range should be carried on with larger sample sizes with a balanced sex ratio. These tests should, however, be based on spontaneous behaviour tests to bypass the motivational problems described above.

Light spectrum in a tunnel

Our model tunnel experiment yielded interesting, though mainly not unexpected results on light propagation/attenuation in a tunnel. It pictured quite well the natural state of a tunnel located superficially; though of course the amount of incoming radiation into an opened tunnel depends on its inclination, it can be assumed that light propagation in superficial

tunnels resembles our results, as tunnels close to surface are often horizontal (personal observation). Vertical radiation into a tunnel hole is thus probable, particularly as in Zambia, close to equator, sunlight radiance occurs vertically on most times of the day. However, the properties of both the material (plastic) and the colour (black) of the model tunnel are, of course, different to those of soil, and this difference might result in 'false' light propagation or attenuation measurements compared to the natural situation.

The strongest intensity applied in our test was approximately 600 μmol $\text{photons} \cdot \text{m}^{-2} \cdot \text{s}^{-1}$ (equalling 33,600 lux). This intensity is likely to occur in Zambian mole-rat habitats frequently: though a cloudless summer day might have up to 2000 μmol $\text{photons} \cdot \text{m}^{-2} \cdot \text{s}^{-1}$ (100,000 lux), infiltration of light always also depends on shading. Vegetation, of which bushes and high grass are frequent in the mole-rat habitat (see fig. 1), as well as soil which might block a tunnel opening partly or nearly totally, are two factors that could decrease incoming solar radiation strongly. Furthermore, conversion factors of standard intensity measures into photon counts are dependent on the light source (McCree 1981), meaning that technically determined 600 μmol photons might differ when being derived from a halogen lamp with 100W or from the sun with its approximately 1.37 kW electric power reaching each square meter of the Earth (http://lexikon.astronomie.info/sonne/index.html). The same emitted radiation might then result in a higher incoming intensity; a pure calculation problem.

The measured wavelength attenuation shows that within a tunnel, there is hardly any blue light contained in the incoming spectrum; only 0.01% of the total light income belongs to the short wavelengths of the 400-500 nm range, already at 5 cm distance (i.e. a mole-rat's head length) from the light source. These short waves are, due to their high frequency, as expected attenuated quickest in a tunnel, as they are, of all visible colours, scattered most along the tunnel walls. Hence, vision in the blue light or even in the UV-light spectrum seems improbable underground. Communication of mole-rats via UV light, that is via urine markings visible in these wavelengths, is however still thinkable, as it has been, in predator-prey interactions, shown e.g. in voles (Viitala et al. 1995; Chávez et al. 2003). Urine in mole-rats is the carrier of immanent information (Heth & Todrank 2007). Even if not within a burrow system, where no UV-light is present to let the urine fluoresce, urine markings could serve as a probate means to orient or exchange information during the still unstudied periods the animals spend above ground. Urine UV properties should be thus examined in mole-rats, as they could give a hint at aboveground activity. To this end, UV absorbance, reflectance and fluorescence should be measured in mole-rat urine according to the standard procedures described in Koivula et al. (1999) and Kellie et al. (2004). Subsequently, a putative spectral

tuning of the shortwave sensitive cone type to the UV-light spectrum should be successively examined, because it has been discussed in Peichl et al. (2004) that the Zambian mole-rat S-opsin may be UV sensitive. This functional shift might be one explanation of the unusual presence of short-wave sensitive opsins in mole-rats. In mammals, ultraviolet vision has been found in e.g. bats (Winter et al. 2003) and in a number of rodents (Jacobs et al. 1991). Though the UV sensitivity of the S-opsin is undoubtedly an ancestral mammalian condition (Hunt et al. 2001), the adaptive meaning in those rodent groups that have retained it, e.g. whether its formation has been driven by the use of territorial urine marks (Chávez et al. 2003), remains an object of discussion.

The wavelengths propagated best, i.e. attenuated least in a tunnel, are green and red, with red being detectable even at 70 cm distance from the light source. Though the amount of detected red light was meagre, it was twice the photon catch in the blue or green range, and well in the area of scotopic vision (see above). Thermal radiation, i.e. infrared radiation, was always detected. This finding did also not, as to the low frequency of long wavelengths, surprise; and it fits also well the findings by Sun et al. (2003), who describe that far-red and near infra-red light might leak out of plant tissue. Here, a second explanation for the blue-light sensitive cone opsin, though a highly speculative one, should be introduced. It is principally imaginable that the blue cones are a kind of infrared-light detector for orientation along longwave radiation within the burrow system. Physically, it would be possible that IR quanta, which are, particularly at low flux rates, difficult to detect for a warm-blooded animal due to thermal contamination, activate photoreceptors in a multi-stage quantal process that would provide the necessary energy for excitation of the cis/trans transfer in the 'blue' visual pigments (K. Götz, personal communication). Another option is the so-called "blue eyes" effect, recently firstly presented at a conference (Kaernbach & Scheibelhofer 2006). The name of the effect is deduced from the blue halos that occur on both sides of a red light spot focused on in a dark room; the authors suggest this effect as being retinal. If both a transfer of this human study to mole-rats and wild speculations are allowed, the rodent could see 'blue', and that is even a symmetrical blue form, by viewing only a single red light spot. By moving the head and perceiving red light from different spatial positions, the shape of the blue halos could then yield information on intensity, direction, and distance of the light source.

In any case, whether mole-rats 'see' the (infra)red light or detect it by another sensory system, it would be advantageous for an animal to recognize an open or collapsed tunnel as soon as possible in order to plug or maintain it. As there are no air currents in an open tunnel (see above), detecting the opening from a distance of already 60 to 70 cm would allow the animal to quickly react and plug the tunnel system. Regarding the red light present in a tunnel, a system sensitive enough to integrate even low photon shares of 0.02% of the total light

income would allow the animal to still react at 30 cm distance from the broken-in tunnel. Within a tunnel system having a main tunnel of 200 m length or more (Hickman 1979), 30 cm is a short distance and would suggest high sensory sensitivity.

»Quelle peut donc être la force physique, partout présente, aussi bien dans les hauteurs de l'atmosphère que dans la profondeur des flots, qui pourra diriger les légions errantes des animaux migrateurs? Il n'en existe, à mon avis, qu'une seule, celle qui nous sert aussi à diriger nos navires sur les mers: je veux dire le magnetisme terrestre.« (*Charles Viguier, 1882*)

B MAGNETORECEPTION

1 INTRODUCTION

1.1 Magnetoreception in Animals

Magnetoreception is the ability to sense/perceive magnetic cues (intensity and/or the orientation of the local geomagnetic field) and transfer them to the nervous system, which extracts, processes, and interprets the relevant information. This information derives from electrical currents evoked by the Earth's core and mantle rotating against each other and creating a magnetic field (cf., Press & Siever 2003). These currents provide relatively constant and reliable information for orientation because they are always available and uninfluenced by external factors such as a swiftly shifting cloud cover. In contrast to other compass mechanisms, such as the star and sun compass, orientation using the magnetic compass is an innate mechanism (shown for warblers in Wiltschko & Gwinner 1974), corresponding to the reliability of the Earth's magnetic field's information, whose use does not require circadian or seasonal movements of an external reference. It seems thus clear to view the magnetic compass as a particularly useful system for the immediate realization of innate nominal directions and for the calibration of other innate systems.

Animals from a number of groups have been described as possessing and orienting with a magnetic compass during navigation (cf., Kirschvink et al. 1985, Wiltschko & Wiltschko 1995). At least in the diverse vertebrate groups, the magnetic compass does not, however, present a uniform system. While birds (Wiltschko & Wiltschko 1972, 1995) and sea turtles (Lohmann & Lohmann 1992; Light et al. 1993) magnetically orient via a so-called inclination compass, fish (Quinn et al. 1981) and subterranean rodents (Marhold et al. 1997a) use a polarity compass (for further information on the compass types, see B1.5). Amphibians seem to use both systems in parallel (Phillips 1986).

Despite Aristotle's observations of regular pre-winterly bird migrations, and despite the strong evidence from the 19th century that migratory birds use components of the

magnetic field as putative orientation factors (Middendorf 1859[1], Viguier 1882), it was not until the 1960s that magnetic compass orientation could be demonstrated in a bird (Wiltschko & Merkel 1966). The first mammal shown to have a magnetic compass was, as mentioned above (III.3), the Zambian Ansell's mole-rat (*Fukomys anselli*) (Burda et al. 1990b). This rodent species still plays the lead when it comes to a refined and continuously expanded knowledge of the magnetic compass sense in rodents.

As in the monotonous world underground, the Earth's magnetic field provides a reliable source of directional, and perhaps also positional, information, this compass mechanism is not a surprising finding in a subterranean mammal, as the Earth derived information helps an animal, in absence of other stimuli, to navigate effectively, i.e. to determine where it is, where it wants to go and how to get there.

Magnetotaxis and alignment behaviour exist in diverse taxa from bacteria to honeybees, and navigation based on magnetic information occurs, amongst others, in lobsters and molluscs (Kirschvink & Gould 1981; Cain et al. 2005).

In terrestrial vertebrates, magnetoreception has been unambiguously demonstrated in sharks, salmonids, newts, turtles and migratory and homing birds (reviewed in Wiltschko & Wiltschko 1995; Lohmann & Johnsen 2000; Meyer et al. 2005). Recently, the bat could be added to the list of mammals that use magnetoreception, showing to use a sunset-calibrated magnetic compass for long-distance navigation (Holland et al. 2006). Furthermore, several rodent species have been proposed to use the magnetic field for compass orientation or responses to gradients or to temporal variations (Wiltschko & Wiltschko 1995), but a magnetic compass sense has been demonstrated unambiguously in only two subterraneous species: the African Ansell's mole-rat *F. anselli* (Burda et al. 1990b, Marhold et al. 1997a,b) and the blind mole-rat (*Spalax ehrenbergi* superspecies) from Israel (Burda et al. 1991; Kimchi & Terkel 1999, 2001; Kimchi et al. 2004). Magnetoreception has also been demonstrated in two epigeic species: the Djungarian hamster (*Phodopus sungorus*) (Deutschlander et al. 2003) and the laboratory mouse (Muheim et al. 2006). Earlier studies of magnetic orientation in rodents provided ambiguous and in some cases questionable results (Mather & Baker 1981; Madden & Phillips 1987; Sauvé 1988; August et al. 1989).

[1] »[...], so liegt der Gedanke nahe, es möge die erstaunliche Unbeirrbarkeit der Zugvögel – trotz Wind und Wetter, trotz Nacht und Nebel – eben darauf beruhen, dass das Geflügel immerwährend der Richtung des Magnetpoles sich bewusst ist, und demzufolge auch seine Zugrichtung genau einzuhalten weiss. […] Gleich dem Schiffer, der seinen Kurs in die Karte einträgt so oft er die Rumbe seiner Richtschnur, der Magnetnadel, wechselt, ist auch der Vogel unablässig sich dessen bewusst, wann und wie viel er abweicht […]. Während aber der Schiffer, bei der Eintragung seiner Kurse, noch die jedesmalige Deklinationsgrösse der Magnetnadel von den Meridianen seiner Seekarten in Abrechnung zu bringen hat, liest sich der Vogel die Grösse des Abweichungswinkels u n m i t t e l b a r ab […].« (Middendorf, 1859)

1.2 The Earth's Magnetic Field

At the end of the 16th century, William Gilbert determined that the Earth is a big magnet, implying that it has a magnetic field (cf., Lanza & Meloni 2006). The Earth's magnetic field (fig. B1) is a dipole field, i.e. a system comprising two magnetic charges (or masses) of equal intensity and opposite signs (cf., Skiles 1985; Lanza & Meloni 2006). These magnetic field's measurements are based on superimposed contributions from different sources.

Corresponding to these different origins, the Earth's magnetic field of force can be separated into: the *main field*, generated in the fluid core by a geodynamo mechanism; the *crustal field*, generated by magnetized rocks in the Earth's crust; the *external field*, generated by electric currents flowing in both ionosphere and magnetosphere through interactions of the solar electromagnetic radiation and the solar wind with the Earth's magnetic field; and the *magnetic field* resulting from an electromagnetic induction process generated by electric currents induced in the crust and the upper mantle by external magnetic field time variations – the Earth is partly an electric conductor, and currents can be induced in its conducting parts by external time variations. The most stable parts of the Earth's magnetic field are the *main* and the *crustal* field, which mainly determine its spatial structure. The field is also subject to time variations. These can be divided into long-term variation due to changes within the Earth, and short-term variation of external origin (see *external field* above) (cf., Lanza & Meloni 2006). The Earth's magnetic field behaves like a small, very strong bar magnet close to the Earth's centre that is tilted against the rotation axis by about 11° (cf., Press & Siever 2003).

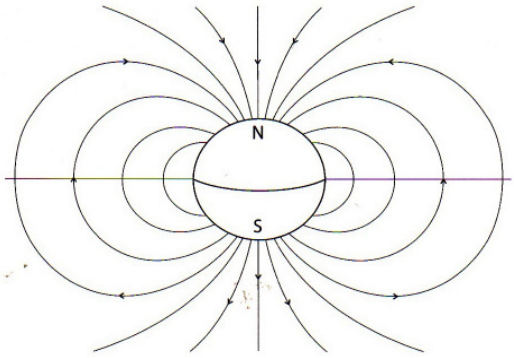

Fig. B1 Schematical view of the Earth's magnetic field lines. The Earth is represented by a sphere, N and S are the ideal magnetic pole positions (from Lanza & Meloni 2006).

Determining exact geomagnetic coordinates, i.e. identifying exact positions of points on the Earth's surface with respect to a geomagnetic reference (similar to geographic coordinates), is enabled by use of colatitudes and longitudes in the geomagnetic dipole frame. This coordinate system also enables the identification of north and south geomagnetic poles as those points on the Earth where the ideal central dipole axis intersects the surface. Accordingly, the geomagnetic equator is the ideal line on the surface representing the intersection of the plane passing through the Earth's centre orthogonal to the central dipole (Lanza & Meloni 2006).

The Earth's magnetic field's strength is given by the intensity (expressed in μT). At the magnetic poles, the total intensity of the natural magnetic field is strongest with more than 60 μT; it decreases down to values of about 30 μT at the magnetic equator, and reaches its minimum with 26 μT at the eastern South American coast. Total intensity depends on the sun's position and this dependency comes with circadian and seasonal changes in a scale from 10 to 30 nT. Magnetic topography is also determined by the presence of underground ore deposits, which can lead to local anomalies that gradually change the magnetic field in addition to its globally asymmetric character. Furthermore, magnetic storms with strengths of up to 500 nT can produce marked changes of the Earth's magnetic parameters (cf., Press & Siever 2003; Lanza & Meloni 2006).

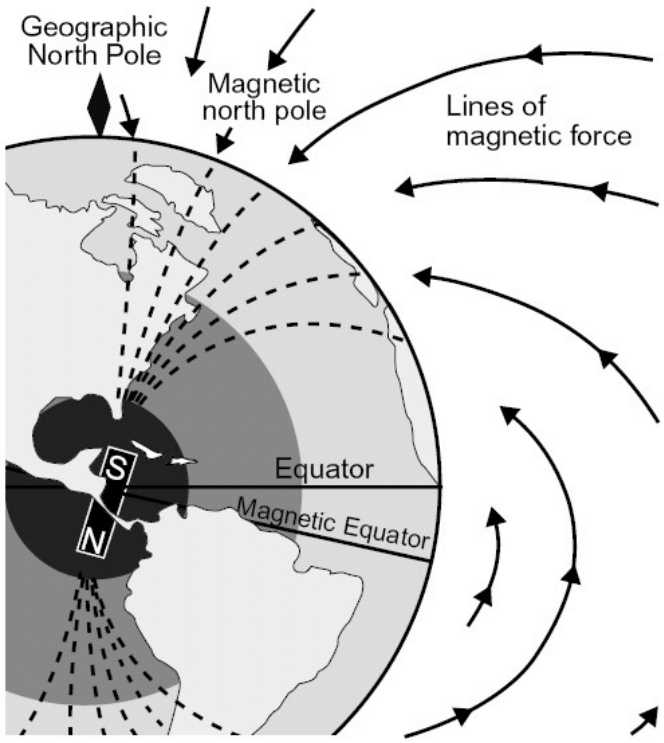

Fig. B2 The schematical Earth's magnetic field. The main field of the Earth is produced in the core and contains both dipole and non-dipole components. The field evoked by the magnetic dipole in the core as represented by the bar magnet is shown by field lines of magnetic forces. These lines demonstrate the course of intensity and inclination between the magnetic equator and the magnetic poles (from Walker et al. 2002).

The magnetic streamlines resulting from the magnetic properties of the electrical currents extrude at the southern geographic pole (equalling the northern geomagnetic pole) and run in concentric circles to the northern geographic pole (the southern geomagnetic pole), where they dive again into the globe (fig. B2). The Earth's magnetic field is thus built up as a

vector field, whose detailed properties as well as its spatial and temporal variations are extensively discussed in Skiles (1985) and Lanza & Meloni (2006).

1.3 Using the Earth's Magnetic Field

Moving through the Earth's magnetic field, an animal induces an electric field across its body. This field is oriented perpendicular to the plane containing the direction of movement and the magnetic field. Its strength is maximal when the animal moves perpendicular to the magnetic field. The moving animal could principally thus relocate its direction until its self-generated electric field is both of appropriate direction and strength (cf., Dusenbery 1992).

Both the regular and gradual magnetic parameters of the Earth's magnetic field can be used by animals to orient. To this end, two types of information are supplied: the magnetic field vector (*F*) provides directional information that can be used as a compass, while total intensity and/or inclination (see below) give information that supports position determination on a magnetic map. For compass orientation, three components of the Earth's magnetic field are of importance. An individual can obtain differential information either from the spatially varying gradients of intensity of the magnetic field or inclination (i.e. the angle between the magnetic field vector and the horizontal plane, see below), or from directional cues provided by horizontal polarity (i.e. direction of the magnetic field lines pointing towards magnetic North, as visualised by a compass needle). Additionally, geological formations may disturb the local magnetic field and serve as characteristic magnetic landmarks (Dusenbery 1992).

The functional mechanism of the magnetic compass, e.g. in birds, is not, however, in contrast to the technical compass, based on the magnetic field's polarity, but on its inclination: the streamlines that leave the Earth at the northern geomagnetic pole in the southern hemisphere and reenter the globe in the northern hemisphere at the southern geomagnetic pole form inclination angles, which alter systematically with geographical width. These inclination angles amount to 90° at the poles and 0° at the equator. By perceiving the streamlines and using these angles, an animal can perceive the course of the magnetic axis. The angles supply the animal with information on the direction the animal is heading, i.e. polewards or equatorwards. That means that e.g. migrating birds interpret the inclination angles and their course for orientation; this system is thus called an inclination compass (Wiltschko & Wiltschko 1972, 1995; Wiltschko et al. 1993). With this compass, birds do not discriminate between "North" and "South", but receive information on the "poleward" and "equatorward" direction, respective to the magnetic poles and the magnetic equator. Birds from the northern and southern hemisphere thus possess the same "migration programme" enticing them to migrate "equatorwards" in their respective autumn (Wiltschko et al. 1993).

Combining the information on the locally varying gradients in inclination and magnetic field intensity, an animal can determine magnetic coordinates of any particular location within a given corridor. Although total intensity and/or inclination may provide positional (map) information, it is the magnetic vector that provides the necessary directional (compass) information (see above; reviewed in e.g. Wiltschko & Wiltschko 1995, 2005, 2006; Bingman & Cheng 2005; Lohmann & Lohmann 2006; Phillips et al. 2006).

1.4 From Earth to Animal: Available Sensory Information

About 50 billion migratory birds travel yearly with single migrating distances of up to 15,000 km (cf., Berthold 1990). Female sea turtles swim hundreds to thousands of km through the Atlantic Ocean to reach their natal beach for nesting. To this end, magnetic information becomes important once they are in the open sea (Lohmann & Lohmann 1996). Subterranean rodents orient successfully in a lightless underground habitat. In air, water and soil, animals use the Earth's magnetic field for deriving location and direction information (Wiltschko & Wiltschko 1995). However, the sensory mechanisms underlying these compass orientation achievements have, until today, largely remained unclear.

To understand the magnetic sense's mechanisms better, three main questions need to be answered: (1) is there a "magnetic sense organ"?, and if so, what kind of structure does it possess, where is it localized, and how is it innervated?; (2) which primary processes underlie the reception of magnetic information?; and (3) which brain structures underlie the processing of the magnetic information?

Dealing with the first question, these structures or receptors could be a relatively simple, easy-to-locate magnetic sense organ, such as the functionally converted electroreceptors in sharks or rays (Kalmijn 1978), but in other animal groups, such a simply structured organ is apparently absent.

The second question regarding the receptor or sensor level, however, seems more promising in terms of research results in diverse taxa. Two primary processes transducing magnetic information are currently mainly discussed. Firstly, processes that depend on permanently magnetic particles of biogenic magnetite, secondly reactions that are triggered or controlled by activated photopigments in the retina (Leask 1977; Yorke 1979; Kirschvink & Gould 1981; Kirschvink et al. 1985; Schulten & Windemuth 1986). These processes and respective recent findings are described in detail in chapter B1.6.

The last question is consecutively addressed in chapters B1.7, B2. and B3.4.

1.5 From Behavioural Experiment to Proof: Compass Modes

Compared to the hitherto studied birds with their light-dependent inclination compass (cf., Wiltschko & Wiltschko 1995), which can be – at least in homing pigeons - switched off or on if the alternative sun compass is disrupted under overcast skies (Keeton 1971), subterranean rodents have only limited access to photic cues. Consequently, the magnetic compass of Ansell's mole-rats has proved to be light-independent, and based on exploiting the magnetic field's polarity, thus behaving like a technical compass (Burda et al. 1990b, Marhold et al. 1997a).

Studying a putative magnetic compass, the researcher receives confirmation from animals' responses to artificial shifts of magnetic North with respective predictable directional changes. Classical experiments make use of homing orientation (reviewed in e.g. Wiltschko & Wiltschko 1995). Whereas plenty of evidence exists for homing abilities in animals of diverse taxa, this experimental approach poses severe limits when examining magnetic compass orientation: homing is realized over longer distances; negative results need to be considered in a motivational context; and being a complex multifactor task, homing can hardly provide evidence for the exclusive use of a particular orientation mechanism. Experimental refinement of this method, practicable in smaller organisms also under laboratory conditions, is based on "simulated magnetic displacements", i.e. when the animal is exposed to a defined artificial magnetic field characterizing the opposite side of its "home", when corresponding changes in the direction of its homing orientation are expected (cf., Fischer et al. 2001; Phillips et al. 2002; Boles & Lohmann 2003). At least males of seasonally breeding solitary subterranean mammals, which seek mates over longer distances (e.g. the silvery mole-rat, *Heliophobius argenteocinereus*; Šumbera et al. 2007), show good orientation abilities presumably based on a magnetic compass. Homing abilities have been demonstrated also in other diverse species of subterranean mammals (cf., Burda et al. 1990a). Nevertheless, examining the proximate mechanisms of homing would be technically very difficult both in the field and in the laboratory, for instance because of the limited availability of animals and probably seasonally limited motivation.

Spontaneous behaviour, specifically innate preference for a certain direction displayed by a migratory direction or positioning of a nest, is an experimental asset. The magnetic orientation assay for rodents, first applied in Ansell's mole-rats (Burda et al. 1990b), is simple: mole-rats are placed in a circular arena with scattered nesting material and food items. In an undisturbed geomagnetic field (in the given case characterized by 66° inclination and 46 μT), the mole-rats preferably place their nest in the south-eastern sector of the arena. Magnetic intensity and polarity in the arena can be manipulated by a pair of Helmholtz coils, by e.g.

shifting magnetic north by a specified angle. The mole-rats place their nests according to the altered magnetic field and relative to their southern magnetic preference direction. This experimental design, which in some studies has been modified to a radial 8-arm-maze with terminal nest boxes, has proven useful for demonstrating magnetic compass orientation, also in the blind mole-rat (Burda et al. 1991; Kimchi & Terkel 2001) and in the Djungarian hamster (Deutschlander et al. 2003).

A modified arena-assay to test whether animals use magnetic cues for orientation when digging in order to hide or escape failed in South American tuco-tucos (*Ctenomys talarum*) (Schleich & Antinuchi 2004) and coruros (*Spalacopus cyanus*) (Begall unpubl.). These results, however, do not conclusively exclude the presence of a magnetic compass in these animals, as it is possible that they do not rely on the magnetic compass in stressful situations. Standard nest-building experiments proved unfeasible in coruros, because no nest was built in most of the trials (82%).

A constructive and innovative modification of this experimental arena design involves learning: the nest position in an arena is imposed upon the animals by using a fixed nest-box, and it is then tested whether the animals locate their nest place or nest box according to the previously learned relationship to the magnetic field, when they are released into a new (clean) arena and/or after the magnetic field has been manipulated. In this way, magnetic compass orientation has been shown in the Djungarian hamster (Deutschlander et al. 2003) and in the laboratory mouse (Muheim et al. 2006). This experimental paradigm certainly harbours a lot of potential, also in the study of spatial orientation in subterranean mammals.

Maze experiments have rarely been applied in the study of magnetic orientation of subterranean rodents. At least Ansell's mole-rats behave in a maze differently than e.g. laboratory rats (Burda, own unpubl. observ.). They learn a maze after the first run, but start to make "false errors", driven by exploration, in later runs. Furthermore, explorative behaviour or xenophobia may be species and gender specific, making the evaluation of maze experiments a more complex task (Heth et al. 1987; Burda, own unpubl. observ.). Nevertheless, in the blind mole-rat, magnetic cues also play a role in maze navigation and path integration (Kimchi et al. 2004).

Indications for magnetic compass orientation may also be derived from field observations. Subterranean mammals in natural habitats with poor food supply tend to build linearly arranged burrow systems with a long, straight main tunnel, the so-called runway, and a nest frequently positioned rather eccentrically with respect to the longest axis of the burrow system (cf., Eloff 1951; Heth et al. 2002 and literature cited therein). It can be speculated that in a uniform habitat, without geomorphologic and other features, such as water streams, slopes, rocks, roads, trees, fields or neighbours, that might potentially canalise burrowing

direction, animals may project their spontaneous directional preference into a predictable orientation of the burrow system. Indeed, the first hints for possible magnetic compass orientation in the Ansell's mole-rat (Burda 1987) were derived from a few then available maps of burrow systems, which exhibited - apparently incidentally - a north-south orientation of their longest axis. Lovegrove et al. (1992) and Schleich & Antinuchi (2004) could not confirm any prevailing directionality of burrows in *Fukomys damarensis* and *Ctenomys talarum*, respectively. Apart from the fact that these studies did not include circular statistics as a method to assess the orientation, the random or directional patterns observed may have been due to the problem that apparently established old systems were examined, where the original primary tunnel might not have been recognizable anymore (or perhaps even no more existent). Burrow systems are not static, but are steadily reworked and rearranged (cf., Šumbera et al. 2003).

Consistent with the subterranean lifestyle, the magnetic compass of Ansell's mole-rats has been specified as a light-independent polarity compass, as neither light nor artificial shifts of inclination affected the preferred south-eastern nesting direction (Marhold et al. 1997a). Similarly, the magnetic compass of the blind mole-rat is light-independent (Kimchi & Terkel 2001) and, although this point has not been addressed explicitly, it is highly probable that its compass is also polarity-based.

The directional positioning of nests in mole-rats may express alignment behaviour towards the magnetic field's polarity and *per se* does not prove that the animals use the magnetic compass also in navigation. However, the findings that the blind mole-rat uses magnetic cues as a stable, external reference (comparable to visual cues in sighted mammals) for orientation within complex maze systems (Kimchi et al. 2004) as well as recent neuroanatomical findings (described below) indicate that the magnetic compass of mole-rats is involved in both path integration and navigation.

1.6 From Signal to Sensor: Transduction Mechanisms

An extensive body of evidence demonstrates that two starkly different magnetoreceptive mechanisms have evolved in terrestrial vertebrates: (1) a light-dependent mechanism involving a photo-induced radical pair reaction occurring in a specialized photoreceptor (the so-called Radical-Pair Mechanism (RPM), and (2) a light-independent mechanism involving particles of biogenic magnetite (reviewed in e.g. Kirschvink et al. 2001; Ritz et al. 2002; Johnsen & Lohmann 2005; Wiltschko & Wiltschko 2005, 2006). Note, however, that despite the behavioural evidence for these two systems, the primary receptors have not yet been identified in any animal with certainty. It should also be noted, that evidently these two distinct

magnetoreceptive systems occur complementarily in newts and birds: apparently, these animals use the light-dependent radical-pair mechanism to derive compass information, and a light-independent magnetite-based mechanism to derive map information (cf., Phillips 1986, Phillips et al. 2002; Munro et al. 1997a, b; Brassart et al. 1999).

1.6.1 Magnetoperception via Biochemical Processes

The radical pair-model (RPM) assumes resonance phenomena of excited photopigments in the optic system and explains the transduction process of magnetoreception by the biochemical transfer of macromolecules to energetically higher states. It has been firstly suggested by Leask (1977, 1978) and then extended and complemented by Schulten & Windemuth (1986) and Ritz et al. (2000). The model assumes that magnetoperception is based on biochemical processes, in which macromolecules of the visual system (e.g. rhodopsin or iodopsin) react in an excited triplet-state dependent on their relative position to the magnetic field's direction. Special receptor structures on the retina are specifically stimulated. All radical pair hypotheses assume that a photopigment is transferred into an excited state via acceptance of a photon. Magnetoreception, in these models, is thus a light-dependent system.

Leask (1977, 1978), in his "optical pumping model", presumes a resonance effect between oscillations of the respective triplet condition of a molecule from the optic system and the oscillation of the surrounding magnetic field. The optical pumping, a by-product of the normal visual process, would explain the non-polar reactions to the Earth's magnetic field.

The newer models by Schulten & Windemuth (1986) and Ritz et al. (2000) resemble Leask's, but they assume a bi-radical reaction, that interacts with the surrounding magnetic field. By acceptance of a photon, specialized photopigments are excited and form singlet radical pairs with an unpaired electron. By singlet-triplet interconversion, excited singlet pairs in antiparallel spin are transferred into excited triplet pairs in parallel spin. The Earth's magnetic field influences the dynamics of this conversion between antiparallel and parallel spin. The triplet gain depends on the strength of the external magnetic field as well as on the orientation of the involved macromolecules towards the Earth's magnetic field (fig. B3). As singlet and triplet products possess different chemical characteristics, magnetic compass information can be derived through the comparison of differing triplet gains in diverse spatial directions. This mechanism, however, presupposes that respective receptors are fixed spherically in a specific order.

Leask (1977), Schulten & Windemuth (1986), and Ritz et al. (2000) suggested the retinal photoreceptors as the *locus* of magnetoreception because of their spherical arrangement. Here, a specific excitation pattern could result from the magnetic field's directions, out of

which the animal (here: the bird) could then deduce the magnetic field's axial direction (Ritz et al. 2000). In accordance with this hypothesis, there are electrophysiological studies showing that neurons in certain areas of the avian visual system, namely in the nuclei of basal roots of the optic nerves (nBOR) and in the optic tectum, respond to directional changes of the magnetic field (Semm et al. 1984; Semm & Demaine 1986; Beason & Semm 1987). These results were only achieved under light conditions and with complete retinas. It thus appears likely that photoreceptors in the avian eye simultaneously serve as magnetoreceptors, and that nBOR and the optic tectum, being identified as visually specific to directions, may be the information suppliers of the magnetic field's direction.

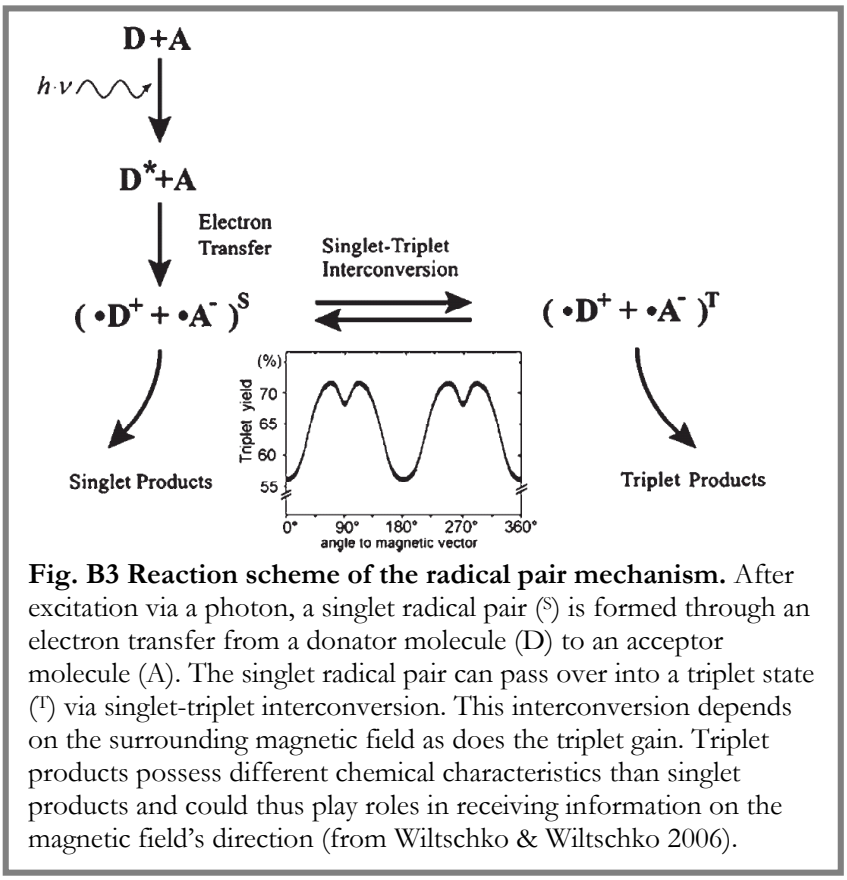

Fig. B3 Reaction scheme of the radical pair mechanism. After excitation via a photon, a singlet radical pair (^{S}) is formed through an electron transfer from a donator molecule (D) to an acceptor molecule (A). The singlet radical pair can pass over into a triplet state (^{T}) via singlet-triplet interconversion. This interconversion depends on the surrounding magnetic field as does the triplet gain. Triplet products possess different chemical characteristics than singlet products and could thus play roles in receiving information on the magnetic field's direction (from Wiltschko & Wiltschko 2006).

Consistent with this model, both compass orientation of birds and newts depend on wavelength and/or light intensity (Phillips & Borland 1992a, b, c; Wiltschko & Wiltschko 2002).

While in newts, the putative receptors are located in the pineal organ (Deutschlander et al. 1999a, b; Phillips et al. 2001), the decisive magnetoreception processes in birds take place in the eye (Wiltschko et al. 2002, 2003). Interestingly, they seem to be restricted to the right eye (Wiltschko et al. 2002), with this strong lateralization already being demonstrable at the receptor level (Möller 2006). Also, recent studies strongly support the RPM-model, showing a

disruption of magnetic orientation by weak, oscillating radio frequency fields in the MHz-range; these affect energy states in radical pair systems (Ritz et al. 2004; Thalau et al. 2005). Despite these results, ethological studies on a putative wavelength dependency of magnetic orientation speak against an involvement of the normal visual pigments in the avian retina (Wiltschko & Wiltschko 2001, 2002). Because of these obvious contradictions, other photopigments are currently discussed as transduction candidates in radical pair based magnetoreception such as cryptochromes (Ritz et al. 2000), a recently discovered class of photoactive flavoproteins. These pigments have been mainly connected with the regulation of circadian rhythms and have meanwhile been demonstrated in diverse plant and animal species (reviewed in Cashmore et al. 1999; Sancar 2003). In magnetoreception, cryptochromes are of special interest, as they possess chemical characteristics that could be functionally crucial for the radical pair model. Firstly, they can, in contrast to opsins, form radical pairs (Giovani et al. 2003); secondly, they absorb light in the shortwave area of the spectrum (Sancar 1994), under which migrating birds orient towards their ancestral migrating direction. Thirdly, since cryptochrome could be demonstrated in the mouse retina (Miyamoto & Sancar 1998), it has also been found in two other vertebrate retinas (Zhu & Green 2001; Bailey et al. 2002; Haque et al. 2002). All here mentioned characteristics support possible involvement of cryptochrome as the supplier of directional information for the magnetic compass, and indeed, cryptochromes may act as the magnetoreceptor molecules in birds, possibly with the highly ordered and constantly directed opsins as potential, spherically fixed, and spatially neighbouring interaction partners (Möller 2006; Möller et al. 2004; Mouritsen et al. 2004).

1.6.2 Magnetoreception via Magnetite

The introduced cryptochrome molecules putatively underlying the RPM obviously work together with the wavelength-dependent avian compass (cf., Möller et al. 2004) and hence represent an unsuitable mechanism for e.g. subterranean rodents living in a photon-deprived ecotope. Light-independent magnetoreception thus supposedly implicates magnetite particles (cf., Kirschvink & Gould 1981; Shcherbakov & Winklhofer 1999; Kirschvink et al. 2001; Davila et al. 2003) as the more likely responsible signal mediator in subterranean mole-rats. The receptor derives its signal transduction from ferromagnetic particles embedded in highly innervated tissue. Ferromagnetism denominates the state of a substance, whose spin moments are all mutually parallel and concordant and impart a total magnetic moment to the domain, i.e. to the link between the atom and the crystal state that is defined by the atoms and the resulting crystal size and shape. In contrast to e.g. a compass needle always pointing north, a ferromagnetic grain harbours many magnetic moments interfering with each other, leading to

an increased magnetization intensity *J* (cf., Lanza & Meloni 2006; for ferromagnetism in a rock see fig. B4).

In the magnetite hypothesis, primary processes are assumed to be based on small particles of magnetite. These magnetite particles are thought to orient like a compass needle corresponding to the magnetic field and thus transfer information to the sensory apparatus. For several decades, ferrous oxide (Fe_3O_4) has been regarded a possible basis for magnetic compass orientation in diverse species (Walcott et al. 1979; Presti & Pettigrew 1980; Kirschvink & Gould 1981; Kirschvink et al. 2001; Winklhofer et al. 2001; Fleissner et al. 2003). This magnetite theory was originally suggested by Lowenstam (1962), who discovered that the teeth of a primitive mollusc were capped with magnetite. But it was probably the Greeks who first reflected upon the wondrous properties of magnetite, the magnetic iron ore $FeO\text{-}Fe_2O_3$ and famed lodestone ("leading stone"). The lodestone appears in Greek writings by the year 800BC (cf., Mattis 1965). For more historical information and interesting details on magnetic characteristics, please see the "Technorama Forum Lecture" by P. Doherty, given in extracts in Appendix AI.

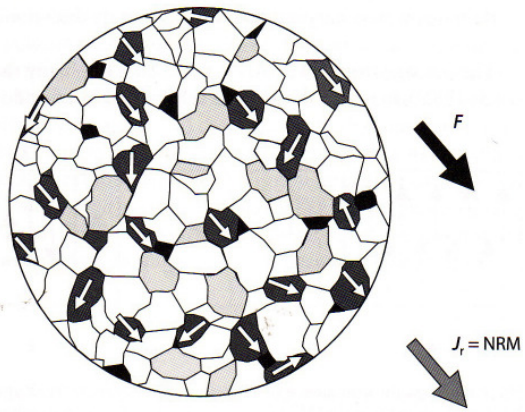

Fig. B4 Ferromagnetic grains in a rock. The grains acquire their spontaneous magnetization J_i according to the easy directions of the Earth's magnetic field, the magnetic field vector *F*. This domain magnetization J_i tends to remain in the original direction, i.e. in the easy direction corresponding to the minimum value of magnetostatic energy. It is however, by the torque of an external magnetic field (*H*), also aligned into its direction. The two directions correspond to two energy states, separated by a barrier. When *H* is strong enough, the barrier is overcome, and the domain's spontaneous magnetization is recreated in the field's direction. This resulting magnetization J_r is the natural remanent magnetization (NRM) (from Lanza & Meloni 2006).

In contrast to the octahedral magnetite crystals found naturally in rocks, biogenic magnetite is always hexagonal and extremely uniform in size and shape. Magnetite's membrane-bound nature rules out the possibility of other than biological origin, because magnetite cannot cross cell membranes (Kirschvink 1983; Credle 1988).

Unlike any other biogenic material, the very dense magnetite is both ferromagnetic and an electrical conductor. As a metallic iron oxide, it has by far the highest electrical conductivity of any known biogenic solid. Its conductivity is roughly 6000 times better than that of the axoplasm in squid neurons and results from electrons hopping between Fe^{2+} and Fe^{3+} ions occupying adjacent gaps in its lattice; this property makes it an excellent transmitter of sensory information (Kirschvink 1983). When of the proper size and shape, magnetite couples

strongly with magnetic fields, producing interaction energies in the order of kT (Kirschvink & Gould 1981). With such a material, a wide variety of magnetoreceptors are theoretically possible in which magnetic fields exert mechanical forces. Magnetite crystals coupled to secondary receptor cells such as muscle stretch receptors (see below) may convert magnetic information into electrical signals, and this signal pattern might then change with the magnetic direction or gradients that the animal faces. In principle, the crystals act as permanently magnetised bar magnets twisting into alignment with the Earth's magnetic field if allowed to rotate freely (Lohmann & Johnsen 2000). Though this magnetotaxis has formerly not been considered sensitive enough to account for the detection of the extremely weak fluctuations of the geomagnetic field (Yorke 1979), the findings of innervated magnetite crystals for instance in the neck musculature and beak tissue of homing and migratory birds (Presti & Pettigrew 1980, Fleissner et al. 2003) show that the sensitivity of the respective particles might well be high enough to at least serve as a donator of reference information. Secondly, magnetite-based receptors might be much more sensitive to changes in field intensity than are chemical reception mechanisms, and the receptors' character might differ between compass types and within their sensitive correspondence to diverse magnetic features (Lohmann & Johnsen 2000).

It has, however, proved difficult to resolve magnetite microscopically. Also, iron oxides are common environmental and histological contaminants. They can also occur as by-products of diverse degenerative biological processes (Johnsen & Lohmann 2005). Fixatives with lower pH also dissolve magnetite (G. Fleissner & H. Burda, personal communication), so that visualization of magnetite crystals within their cellular environment remains a challenging task (Johnsen & Lohmann 2005).

Magnetite follows the molecule ferrihydrite, and it is the iron storage protein ferrin in the molecule's core that has been thought to be responsible for the mineralization of magnetite e.g. in pigeons (Walcott et al. 1979). Yorke (1979) and Kirschvink & Gould (1981) both created hypotheses on how magnetoreceptors based on magnetite particles could work. Magnetite's properties vary directly as a function of its crystal sizes and shapes, resulting in a classification of two basic types of ferromagnetic organelles, described as domains (see above): the single-domain (SD) and the superparamagnetic (SP) particles (Shcherbakhov & Winklhofer 1999). Principally, domains are divided into SD and multi-domain (MD). The transgression from SD to MD occurs when the internal magnetostatic energy E_m of a ferromagnetic grain, proportional to the grain's volume, increases until E_m can be reduced and the grain subdivides into two (or more) parts in which the alignment of the spin moments is anti-parallel (fig. B5), and the total magnetostatic energy is diminished (Lanza & Meloni 2006).

In the case of magnetite, the MD behaviour can be found for particle sizes between 1to10 μm, and the SD behaviour for sizes between 0.03 to1 μm.

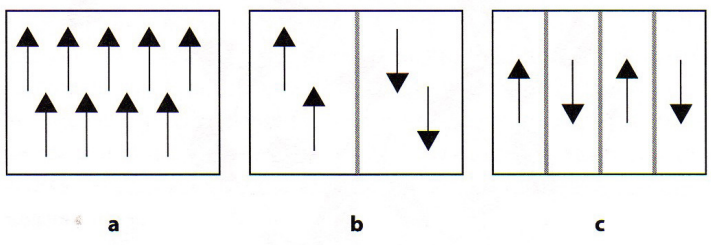

Fig. B5 Magnetic domains. The spin moments in a single domain (SD) grain are parallel (a); in multi-domain (MD) grains (b, c), a certain number of magnetized domains minimize magnetostatic energy. The passage from a SD to a MD grain covers a state with the grains subdivided in a few domains; this state is called pseudo-single domain (PSD) (from Lanza & Meloni 2006).

Ultra-fine grains have a particular behaviour, called superparamagnetic (SP; approximately <0.05μm) (fig. B6; Lanza & Meloni 2006). SD magnetite crystals act as permanently magnetised bar magnets.

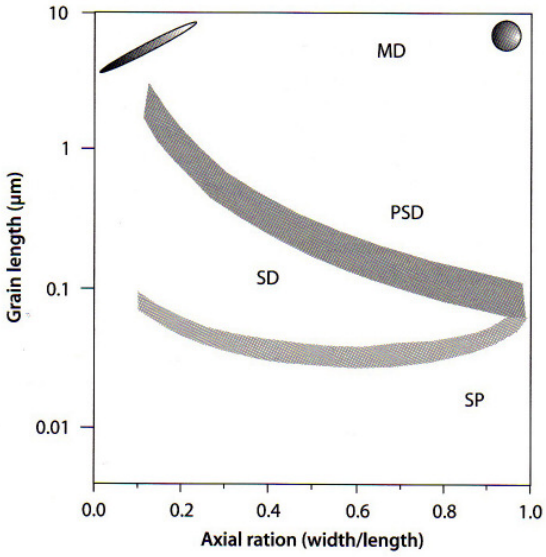

Fig. B6 Magnetite grain sizes and shapes. Ranges in grain sizes and shapes for SP (superparamagnetic), SD (single domain), PSD (pseudo-single domain) and MD (multi-domain) particle behaviour. To the left, acircular grains, to the right, equidimensional grains are shown (from Lanza & Meloni 2006).

Their magnetic orientation remains extremely stable until a magnetic moment occurs that is large enough to twist them passively into alignment with the magnetic field if allowed to rotate freely (fig. B7).

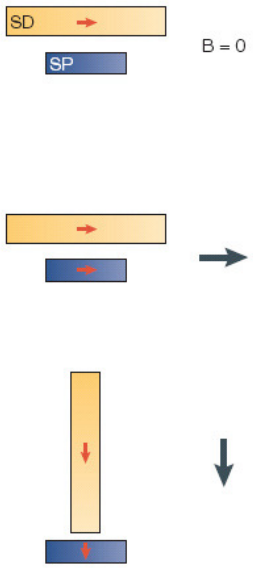

Fig. B7 Properties of magnetic domains. SD crystals show permanent magnetic moments (red arrow) even when an external magnetic field (MF) is absent (B=0); SP crystals do not. If an external MF is present (black arrow), SD crystals align with this field. SP crystals develop a magnetic moment that changes with the external field, with the crystal itself not rotating (from Johnsen & Lohmann 2005).

A chain of SD crystals (as found in the rainbow trout, see below) may exert torque or pressure on secondary receptors such as stretch receptors, hair cells or mechanoreceptors. Alternatively, rotation of intracellular crystals might open ion channels directly, if cytoskeletal filaments connect the crystals to the channels (fig. B8, see next page; Kirschvink et al. 2001). SP magnetite crystals do not have a permanent magnetic moment and so cannot physically rotate into alignment with the Earth's field; in an external field, they nevertheless develop a magnetic moment. The magnetic direction of a particle can change without moving the grain at all, as the grain size is below the critical size for stability (Banerjee & Moskowitz 1985). In an Earth-strength magnetic field, clusters of superparamagnetic particles (as found in the pigeon, see below) can attract or repel one another, depending on the orientation of the external field (Davila et al. 2003). These interactions can deform the matrix (e.g. the cell membrane) in which they are embedded (fig. B9, see next page). Moreover, SP particles often form clusters, whose sizes can be enlarged by the factor 10^8 compared to their constituent particles (Banerjee & Moskowitz 1985); recent simulations and experiments have demonstrated that a group of superparamagnetic clusters self-assembles into a chain-like structure that behaves like a compass needle in an external field (Davila et al. 2003).

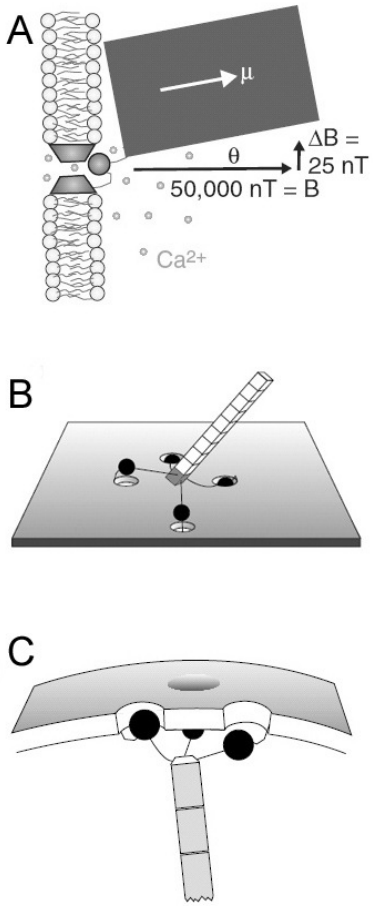

Fig. B8 Possible magnetite-based receptor models for SD crystals. These models are based on mechanical forces of a chain of magnetic SD particles. (A) The grey rectangle represents a magnetic particle chain being anchored to a mechanically activated trans-membrane ion channel through a cytoskeletal filament. The two lower figures show 3D-models of an SD chain linked to mechanically gated ion channels in a receptor cell membrane. In (B), the chain is connected with a pivot (dark grey cube), that is embedded in the cell membrane and connects the chain with the cell membrane via microtubule-like strands (black), while in (C), the magnetite particle row is linked with the membrane directly through microtubule-like strands. In (A), (B) and (C), torque and thus movement from the magnetite chain following changes of the external MF, will cause the chain to pull open one (or more in B, C) ion channel(s), allowing ions to cross and thus lead to depolarization of the receptor cell (after Kirschvink et al. 2001 ; Walker et al. 2002).

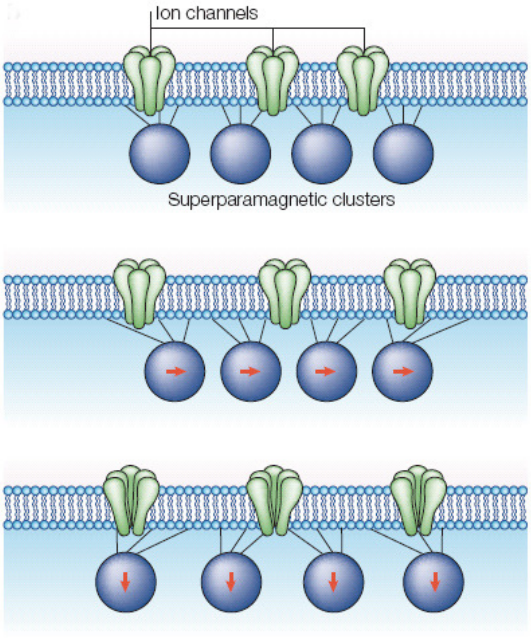

Fig. B9 A possible magnetite-based receptor model for SP crystals. Interacting clusters of superparamagnetic crystals in the membranes of neurons, following the orientation of the external MF, attract or repel each other, deforming the membrane and opening or closing ion channels. With the MF parallel to the cell membrane, e.g., the crystals' internal MFs' alignment (red arrows) attract adjacent clusters like bar magnets being aligned in an end-to-end row (middle). This alignment results in a compression of the membrane and ion channel closure. With the MF perpendicular to the cell mebrane (bottom), the adjacent clusters behave like bar magnets in a side-to-side row, resulting in interactions stretching the membrane and opening ion channels (from Johnsen &Lohmann 2005).

Magnetite particles associated with afferent trigeminal terminals, specifically the ophthalmic nerve branches, have been found in the upper beak tissue of birds (cf., Hanzlik et al. 2000; Williams & Wild 2001; Fleissner et al. 2003), and also within the olfactory lamellae of the rainbow trout (Walker et al. 1997; Diebel et al. 2000). Congruently, impairment experiments involving anaesthesia and bilateral section of the ophthalmic nerve confirmed that this nerve might well be the carrier of magnetic field information to the brain (Beason & Semm 1996; Mora et al. 2004). Electrophysiological recordings (Semm & Beason 1990; Walker et al. 1997) as well as conditioned-choice experiments (Walker et al. 1997; Mora et al. 2004) suggested further that the magnetoreceptors associated with the ophthalmic nerve do not participate in the compass, but instead yield map information. This suggestion arose because the neurons reacted solely to intensity but not direction changes of the magnetic field, for instance shown in recordings of the corresponding nerve of the trout (Walker et al. 1997). In Ansell's mole-rats, our preliminary histological (Burda unpubl.) and experimental behavioural studies (Chapter B2.3) suggest that the cornea, i.e. a paired, highly mechano-sensitive ocular structure innervated by the ophthalmic nerve, may be the seat of magnetite-based receptors (for a vertebrate model of such receptors see fig. B10). In contrast, Cernuda-Cernuda et al. (2003) reported findings of crystalloid bodies in the inner segments of retinal photoreceptors of the Ansell's mole-rat. The authors interpreted these structures as potential magnetite grains, suggesting the retinal photoreceptors as the respective magnetite-based structure.

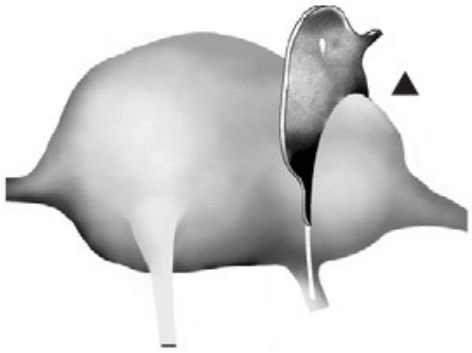

Fig. B10 A possible magnetite-based receptor type. Three-dimensional reconstruction of the putative magnetite-based receptor cell in the trout visualized by confocal microscopy. One single optical slice taken at the level of the magnetite particle chain (arrow) is shown offset from the rest of the receptor to show its placement (Diebel et al. 2000).

Other studies aimed at identifying a magnetite-based receptor, worked with a change of the particle magnetization. In Ansell's mole-rats, exposure to a strong, short magnetic pulse (0.5 T, 5 ms) resulted in an immediate, long-term shift of the preferred nesting direction from South-East (160°) to East (86°) (Marhold et al. 1997b), hinting at a change in magnetic properties of the responsible receptor. In migrating birds, a similar pulse magnetization induced a change of the preferred migrating direction, depending on the applied pulse's direction (Beason et al. 1995). With the ophthalmic nerve anaesthetised, pulsing did not disturb the bird's magnetic migration orientation (Beason & Semm 1986). These results also suggest that birds have magnetite-based receptors that yield information on the magnetic

field's intensity, but not on its direction (e.g. compass information). With help of such information on intensity differences, animals can theoretically build up a „navigation map" over time, to assist in locating their position and searching for known places. The trigeminal character of the directional and not positional magnetic field information has been supported by Němec et al. (2001, 2004).

1.7 From Sensor to Brain: Neuronal Processing

In contrast to the wealth of information on the role that the magnetic sense plays in animal orientation, on its distribution across animal taxa, and on its behavioural characterization, our knowledge of the neural substrate subserving magnetic orientation remains meagre (reviewed in Johnsen & Lohmann 2005; Němec et al. 2005; Wiltschko & Wiltschko 2005): only a few studies have tried to shed light on the neural aspects of magnetoreception in mammals.

Early electrophysiological studies have demonstrated the presence of magneto-responsive units in the pineal organ of the guinea pig (Semm et al. 1980), the laboratory rat (Reuss et al. 1983), and the Mongolian gerbil *Meriones unguiculatus* (Stehle et al. 1988). Magnetic stimulation was reported to affect pineal melatonin synthesis in the laboratory rat (Olcese et al. 1985; Reuss & Olcese 1986; Welker et al. 1983). Interestingly, these effects appeared to be light- and vision-dependent (Olcese et al. 1985, 1988; Reuss & Olcese 1986), indicating the involvement of a photoreceptor-based magnetoreception mechanism.

Another mechanism comprises so-called second messenger signal cascades, on which the stimulation effect is of a longer-acting character. These cascades involve *immediate-early genes* (IEGs; also called *second messengers*), genes expressed rapidly, i.e. within minutes after a stimulus. Thus, they are also called *primary response genes*. IEGs induce many functionally different products. Among others, they encode, very quickly after stimulation[2], the production of 'inducible transcription factors' (ITF; e.g. Jun or Fos)[3]. Subsequently, transcription and/or repression of other genes is controlled by pre-existing transcription factors and results in a change of neuronal response to the subsequent stimuli (Herdegen & Leah 1998)[4]. In this context, the stimulus inducing ITF production does not have to be a 'fixed' event. Also 'disinhibition' or 'negative stimuli', i.e. the absence of the 'positive stimulus' (e.g. deprivation of light), can effectively induce ITFs (Herdegen & Leah 1998). Mapping of the expressed gene

[2] The transcription factors represent "proteins that control the expression of genes, and as such they are the master regulators of every cell's development and functioning." (Herdegen & Leah 1998)
[3] So-called 'proto-oncogenes' denominate mutated IEG-encoded proteins that cause transformation. Transformation can however also result from other IEG-encoded proteins such as JunB and FosB that co-operate with proto-oncogenes (Herdegen & Leah 1998).
[4] The pre-existing transcription factors, that control the onset of IEG-expression quickly after cellular stimulation, can be found e.g. in the nervous system when external stimuli are absent. They are thus called 'constitutive transcription factors' (CTFs).

products yields a timely picture of the actual activity in response to the stimulus. Obviously, transcription factors play roles in both development and functions of the nervous system, and also in its responses to diverse stimuli. In animals, the extent of ITF expression seems related to the importance of the stimulus (Herdegen & Leah 1998). Recently, functional neuroanatomical mapping based on monitoring this stimulus-evoked expression of ITFs has been introduced into magnetoreception research (Němec et al. 2001). This mapping method can be used e.g. to identify neurons specifically activated by magnetic stimuli, and it also offers cellular resolution and the possibility to screen for neuronal activation throughout the central nervous system (reviewed in Němec et al. 2005). Previous experiments performed in Ansell's mole-rats provided evidence for magnetic input to the superior colliculus (Němec et al. 2001). Interestingly, homologous brain regions of birds and mammals seem to be co-opted independently into magnetic information processing: while in birds, magneto-responsive neurons could be identified in superficial layers of the optic tectum receiving a robust visual input (Semm & Demaine 1986), magneto-responsive neurons in mole-rats, on the other hand, were found within the intermediate layers of the superior colliculus dominated by trigeminal input (Němec et al. 2001) - visual input to the superior colliculus is extremely reduced in these rodents (Němec et al. 2004). Since it has been repeatedly demonstrated that magnetite-based magnetoreception is associated with the trigeminal nerve system, the data provided by Němec et al. (2001) indirectly support the hypothesis of a magnetite-based compass mechanism in Ansell's mole-rats.

1.7.1 Immunocytochemical methods

Immunocytochemistry (ICC) is a combination of immunology and microscopy. Its principles are based on visualising gene products expressed under certain conditions or activities, i.e. *antigens* that display neuronal activity (e.g. "c-Fos", the protein expressed by the gene "c-*fos*", the cellular counterpart to the viral gene "*fos*") (Beesley 1993; Herdegen & Leah 1998). These proteins can be marked by appropriate *antibodies* (AB) that bind very specifically to diverse parts of 'their' antigen in the tissue. The reaction can be localised with respect to cell structure by the attachment of a marker to the antigen-antibody complex. This marker is microscopically dense, and thus allows visualisation of the complex distribution across a tissue. ICC is a highly specific and a relatively quick and sensitive routine method. However, to achieve a high signal to background ratio for unambiguous results, several aspects such as the antibody, the marker or the labelling technique need to be considered. The exact antibody choice determines the full range of all other used immunocytochemical reagents, as they depend on one another consecutively (cf., Beesley 1993).

Polyclonal and monoclonal antibodies, each with distinctive characteristics, can be used in ICC. Whereas polyclonal antibody sera comprise a mixture of high affinity antibodies, that are active against different epitopes on the antigen, monoclonal antibodies are pure sera with one of the polyclonal constituents. The antibodies, glycoproteins, derive from the sera of host animals after antigen injections that initiate antibody production in the host's spleen by B lymphocytes and plasma cells; these hosts are, in most cases, rabbit, sheep, or goat (cf., Beesley 1993).

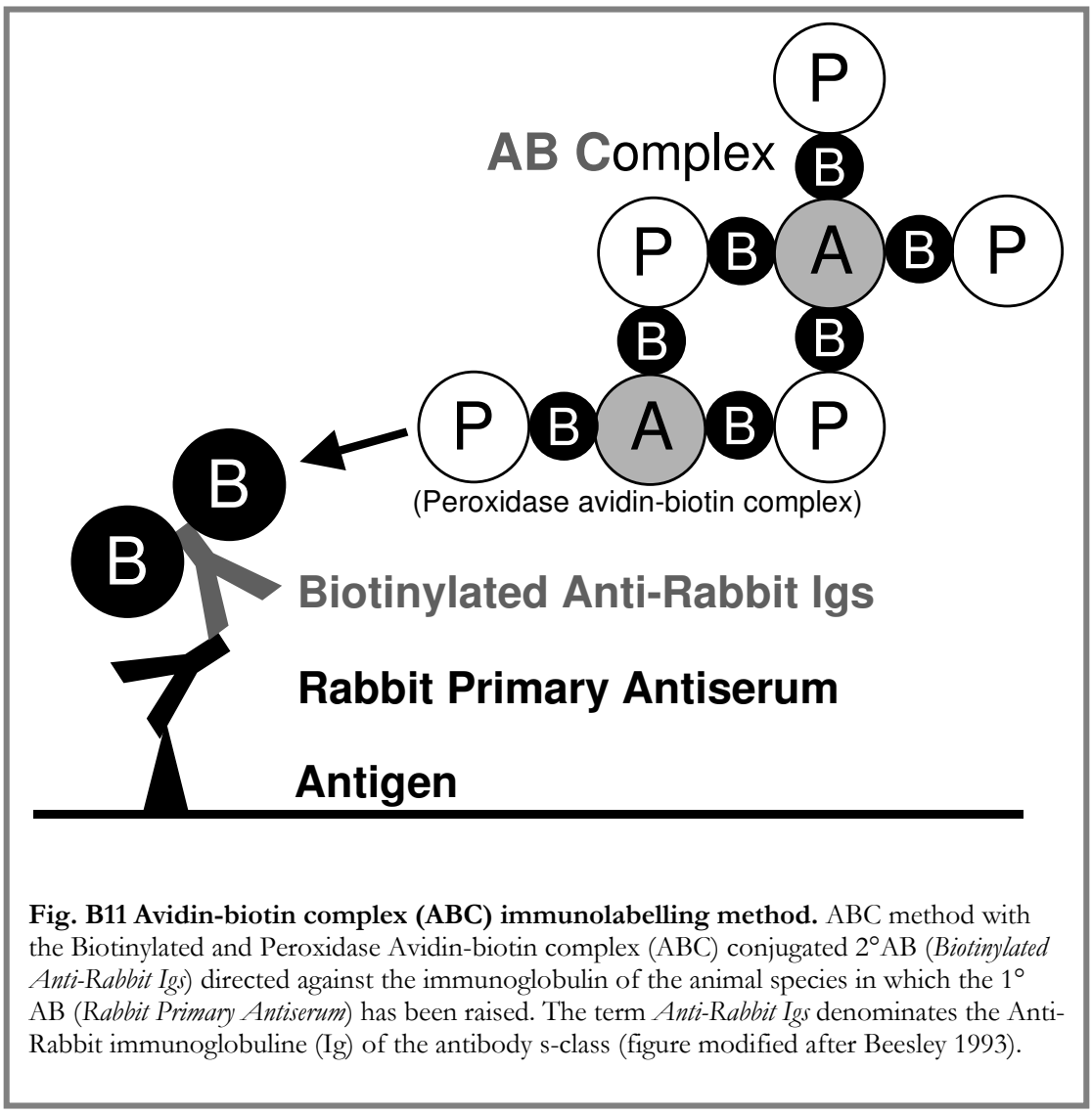

Fig. B11 Avidin-biotin complex (ABC) immunolabelling method. ABC method with the Biotinylated and Peroxidase Avidin-biotin complex (ABC) conjugated 2°AB (*Biotinylated Anti-Rabbit Igs*) directed against the immunoglobulin of the animal species in which the 1° AB (*Rabbit Primary Antiserum*) has been raised. The term *Anti-Rabbit Igs* denominates the Anti-Rabbit immunoglobuline (Ig) of the antibody s-class (figure modified after Beesley 1993).

To localise antigens via antibody marking, several possible immunocytochemical methods can be applied, the choice of which depends on diverse parameters. Here, only the applied Avidin-Biotin method will be introduced in detail (fig. B11). Other techniques (Direct method; Two-step indirect method; Protein A method; Unlabelled antibody methods; or Immunogold methods) can be found in the respective literature (e.g. Beesley 1993). Generally, methods using primary (1°) and secondary (2°) antibodies are based on the premise that the

unlabelled 1° AB is visualised by a labelled 2° AB, that is directed against the immunoglobulin of the animal species the 1°AB derives from (e.g. *rabbit* primary antiserum). The avidin-biotin techniques go a step further: Avidin is a basic glycoprotein with a high affinity for the small water-soluble vitamin biotin. Biotin can be conjugated to various biological molecules, including ABs. As many biotin molecules can be attached to a single molecule of protein, the biotinylated protein can bind to more than one avidin molecule. However, still the colourless chromogen needs to be converted into visible, coloured end products. This job is done by enzyme-substrate reactions, such as the hydrogen peroxide-diaminobenzidene reaction that produces a brown end product insoluble in alcohol, xylene, and other inorganic solvents (cf., Beesley 1993).

1.8 Arising questions

The picture of how animals perceive and process directional information from the Earth's magnetic field is still incomplete, as our knowledge of the associated physiological and neurobiological processes is sketchy. Though initial magnetoreception studies in subterranean rodents hint at the involvement of the superior colliculus (Němec et al. 2001), the largest enigma is connected with the receptor level, because it is still not clear which transduction mechanism (and thus which underlying receptor type) plays roles in this mammalian magnetic orientation system. With the sensory receptor for magnetic information, a coherent process from receptor cell to ethological response could be described and could thus interconnect the state-of-the-art neurobiological with ethological and functional morphological results.

As it is highly probable that there is no general vertebrate "magnetic sense", and as a retinal receptor type has already been described in migrating birds (in detail in Möller 2006), it would be of interest to better describe the respective, maybe differing, receptor type in a mammal, the magnetoreception model species *Fukomys anselli*. Questions relevant to this thesis include: Is the transduction mechanism in mammals the same as in birds, i.e. can biochemical processes be excluded and magnetite be supported, as earlier studies suggest? Where does the transduction mechanism take place, i.e. where are the sensory receptors located in the Zambian mole-rat? Can they be visualized? Is magnetoreception, as in birds, lateralised?

2 MATERIAL AND METHODS

2.1 Study Animals

The test animals for all studies in this part (B) were wild captured Zambian mole-rats or their captivity-born offspring derived from the breeding stock at the Department of General Zoology, University of Duisburg-Essen (see also Chapter A2.1). The tested adult mole-rat pairs belonged to the two closely related sibling *Fukomys*-species, *F. anselli* and *F. kafuensis* as well as to their hybrids. Importantly, as evidenced in many previous as well as current control experiments, both species do not differ in their directional preferences in nesting experiments. Most pairs used in this study consisted of a male and a female breeder, and occasionally of sibling pairs. Each animal carried a tissue compatible, subcutaneous transponder (bio-capsule, 12 x 2.1 mm, ISO-standard 11784) with a unique number code (ALVIC-transponder, ALVETRA GmbH, Neumünster, Germany), ensuring individual identification. Mole-rats were, if not described otherwise, housed at ambient room temperature under natural daylight in glass cages filled with a layer of horticultural peat and were fed *ad libitum* with carrots, potatoes, lettuce and apples. Experiments were performed under the local geomagnetic field of Essen, Germany (45 μT; 66° inclination); exceptions are marked within the text.

2.2 Ruling out Biochemical Processes

Assuming that the radical pairs within a cell are sufficiently ordered, the sensitivity of radical reactions on the direction of an external magnetic field can provide the basis for a magnetic compass sense (see chapter B1.5.1.; Ritz et al. 2000). Weak intensity high frequency fields in the MHz range interfere with the singlet-triplet interconversion and thus provide a diagnostic tool to identify radical pair processes: the pattern of high frequency effects on the migrating behaviour has for instance shown that the avian magnetic compass is based on radical pair processes (Ritz et al. 2004; Thalau et al. 2005; Wiltschko et al. 2005).

2.2.1 Study rationale

These findings raise a question about the nature of the primary processes underlying magnetic compass mechanisms of other vertebrates than birds, like marine turtles and mammals (Wiltschko & Wiltschko 1995, 2005). We analyzed the magnetic compass mechanism of Ansell's mole-rats. In captivity, these subterranean rodents tend to build their nests preferably in the southern half of a round arena, a reliable spontaneous behavior that has been used

before to analyze the functional mode of their magnetic compass (e.g. Burda et al. 1990; Marhold et al. 1997a). Though magnetite seems a better candidate as the responsible mediator (see above B1.5.2) in subterranean mole-rats, we wished to exclude RPM behaviourally with the described set-up used successfully in birds by examining the mole-rats' directional nest building preference in a circular arena under certain oscillating magnetic fields. Our hypothesis was that mole-rat directional orientation should not be affected under oscillating magnetic fields, thus hinting at a magnetic signal transduction principle other than RPM, supposedly magnetite.

2.2.2 Study procedure

The experimental protocol followed the standardised protocol for nesting experiments in circular arenas as described in Burda et al. (1990b) and Marhold et al. (1997a). Eight mole-rat pairs (*Fukomys* spec.) were transported from the laboratory in Essen to the Biological Institute (Physiology and Ecology of Behaviour), University of Frankfurt am Main, two weeks prior to testing for habituation and avoidance of potential homing behavior. They were housed in animal housing facilities in plastic rodent cages at ambient room temperature and under a 12:12 light regime. Testing took place in darkness in four wooden huts in the garden of the Frankfurt institute where the local geomagnetic field of 46 μT, 66° inclination was undisturbed (fig. B12).

Fig. B12 Wooden hut with circular arena plus Helmholtz coils. Wooden huts with indoor arenas and Helmholtz coils in the garden of the Department Physiology and Ecology of Behaviour, J. W. Goethe-University, Frankfurt/Main. Local geomagnetic conditions: 46μT, 66° inclination. (A) Wooden hut with coil control elements in white box placed outside. (B) Helmholtz coil around plastic arena inside wooden hut. (C) Arena with randomly scattered nesting material and food items before releasing the mole-rats.

The animals were tested in pairs. Six pairs came from two colonies consisting of six animals; here, tested animals were returned to their colony directly after testing. The experiments were performed in spring 2004 and 2005, using the same pairs in both years except for one group that had to be replaced.

We exposed the mole-rats to a broad-band high frequency field with frequencies ranging from 0.1 to 10 MHz (intensity of 85 nT) and to a 1.315 MHz field of 480 nT and 4800 nT intensity, both presented vertically, i.e. with the high frequency field vectors at a 24° angle to the vector of the static geomagnetic field. In previous studies, these high-frequency fields had completely disrupted the orientation of birds (Ritz et al. 2004; Thalau et al. 2005).

To produce the broad-band high frequency field and the 1.315 MHz-field of 480 nT, we used the equipment from the corresponding bird experiments (Ritz et al. 2004; Thalau et al. 2005): a coil antenna of a single winding of coaxial cable with 2 cm screening removed opposite the feed was mounted horizontally on a wooden frame surrounding the test arena. Oscillating currents from a high frequency-generator were amplified by a HF-amplifier and were fed into the coil through a resistance of 51Ω. For the 1.315 MHz-field of 4800 nT, the arena was surrounded by a double winding of coaxial cable also with 2 cm of the screening removed. The high-frequency fields were measured before each test session with a spectrum analyzer. For details on the equipment used, see Ritz et al. (2004). In 2004, we performed a series of control tests in the geomagnetic field before we started the tests in the high-frequency fields and another control series interspersed with the high-frequency tests. Several controls were undertaken: *Apriori* controls were all performed before the particular pairs of mole-rats were tested in the high-frequency field for the first time to document their normal behaviour; the *Intermediate* controls were interspaced with the tests in the high frequency (HF) fields. Since there was no difference between the mole-rats' behaviour, thus indicating no aftereffects, the control tests in 2005 were performed before and between the high-frequency tests (*Alternating* controls).

For testing, the mole-rat pairs were moved in closed opaque plastic buckets to the round test arenas in the wooden huts. We used four huts with four arenas during the trials and randomly changed distribution of tested pairs among the huts. The plastic arenas had a diameter of 80 cm and a wall 30 cm high, they were placed on wooden tables 60 cm high. A plastic bucket of 17 cm diameter was placed in the center to ensure analyzable nest positions by preventing the animals from building nests in the arena's middle. The ground of the arena was covered with peat; a sufficient amount of strips of tissue paper was homogeneously scattered to provide nesting material, and food items (potatoes and carrots) were arranged radially (for details, see Burda et al. 1990b). When the test began, the animals were left in the middle of the arena in their transport bucket for a 30 min. habituation; then they were released

into the arena. The arena was closed with an opaque plastic lid, resulting in a light level of less than 0.005 μmol $\text{photons} \cdot \text{m}^{-2} \cdot \text{s}^{-1}$ inside the arena (measured in mW/m^2 and converted) with an Optometer P9710-1 (Gigahertz-Optik, Puchheim, Germany) with a radiometric probe (silicon photoelement, RW-3703-2, 400-800 nm). A nest was considered complete when most of the available paper strips were gathered, when animals slept in it or when the tissue pile showed signs of having been used for sleeping. The position of the nest was recorded and its direction with respect to geographic north was determined. The animals were tested once per day, in the morning or in the afternoon, mostly with a day between tests. The time until a nest was constructed varied between 30 min and about 6 h, with great differences between individual groups, as some animals regularly built faster than others. The outside temperature also had a certain influence, with nest building usually being faster at low temperatures. When the animals had not built a nest within 6 h, they were normally removed to their housing cages; in exceptional cases, they were left in the arena and built a nest after up to 9 h. After each test session, the peat was removed and the arena cleaned and washed with 10% acetic acid. Each group of animals was tested with its individual peat.

2.3 Narrowing down the Receptor Site

After exclusion of biochemical processes underlying the magnetoreception transduction mechanisms in Ansell's mole-rats, the second discussed mechanism, magnetite, seemed much more likely. The responsible signal transmission has been frequently associated with magnetite-based receptors innervated by the ophthalmic nerve, or with the involvement of the eye, particularly the retina. In trouts (Walker et al. 1997) and some bird species (Fleissner et al. 2003; Hanzlik et al. 2000; Williams & Wild 2001; Winklhofer et al. 2001), clusters of tiny magnetite crystals (diameter ~1-3 μm) were found in regions innervated by the ophthalmic branch of the trigeminal nerve. Physiological studies confirmed that this nerve might well carry magnetic field information to the brain (Beason & Semm 1996; Mora et al. 2004). The cornea, being a distinct, paired, and highly mechano-sensitive ocular structure innervated by the ophthalmic nerve, appeared predestined as a seat for receptors translating magnetic field information into mechanical signals, as suggested in some models (Walker et al. 2002). Preliminary findings of ferrous inclusions in its epithelium (Burda H. unpublished; fig. B14, following page) match its characteristics as a distinct and highly mechano-sensitive ocular structure arranged in pairs - and as being innervated by the ophthalmic nerve. We thus studied a putative involvement of the eye, i.e. the cornea, in mole-rat nesting behaviour. To this end, local anaesthesia was applied to the cornea in order to affect putative respective primary magnetoreceptors.

Because of the limitations that behavioural experiments impose on our understanding of magnetoreceptive mechanisms, it is important to narrow down the receptor site in order to identify the primary receptors unambiguously by means of neuroanatomy.

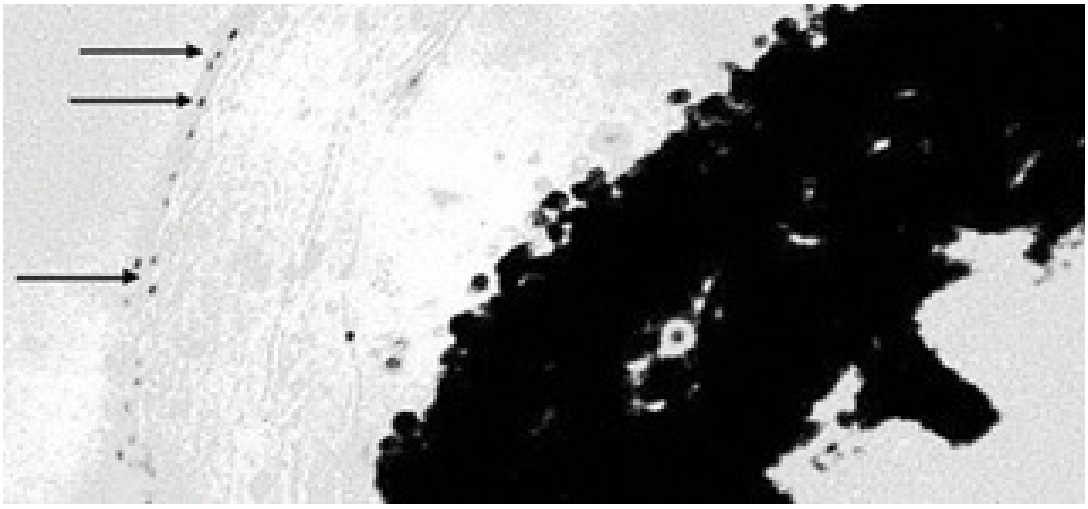

Fig. B13 Ferrous inclusions in the mole-rat corneal epithelium. Inclusion particles in a *Fukomys anselli* cornea are visualized by Prussian blue staining as indicated by arrows (photo: Hynek Burda).

Refining the current knowledge on both seat and character of the putatively magnetite-based magnetoreceptors is a crucial procedure in Ansell's mole-rat, particularly as magnetite, in contrast to chemical magnetoreception, enables, next to positional information via perceiving intensity changes, gathering directional information about the field polarity (Kirschvink & Gould 1981, Ritz et al. 2000); it thus matches the compass mode of subterranean mole-rats.

2.3.1 Study rationale

We again used the spontaneous nest-building drive of *Fukomys* mole-rats to examine whether mechano-sensitive desensitisation due to local anaesthesia of the corneal region affects their magnetic compass orientation. In our established experimental design (see above), mole-rats place their nests predominantly in the southern sector of a circular arena under control conditions (cf., Burda et al. 1990b). We expected that any direct impairment of primary magneto-receptors would result in random nest placement rather than in the usual directional behaviour.

Although the magnetic compass of these rodents has been described as light-independent (Marhold et al. 1997a), the possibility that corneal anaesthesia actually disrupted a photoreceptor-based magneto-sensory system in the mole-rats' eyes had to be excluded. We

thus used a two-armed maze preference test to assess the effect of the same anaesthetic treatment on the animals' ability to discriminate light from dark and to nest preferentially in darkness (see Chapter A2.2 & A3.1).

As the results suggested that the receptors involved in magnetoreception lie in the area innervated by the ophthalmic nerve, we thus performed further nesting experiments in a circular arena under the normal, local geomagnetic field. This time, one study group was supposed to undergo a neurotomy of the ophthalmic nerve, and the second study group bilateral enucleation. The hypothesis was that transsecting the ophthalmic nerve would result in a behavioural response, that would, together with the nesting response after enucleation, narrow down the still unclear receptor location: still, the first study did not show whether it was the nasal region, the retina, the Harderian gland or the cornea harbouring the receptors, as the anaesthetic fluid might have anaesthetised e.g. the nose via the lacrimal duct. For visualization, the hypothetical framework is given in tab. B1.

Table B1 Hypothetical framework to locate the magnetoreceptor site. The table gives the hypothetical framework of the experiments undertaken to narrow down the receptor site of magnetoreception in Zambian mole-rats (2.4). Neurotomy denotes the transsection of the ophthalmic nerve in both eyes of the animals of experimental group 1, enucleation denotes the enucleation of both eye-balls of the animals of experimental group 2. Experiment 3 comprises enucleation of animals of experimental group 1 in case of no neurotomy effects. H. gland = Harderian gland.

Experiment	Nesting behaviour	Putative site	Resulting site
1 - Neurotomy	a - disturbed	nose, cornea or H. gland →	cornea
	b - undisturbed	retina? → Exp. 3	
2 - Enucleation	a - disturbed	eye →	
	b - undisturbed	any other side	
[3 - Enucleation]	a - disturbed	retina	retina
	b - undisturbed	any other side	

Should the nesting behaviour be disturbed in the experiment following enucleation, it would be clear that the receptors are located in the eye. The cornea would then be clearly supported as the site for magnetoreceptors. Should (a) nesting behaviour of Zambian mole-rats be disturbed in the experiment following neurotomy of the ophthalmic nerve, this result would confine the location of the receptor site to the cornea, the nose, or the Harderian gland. However, together with possible scattered nesting results from the enucleation experiment, nose as well as Harderian gland could then be excluded. Should nesting behaviour be (b) undisturbed after transsection of the ophthalmic nerve, this result would hint at the retina rather than the cornea as the receptor site because the afferent pathway of the retina is via the optic nerve. After a subsequent enucleation in the same animals, the nesting behaviour should in this case be disturbed.

Due to complications in the timely preparation of the nerve transsection and due to seasonal restrictions on the outside experiments following this operation, this PhD thesis presents results solely from the corneal anaesthetic and enucleation experiments and leaves the still pending nesting-after-neurotomy tests to the future (see Outlook).

2.3.2 Study procedure

The experimental protocol applied to the standardised protocol for nesting experiments in circular arenas as described in 2.3 and 2.4 (Burda et al. 1990b; Marhold et al. 1997a).

In the timely preceding anaesthesia experiments, we repeatedly tested orientation in six adult pairs of mole-rats (breeding pairs or siblings from larger colonies) with four replications in each condition. Next to this commonly used second order data, we tested all available pairs of mole-rats from our breeding stock once per condition (n = 40 in controls; n = 42 in treatments with two more pairs due to recent mating) obtaining thus a large data set without replicates (Batschelet 1981). For control, the cornea was treated with sodium chloride solution used for medical and physiological purposes. Mole-rat pairs were tested on warm days in the year 2005 in an opaque plastic arena (80 cm diameter; 0.5 mm thick) in silent outside premises of the University campus in Essen, in the undisturbed local geomagnetic field. The arena floor was covered with a thin layer of peat; tissue paper strips and carrot pieces were spread radially on the surface. During testing, the arena was closed with a light impervious lid to exclude possible visual orientation. Mole-rats collected the tissue paper and built a nest; the exact nest position was then recorded referring to geographic North (Fig. B14, next page). To exclude order effects, half of the subjects of the singular tested group (tested once per condition) were tested first in controls with sodium chloride treatment, the other half first in the treatment condition with corneal anaesthesia. In the repeated tested group, the mole-rat pairs were

tested alternating under control and corneal treatment conditions with at least a day between subsequent tests. Tests lasted about 30 minutes to an hour. Anaesthesia was applied repeatedly when no nesting behaviour had begun after half an hour.

Sodium chloride solution or 2% Xylocain® solution (active substance: Lidocain hydrochloride; Astra GmbH, Wedel, Germany), a surface anaesthetic used routinely in medical practice for mucous membrane anaesthesia, was gently dropped into (NaCl) or applied generously to the opened eyes with a soft brush (viscous Xylocain®). During neither control nor treatment application did the animals show any adverse behaviour such as teeth chattering, distress or aggression vocalisations. No efforts to clean their eyes were observed.

In following tests on a possible effect of Xylocain® on vision, i.e. on the mole-rats' retinal performance, mole-rat pairs had to make a choice between a dark and an illuminated chamber for nesting with the same anaethesia treatment; their choice was recorded.

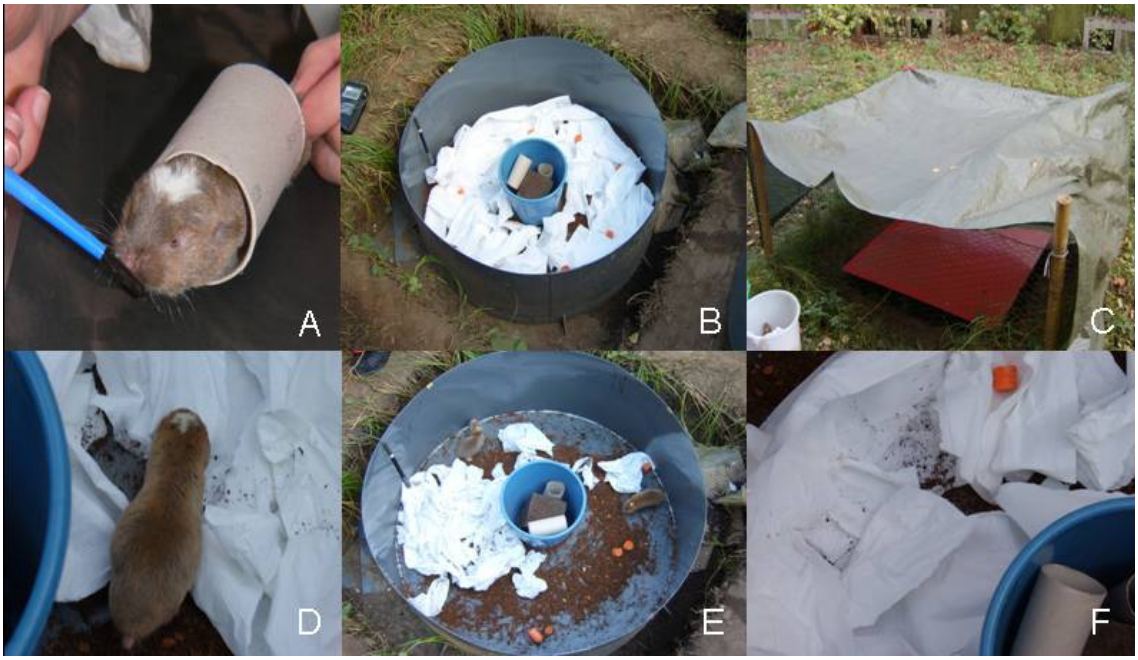

Fig. B14 Study set-up during nesting experiments in circular arenas. Nesting experiments in circular arenas were performed in outdoor premises of the Department of General Zoology, University Duisburg-Essen. Local geomagnetic conditions: 45µT, 66° inclination. (A) Application of Xylocain® with soft brush during fixation in a paper roll. (B) Preparation of the circular arena with nesting material and food items. The arena was inserted into an earth hole. On the left side, a thermometer is hanging into the arena. (C) Arena closed and shielded during experiments with mole-rats nesting. (D) Mole-rat gathering paper material. (E) Nesting finished. (F) Nesting swale.

In the enucleation experiments, we tested six adult mole-rat pairs (six females and six males) under the local geomagnetic field of Essen, Germany. Animals were either breeding pairs without any offspring or siblings from a larger colony. Animals were tested on warm

days in the year 2006 as described above, but in a different outside location of the Essen University campus, i.e. within an unoccupied greenhouse made from plastic walls with an aluminium frame. Each mole-rat pair underwent four replications under control conditions and six replications under experimental conditions after enucleation in order to obtain second order data sets. The difference in replicate numbers resulted from the circumstance that temperature conditions were favourable for outside testing until October and allowed a longer testing period than previously assumed. As the definite nature of the enucleation operations did not allow us to mix control experiments with treatment experiments, we could neither enlarge sample size in controls nor exclude order effects by mixing controls and treatments. Enucleation had no negative effect on the animals' health state of their behaviour or status within the colony after return (fig. B15).

Fig. B15 Mole-rats after enucleation operations. (A, B) Two enucleated mole-rats sitting in their nest six days after enucleation. The left animal's left eye is covered with a piece of substrate. (C) Another enucleated mole-rat four days after the operation.

We also performed four replicates with six different mole-rat pairs designated for the future neurotomy without knowing that the operations would be postponed. The available data, however, enabled us to compare the two control data sets and thus to test the control results for variabilty and/or stability of the directional preference.

Animals were deeply anaesthetised with an intramuscular injection of 0.04 ml/100g ketamine/rompun (10% ketamine and 2% rompun) (Pitman-Moore GmbH, Burgwedel, Germany). Body temperature was maintained at 36°C with a homeothermic blanket, and heart rate (pulse) and respiration were closely monitored. The eye region was carefully shaved with small titan scissors (World Precision Instruments, Sarasota, FL, U.S.A.). For local anaesthesia and a myorelaxant effect on the musculus retractor bulbi, 0.2 ml of a Lidocain solution (0.1%) was injected behind the eyeball with a 1 ml BD Micro-Fine syringe (0.33 mm(29G) x 12 mm; BD Consumer Healthcare Europe, Le Pont de Claix, France). Eyes were then removed with titanium surgery instruments (World Precision Instruments, Sarasota, FL, U.S.A.) and transferred into PFA for 30 min. and then into PBS for storage and later analysis. The wound

was covered with Tyrosur® antibiotic powder (active substance: 1% Tyrothricin; Engelhard Arzneimittel, Niederdorfelden, Germany). After an injection of 0.05 ml antibiotics (9.6 mg/kg) (Borgal®; Intervet, Unterschleißheim, Germany) and 0.125 ml Rimadyl® (4 mg/kg) for post-surgical pain relief (Pfizer, Karlsruhe, Germany). Animals were placed on layers of tissue paper in glass cages under warming lamps until they had fully recovered and could be placed back into their home colony. Recovery lasted from about 30 min. in large males to 90 min. in small females. After 12 hours and then daily, postoperational treatment was applied by subcutaneous injections of 0.05 ml Borgal® (9.6 mg/kg) and 0.25ml Rimadyl® (4 mg/kg).

Experiments, Xylocain®-treatment and enucleations conformed to the relevant regulatory standards and were approved by the authorities of the University of Duisburg-Essen and the District Government, Düsseldorf (50.05-230-37/06).

2.4 Magnetic Orientation is Binocular

2.4.1 Study rationale

Following Bisazza et al. (1998), a brain is defined as lateralised (or asymmetrical) if one side structurally differs from the other, or if it exercises different functions. Lateralization may then be expressed in an organism with one body side being structurally, or behaviourally different from the other side (Byrne et al. 2004). Lateralization of brain functions appears widespread among vertebrates (cf., Bradshaw & Rogers 1993; Bisazza et al. 1998; Vallortigara 2000; Rogers & Andrew 2002). By some scientists, brain lateralization is currently being considered as a homologous trait across all vertebrates (Rogers & Andrew 2002).

In European robins, e.g., the visual system associated with magnetoreception has been reported to function in a lateralised way (Wiltschko et al. 2002), and there is strong evidence that lateralization already takes place at the receptor level, long before the brain is involved in information processing (Möller 2006).

Regular observations of mole-rats running clockwise along the wall in a transport bucket or in a circular arena (Burda 1987) inspired us to take a closer look towards possible lateralised orientation behaviour of *Fukomys* mole-rats. Such lateralised behaviour could show in differing nesting behaviour with the left and the right eye, respectively, being blocked from magnetic perception by anaesthetic treatment.

Our aim was to test whether the receptors receiving magnetic stimuli for nesting orientation may be distributed in a lateralised way. Should magnetoreception be lateralised, nesting directions with one (or the other) eye anaesthetised would be expected to differ sharply from control directions.

2.4.2 Study procedure

In the nesting experiments with the left or the right eye anaesthetised, the experimental protocol and the treatment followed closely the one described in B2.2, the only difference being that these experiments took place in the location described in B2.3. Eight mole-rat pairs were tested four times in control conditions in the undisturbed geomagnetic field with a sodium chloride treatment applied to the eyes. In an alternating manner, the same study animals were tested four times with the left eye anaesthetised with Xylocain®, and also four times with the right eye anaesthetised with Xylocain®, with at least a day between subsequent tests; this was done to exclude order effects.

As the experimental data did not differ, we pooled them for the treatment condition into "monocular condition" data, and compared it to the control data ("binocular condition").

2.5 Revealing Hippocampal Involvement

2.5.1 Study rationale

Since Němec et al. (2001) showed the involvement of the superior colliculus in magnetic orientation in *Fukomys* mole-rats, there was the need to examine the participating neuronal structures further.

Our aim was to use immunocytochemical methods to map ITFs (*Inducible Transcription Factors*) (B1.6) in order to display neuronal structures involved in magnetoreception under certain manipulations of the magnetic field that should alter the neuronal response of the animals. As a change from a familiar situation (with continuous stimuli that are natural and of importance to the animal) towards a situation without the stimuli (e.g. darkness to light; MF to altered MF) may enhance c-Fos expression in rats (Herdegen & Leah, 1998), we examined and compared putative c-Fos expression changes in animals under certain MF manipulations.

2.5.2 Study procedure

We examined neuronal activity in shifted horizontal component and increased intensity magnetic fields in 6 adult mole-rats (5 females and 1 male) of the species *Fukomys anselli*. Four adult animals (1 female and 3 males) served as a control group in the undisturbed geomagnetic field. The animals were wild captured or laboratory-born and -raised. Experiments were performed in darkness in wooden huts in the garden of the Biological Institute in Frankfurt (Physiology and Ecology of Behaviour) (local geomagnetic field 46 μT; 66° inclination). The experimental and control groups were habituated in standard rodent plastic boxes within the

wooden huts for three consecutive days. Early on the fourth day, they were then placed in transparent plastic terrariums (33 cm length; 18 cm width; 19 cm height) filled with substrate (horticultural peat) and supplied with nesting material (tissue strips). After the control and treatment experimental time had run out (tab. B2), the animals were deeply anaesthetised with halothane and then transcardially perfused with heparinised saline followed by paraformaldehyde (PFA, 4% in 0.1M phosphate buffer, PB, pH 7.4) fixative. Animals were decapitated, the skulls were rapidly dissected, carefully opened at one or two points to allow the fixating liquid to penetrate and placed in chilled PFA.

Table B2 Mole-rats under magnetic field manipulations prior to neuronal activity mapping. Animals examined for neuronal activity under certain magnetic field manipulations derived from four different colonies of Ansell's mole-rats. Magnetic field conditions were the natural geomagnetic field with 46 μT and 66° inclination (Control), the natural geomagnetic field with the horizontal component inversed (-H), and the natural geomagnetic field with intensity increased by 1000 nT.

Animal	Colony	Sex	Condition	Experimental time
1	KAI2x(a)	male	Control	06:00-09:10
2		male		
3	CA11	female	Control	06:00-09:50
4		male		
5	KAI1	female	-H	09:15-10:45
6		female		
7		female		
8	KAI3	female	I+1000	09:50-11:20
9		male		
10		female		

The skulls were transferred to the Anatomy III laboratory of the Frankfurt Johann Wolfgang Goethe University hospital (Dr. Senckenbergische Anatomie); the brains were dissected from the skulls and postfixed overnight in the same fixative. Following this, the brains were transferred into PB-sucrose buffer (30%) for cryo-protection prior to cryo-microtome sectioning. Before sectioning, the brains were embedded in sucrose-gelatine (30% sucrose, 10% gelatine (300 bloom) in distilled water). The gelatine blocks were fixed in sucrose-PFA solution (30% sucrose, 4% PFA in PB), trimmed and properly oriented for sectioning. Gelatine-embedding and cryo-microtome cutting was chosen as free-floating gelatine sections rapidly return to their original form after cutting. Also, certain cell membrane

antigens do not survive routine fixation and paraffin wax embedding, the most widely used embedding medium (Beesley 1993). After trimming, the brain-blocks were put back into the PFA-sucrose for 48 h.

Brain blocks were glued to the moisted microtome's holding device with Tissue-Tec® (Miles Inc., Diagnostics Division, Elkhart, U.S.A.) and cooled to -50°C. Free-floating sections of 60 µm thickness were cut in the coronal plane with a rotation microtome (MICROM, type HM340, Heidelberg, Germany) and equally distributed into laboratory wells with a content of 5 ml each and ca. 45 sections per well) for immunocytochemistry (ICC). The wells were filled with phosphate buffer (PB) and 3 drops of azide each to prevent contamination. Sections were then transferred to reaction jars with a net on the bottom. The following procedure was applied to the sections within the net-jars on a shaker. All solutions were applied freshly. Net-jars were only used once per treatment series and then recycled.

Washing procedure prior to primary antibody treatment was applied within the net-jars on a shaker as follows:

(a) 1 wash with H_2O_2 (30 min.) to remove endogenous peroxidase
(b) 3 washes with PBS (10 min. each)
(c) 1 wash with "SAPJE" (30 min.)
(d) 1 rinse with PBS (5 min.)
(e) Avidin-blocking (15 min.) to remove endogenous Avidin
(f) 1 wash with PBS (max. 5 min.)
(g) Biotin-blocking (15 min.) to remove endogenous Biotin
(h) 3 washes with PBS (10 min. each)
(i) application of primary antibody (1° AB) and overnight incubation.

Secondary antibody application and preparation prior to light microscopy analysis were performed as follows:

(a) 3 washes with PBS (10 min. each)
(b) application of secondary antibody (90 min.)
(c) 3 washes with PBS (10 min. each)
(d) application of ABC (120 min.)
(e) 3 washes with PBS (10 min. each)
(f) pre-incubation in DAB.
(g) reaction stop.

The polyclonal 1° ABs for certain ITFs were applied according to tab. B3. Tested antibodies were chosen after those that had been tested in the Němec et al. (2001) mole-rat study, an ideal case, as a good antibody for one purpose or on one positive tissue may not always work

with another (Beesley 1993). From the tested 1° ABs, c-Fos (K-25), c-Jun (N), Egr-1 (C-19) and JunB (N-17) were working well during staining. Due to time restrictions, only c-Fos (K-25) was used for analysis.

The 2° AB used was 1:300 biotinylated goat anti-rabbit immunoglobuline (Vector BA-1000, Vector Laboratories Inc., Burlingham, U.S.A.).

Table B3 Primary polyclonal antibodies applied to ITFs during ICC in mole-rat brain sections. The table gives the tested concentrations of primary polyclonal antbodies against four ITFs in the mole-rat brain. Isotype of all antibodies was IgG (Immunoglobulin G; rabbit polyclonal IgG, 200 μg/ml), indicating the antibody's class referring to the respective heavy chain type (all antibodies: Santa Cruz Biotechnology, Inc., Santa Cruz, CA, U.S.A.). Each AB was tested in the concentrations of 0.05 μg/ml, 0.1 μg/ml and 0.5 μg/ml. The concentration that yielded best neuronal labelling is indicated in the last column with the concentration used for analysis highlighted in bold.

ITF	1°AB	catalog #	Good concentration
Egr-1 (Krox-24)	588	sc-110	-
Egr-1 (Krox-24)	C-19	sc-189	0.1 μg/ml
c-Fos	K-25	sc-253	**0.1 μg/ml**
c-Fos	4	sc-52	-
c-Jun	D	sc-44	-
c-Jun	N	sc-45	0.05 μg/ml
JunB	N-17	sc-46	0.5 μg/ml

Control sections were incubated with normal rabbit serum or with 1° AB pre-absorbed with native peptide (0.1 μg/ml), both of which prevented all nuclear staining for tissue differentiation. Every fourth section was stained with cresyl violet for subsequent Nissl-staining (for recipe see Appendix AH) and used for general orientation. To determine the specificity of the 1° AB, single sections from different compartments were incubated with 1) normal bovine serum albumin (BSA) solution only, with 2) 1° AB preabsorbed by a multiple surplus of synthetic antigen c-Fos (0.1 μg/ml; preadsorption test, blocking experiment; Dragunow & Robertson 1987; Oelschläger & Northcutt 1992).

Glass-slides were coated with gelatine. After stopping the reaction, the sections were washed three times with PB and then mounted on glass slides and dried overnight in the cabinet dryer at 37°C. Sections were then dehydrated by an ascending ethanol series, transferred into Xylol and coverslipped for light microscopy with Eukitt® (Kindler, Freiburg, Germany).

Analysis of positive neurons was performed in Prague, Czech Republic by T. Burger (Charles University) using analySIS® D software (Version 1.10, Soft Imaging System, Münster, Germany). The experimental procedure was approved by the District Government, Frankfurt.

A complete protocol of the perfusion, the preparation and immunohistochemical procedure, including gelatine coating, can be found in the Appendix (AF & AG).

2.6 Statistical analysis

From the nest positions of each animal pair, we calculated the mean vectors for both test conditions, with direction α_p and length r_p. The mean directions α_p of the six repeatedly tested pairs were averaged in grand mean vectors for each testing condition, with direction α_M and length r_M. From the nesting data of the tested pairs, we calculated the overall mean vector with direction α_A and length r_A. The group mean vectors α_p as well as the mean vector of the tested pairs α_A were examined for significant directional preferences with the Rayleigh-test of uniformity (Batschelet 1981) (ORIANA 2.02, Kovach Computing Services, Anglesey, UK); grand mean vectors α_M and the two mean vectors of the tested pairs were tested for differences in distribution between the study conditions with the Watson's U^2 Test (Batschelet 1981) (ORIANA 2.02). The vector length indicates the inter-group variance; the median gives the vector lengths based on the directions of the nests of each group, indicating the intra-group variance of the directional choices

Circular figures were created in Microsoft Excel® via GhostView® and then arranged in panels in Adobe Photoshop®.

The data from the two-arm maze preference tests regarding a possible influence of the anaesthetic on the animals' retinal performance was analyzed for a preferential choice using Chi-square tests (SPSS® 12.0 for Windows).

For comparison of mean numbers of immunoreactive neurons, a ONE-WAY ANOVA was conducted (SPSS® 12.0 for Windows).

3 RESULTS

3.1 Ruling out Biochemical Processes

In control tests in the local geomagnetic field of 46 000 nT, the mole-rats preferred to build their nests in the southern part of the arena (fig. B16A & B). Under the oscillating magnetic fields added to the natural geomagnetic field, the mole-rats continued to build their nests in the same part of the arena (fig. B16C). Even increasing the intensity of the 1.315 MHz-field tenfold to 4800 nT did not disrupt their orientation: their nests were still preferably situated in the south (Fig. B16, lower panel).

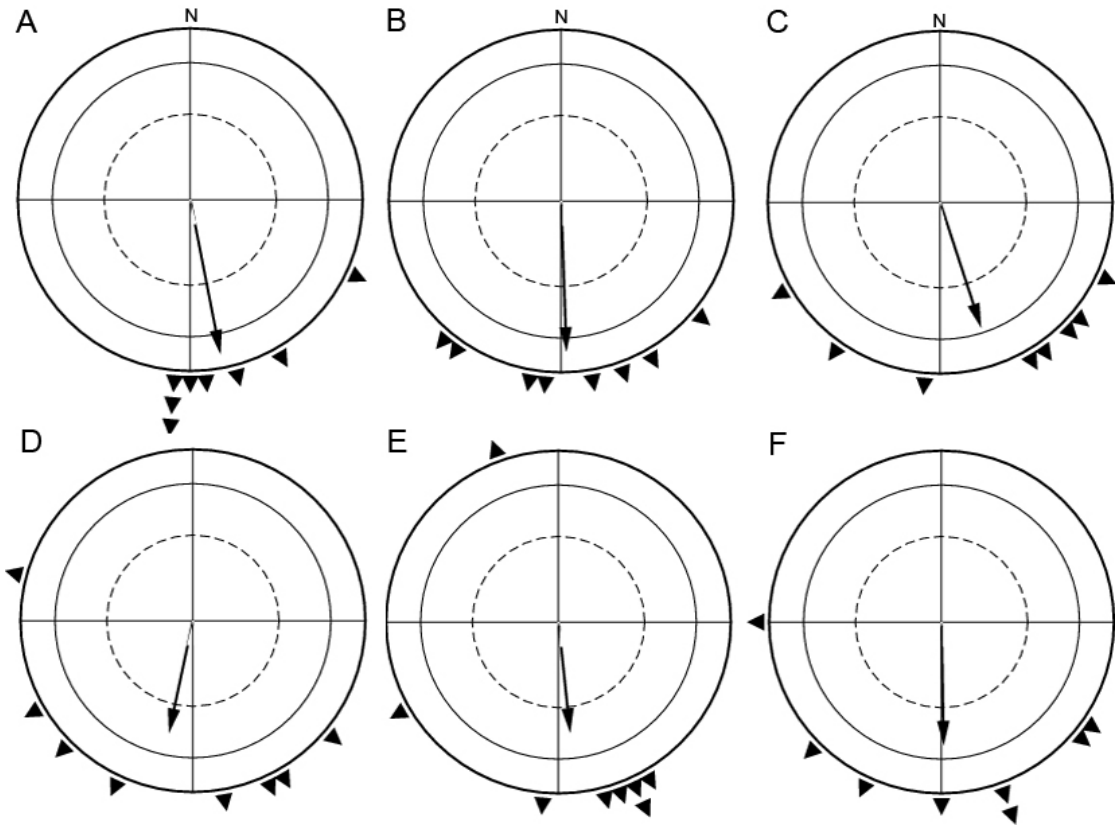

Fig. B16 Orientation of nests built by mole-rats under various test conditions. Figures of the upper panel (A, B, C) derive from 2004, with A displaying the *A-priori Control* data, B the *Intermediate Control* data and C the experimental data with *a Broad-band High-Frequency-Field* of 85nT intensity and 0.1-10 MHz frequency added. Single figures of the lower panel (D, E, F) show the results from 2005, with D displaying the *Alternating Control* data, E the experimental data with a Field of 1.315 MHz and 480nT added, and F the experimental data with a Field of 1.315 MHz and 4800nT added. The triangles at the periphery of the circle marks the means of the nests of the eight test groups; the arrows represent the grand mean vectors based on their single means, drawn proportional to the radius of the circle = 1. The two inner circles represent the 1% (dotted) and 0.1% (bold) significance border of the Rayleigh test in the upper panel (Batschelet 1981). In the lower panel, the dotted circle gives the 5% and the bold circle the 1% significance border. For numerical data, see table 4.

The vectors of the individual pairs of mole-rats in each test condition are given in tab. B4. There were no significant differences in the distribution of nests in the various experimental conditions ($P > 0.05$, Watson's U^2 test; Batschelet 1981).

There was no difference between the two data sets of the *Apriori* control and the *Intermediate* control, indicating that the treatment with high frequency fields had no aftereffects. Overall data are given in tab. B5.

Table B4 Mean vector data of Zambian mole-rats under oscillating fields. Control tests were performed in the local geomagnetic field; in the other test conditions, the respective high frequency field was added. α_p and r_p give the direction and length of the mean vectors of each pair based on the 5-9 replications.

2004	A-priori Control		Intermediate Control		Broad-band HF-Field [85 nT]	
Pair	α_p	r_p	α_p	r_p	α_p	r_p
P1	148°	0.65	162°	0.50	114°	0.26
P2	181°	0.28	131°	0.26	151°	0.21
P3	165°	0.40	217°	0.34	136°	0.60
P4	187°	0.14	184°	0.72	131°	0.82
P5	187°	0.16	169°	0.95	238°	0.28
P6	186°	0.53	219°	0.12	186°	0.59
P7	115°	0.33	150°	0.03	214°	0.57
P8	173°	0.63	192°	0.69	145°	0.24
2005	Alternating Controls		1.315 MHz, 480 nT		1.315 MHz, 4800 nT	
Pair	α_p	r_p	α_p	r_p	α_p	r_p
P1	286°	0.17	242°	0.34	131°	0.56
P2	172°	0.82	157°	0.94	161°	0.67
P3	152°	0.68	159°	0.41	127°	0.82
P4	206°	0.59	164°	0.86	158°	0.66
P5	130°	0.35	157°	0.19	268°	0.27
P6	224°	0.60	151°	0.22	180°	0.71
P7	240°	0.20	339°	0.42	224°	0.32
P9	155°	0.58	187°	0.52	205°	0.78

Table B5 Orientation of Zambian mole-rats under oscillating fields. Eight mole-rat pairs were tested between 5 and 9 times. The values α_p and r_p give the direction and length of the grand mean vectors based on the eight mean directions, with the asterisks indicating the vectors' significance. "med" gives the median of the vector lengths based on the nesting directions of each group. The last column indicates significance between the distributions of controls and treatments.

Year	Test condition	α_p	r_p	med	
2004	A-priori Control	169°	0.92***	0.37	
	Intermediate Control	178°	0.88***	0.42	ns
	Broad-band 0.1 -10 MHz -field, 85 nT	162°	0.77**	0.43	ns
2005	Alternating Controls	192°	0.67*	0.58	
	1.315 MHz field, 480 nT intensity	174°	0.65*	0.41	ns
	1.315 MHz-field, 4 800 nT intensity	179°	0.72*	0.66	ns

3.2 Narrowing down the Receptor Site

In the anaesthesia experiments under control conditions, the mole-rats stuck to their preference for nesting in a southern sector of the arena both in the repeated testing group (fig. B17A) and the singular tested group (fig. B17C). With corneal anaesthesia, the mole-rats still built their nests, however, without any directional preferences, showing a random distribution (fig. B17B, D). This difference between corneal anaesthesia and control groups was significant for both the repeated testing group ($U^2 = 0.206$, $P < 0.05$) and for the singular tested group ($U^2 = 0.218$, $P < 0.05$). Data are given in tab. B6.

In the experiment examining a possible retinal disturbance through Xylocain®, the mole-rats' behavioural response clearly showed that corneal anaesthesia did not affect photoreceptor performance; their ability to perceive light and prefer darkness for nesting was undisturbed ($n = 11$, $\chi^2 = 7.4$, $P = 0.007$).

In the neurotomy/enucleation experiments, both controls showed the usual South-Easterly preference; they did not differ ($U^2 = 0.16$, $p > 0.1$). Animals after enucleation showed a random nesting distribution, but the enucleation control and the after-enucleation data did not differ ($U^2 = 0.12$, $p > 0.2$; fig. B18A, B). However, taking all nesting directions together in a first order test, there was a significant difference between directions from the control group ($N = 24$) and from the enucleation group ($N = 36$) ($U^2 = 0.27$, $p < 0.01$; fig. B18C, D). The data are given in tab. B7.

The figures and the related tables are given on the following pages.

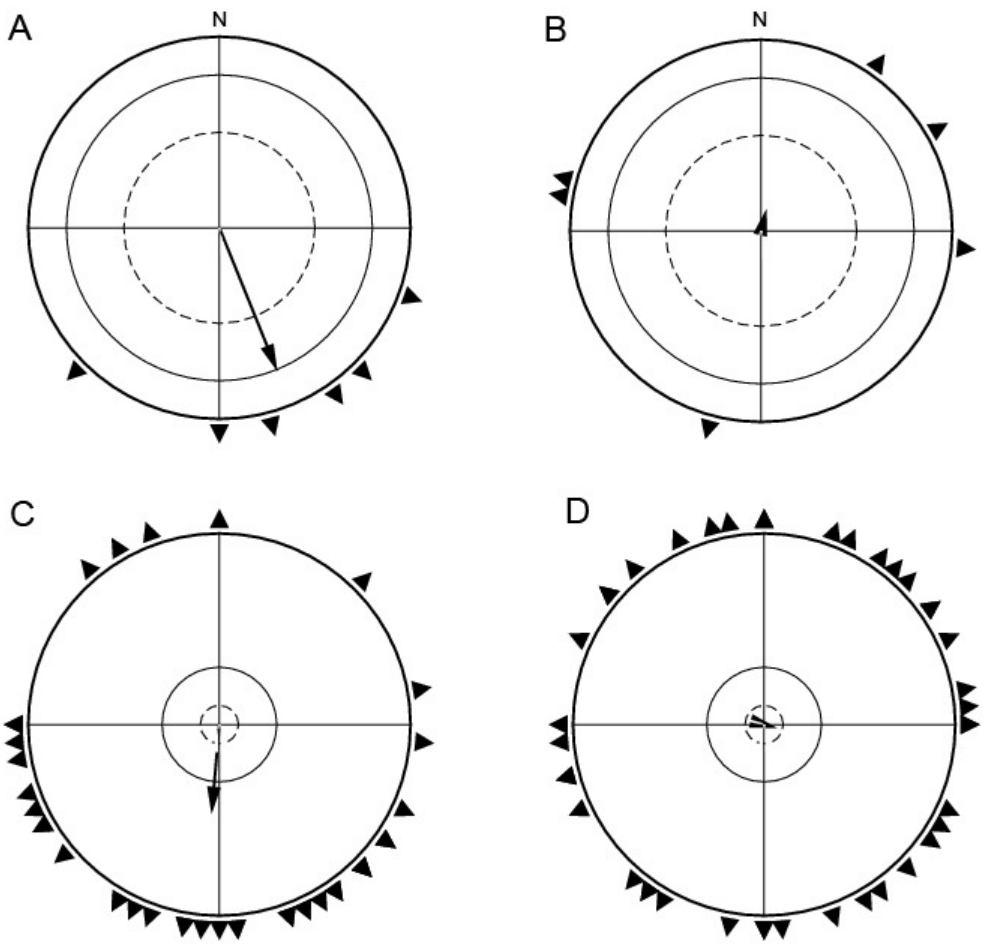

Fig. B17 Random nest distribution of mole-rats under corneal anaesthesia. Triangles display mean nesting directions of the repeatedly tested six pairs in control (A) and under anaesthesia (B), and nesting directions of the singular tested group in control (C; $n = 42$) and treatments (D; $n = 40$). The arrows proportional to the outside radius (= 1) mark the grand mean vector based on the pairs' mean directions (A, B) or the mean vector of all single decisions (C, D). The inner circles mark the Rayleigh significance thresholds: 5% (dashed) and 1% (solid) in A, B; 1% (dashed) and 0.1% (solid) in C, D. Table B6 gives numerical values.

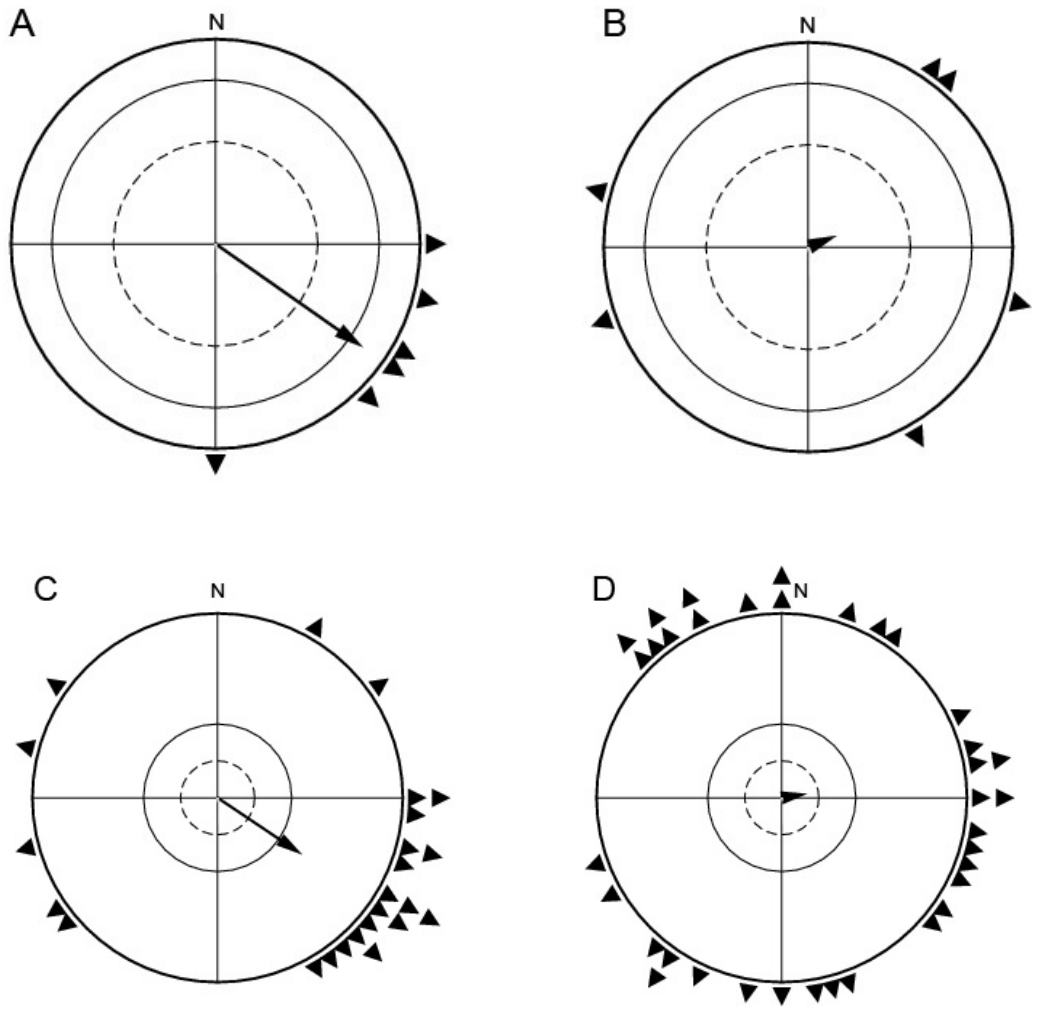

Fig. B18 Nest distribution of six mole-rat pairs before and after enucleation. Triangles display mean nesting directions of six repeatedly tested pairs in controls (A) and after enucleation (B), and the single nesting directions in controls (C) and after enucleation (D). The arrows proportional to the outside radius (= 1) mark the grand mean vector based on the pairs' mean directions. The inner circles mark the Rayleigh significance thresholds with 5% (dashed) and 1% (solid) (A, B) and 5% (dashed) and 0.1% (solid) (C, D). Table B7 gives numerical values.

Table B6 Orientation of Zambian mole-rats after corneal anaesthesia. The α_P and r_P values indicate direction and length of the six pairs' mean vectors based on four trials; α_A and r_A give direction and length of the mean vectors of all single directions in the singular tested group. Grand mean vectors and Mean vectors are displayed with significance marked by asterisks; median individual vector lengths are given for the repeated testing condition. Deviation of directions between control and treatment is given with significance indication.

	Control		Corneal anaesthesia	
Repeatedly tested pairs	α_p	r_p	α_p	r_p
P1	143°	0.77	283°	0.48
P2	108°	0.57	279°	0.21
P3	180°	0.88	35°	0.33
P4	225°	0.86	197°	0.47
P5	163°	0.74	59°	0.22
P6	137°	0.45	94°	0.30
Grand mean vector	158°, 0.81*		14°, 0.12ns	
Median vector length	0.76		0.32	
Direction deviation	144°, $P < 0.05$			
Singular tested pairs				
Mean vector	185°, 0.47***		105°, 0.07	
Direction deviation	80°, $P < 0.05$			

Table B7 Orientation of mole-rats after enucleation. The α_P and r_P values indicate direction and length of the six pairs' mean vectors based on four (controls) and six trials (enucleation). Grand mean vectors and mean vectors are displayed with significance marked by asterisks; median individual vector lengths are given. Direction deviations are given with significance indication for the comparison of directions. Data are also given for all single nesting directions.

	Control Enucleation Group		Control Neurotomy Group	
Tested pairs	α_p	r_p	α_p	r_p
P1	105°	0.43	189°	0.13
P2	119°	0.99	139°	0.69
P3	89°	0.68	209°	0.51
P4	182°	0.59	210°	0.36
P5	127°	0.46	174°	0.49
P6	134°	0.58	141°	0.96
Grand mean vector	125°, 0.88**		177°, 0.88**	
Median vector length	0.58		0.50	
Direction deviation	52°, ns			

	Control Enucleation Group		After Enucleation	
Tested pairs	α_p	r_p	α_p	r_p
P1	105°	0.43	150°	0.31
P2	119°	0.99	106°	0.67
P3	89°	0.68	285°	0.32
P4	182°	0.59	37°	0.32
P5	127°	0.46	41°	0.38
P6	134°	0.58	250°	0.11
Grand mean vector	125°, 0.88**		68°, 0.15 ns	
Median vector length	0.58		0.32	
Direction deviation	57°, ns			

	Single Nests Control Group	Single Nests After Enucleation
Grand mean vector	124°, 0.55***	81°, 0.14 ns
Pairs tested	24	36

3.3 Magnetic Orientation is Binocular

The eight tested mole-rat pairs significantly confirmed the preferred southern direction for nesting in controls (fig. B19A). Roughly the same directional behaviour showed also in the data of the mole-rat pairs with the left eye anaesthetised (fig. B19B) and with the right eye anaesthetised (fig. B19C). With the right eye anaesthesia, however, the mean direction was not significantly expressed, and directional significance of the data after left eye anaesthesia was weak (P = 0.046). Controls and the right-eye group differed significantly (U^2 = 0.296, P < 0.01). However, the directions of the left-eye and right-eye groups did not differ (U^2 = 0.074, P >0.5); neither did the control and the left-eye group (U^2 = 0.131, P > 0.1). All data are given in tab. B8 on the next page.

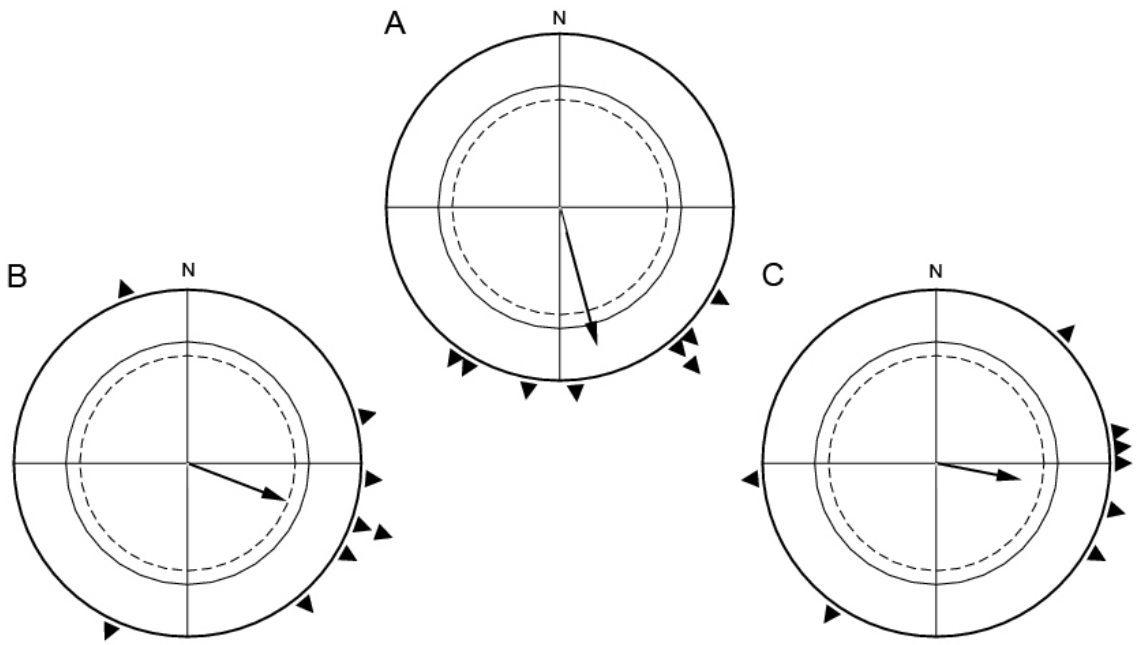

Fig. B19 Nest distribution of mole-rat pairs under lateralised corneal anaesthesia. Triangles display mean nesting directions of the repeatedly tested eight pairs in control (A), under corneal anaesthesia of the left eye (B), and under corneal anaesthesia of the right eye (C). The arrows proportional to the outside radius (= 1) mark the grand mean vector based on the pairs' mean directions. The inner circles mark the Rayleigh significance thresholds: 5% (dashed) and 1% (solid). Table 8 gives numerical values.

Table B8 Orientation of mole-rats after monocular anaesthesia. The α_P and r_P values indicate direction and length of the eight pairs' mean vectors based on four trials; r_P values are given with significance indications. Grand mean vectors and Mean vectors are also displayed with significance marked by asterisks. Median vector lengths are given (MED). Direction deviations are given with significance indication for the comparison of controls and treatments.

	Control		Right Eye Anaesthesia	
Tested pairs	α_p	r_p	α_p	r_p
P1	174°	0.49	217°	0.10
P2	189°	0.13	107°	0.76
P3	139°	0.69	90°	0.10
P4	209°	0.51	84°	0.93*
P5	134°	0.46	79°	0.24
P6	210°	0.36	122°	0.43
P7	119°	0.99**	263°	0.69
P8	141°	0.96**	46°	0.71
Grand mean vector	164°, 0.84**		101°, 0.50 ns	
MED	0.50		0.56	
Direction deviation	63°, $P < 0.01$			
	Control		Left Eye Anaesthesia	
Tested pairs	α_p	r_p	α_p	r_p
P1	174°	0.49	94°	0.32
P2	189°	0.13	108°	0.96**
P3	139°	0.69	341°	0.40
P4	209°	0.51	141°	0.88*
P5	134°	0.46	122°	0.92*
P6	210°	0.36	206°	0.65
P7	119°	0.99	75°	0.66
P8	141°	0.96	112°	0.91*
Grand mean vector	164°, 0.84**		111°, 0.61*	
MED	0.50		0.77	
Direction deviation	53°, ns			
Treatment deviation	10° ns			

Pooling together the non-differing right eye and left eye group and then comparing this monocular treatment condition with the binocular control condition (fig. B20), a significant difference was found between these groups ($U^2 = 0.25$, $P < 0.01$). Data are given in tab. B9.

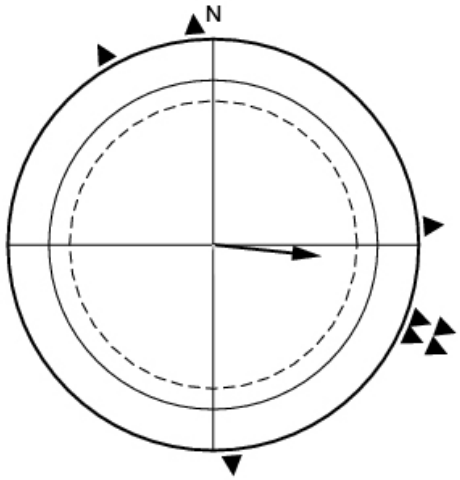

Fig. B20 Pooled experimental data of nest distribution of mole-rat pairs under lateralised corneal anaesthesia. Triangles display mean nesting directions of the eight repeatedly tested pairs. The arrows proportional to the outside radius (= 1) mark the grand mean vector based on the pairs' mean directions. The inner circles mark the Rayleigh significance thresholds: 5% (dashed) and 1% (solid). Table B9 gives numerical values.

Table B9 Orientation of mole-rats after lateralised anaesthesia with pooled data. The α_P and r_P values indicate direction and length of the six pairs' mean vectors based on the eight pooled trials; r_P values are given with significance indications. Grand mean vectors and mean vectors are also displayed with significance marked by asterisks. Median vector lengths are given (MED). Direction deviations are given with significance indication for the comparison of controls and treatments.

	Control (Binocular) data		Monocular data	
Tested pairs	α_p	r_p	α_p	r_p
P1	174°	0.49	111°	0.14
P2	189°	0.13	108°	0.86
P3	139°	0.69	353°	0.20
P4	209°	0.51	111°	0.80
P5	134°	0.46	114°	0.56
P6	210°	0.36	174°	0.41
P7	119°	0.99	331°	0.05
P8	141°	0.96	84°	0.68
Grand mean vector	164°, 0.84**		96°, 0.53 ns	
MED	0.50		0.50	
Direction deviation	68°, $P < 0.01$			

Results from an older study exerting a strong, short magnetic pulse on mole-rats (Marhold et al. 1997b), hinted at a change in magnetization of the responsible receptor (control 160°: N = 15-40, r = 0.9, $P < 0.001$; pulse 86°: N = 18-22, r = 0.98, $P < 0.01$), and are given here for better comparison and with permission of the author (fig. B21). The two conditions differed significantly ($U^2 = 0.264$, $P < 0.05$). However, the directions from the monocular data and the pulsing data were not similar, but showed a significant difference ($U^2 = 0.256$, $P < 0.05$).

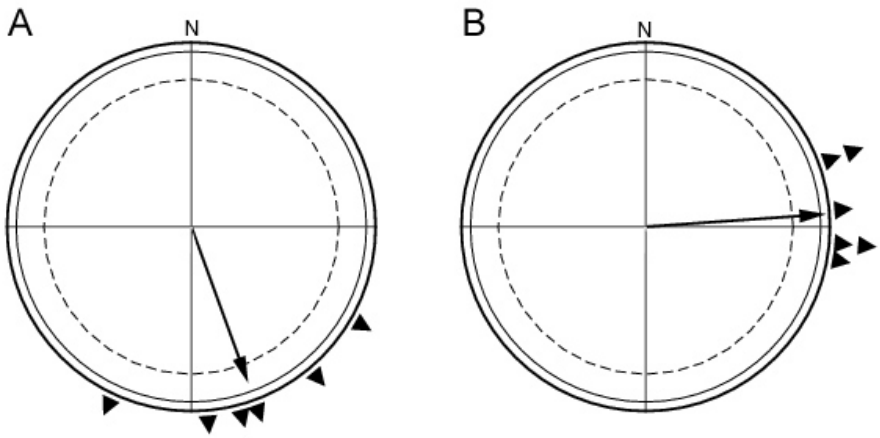

Fig. B21 Nest distribution data of six mole-rat pairs before and after magnetic pulsing (Marhold et al. 1997b). Triangles display mean nesting directions of repeatedly tested pairs in controls (N between 18 and 22) (A) and after exposure to a strong (0.5T), short (5ms) magnetic pulse (N between 15 and 40) (B). The arrows proportional to the outside radius (= 1) mark the grand mean vector based on the pairs' mean directions. Inner circles mark significance thresholds: 1% (dashed) and 0.1% (solid) (Figures by the author using original data with kind permisssion from S. Marhold.).

3.4 Revealing Hippocampal Involvement

Significant neuronal activity under magnetic field manipulations could be found in regions of the hippocampal formation.

Distribution patterns of c-Fos immunoreactive neurons in the hippocampus are shown in fig. B22. Differences in the number of immunoreactive neurons between the control condition and manipulations of the magnetic field were significantly displayed in the CA1 region of the hippocampus (fig. B23C). Mean numbers differed strongly between the control group and the intensity change group ($P = 0.003$), with neuronal activity being starkly depressed in the latter. This effect was also shown in the significant difference between the two experimental groups ($P = 0.004$). In the hippocampal CA3 region, there were differences between control and the experimental conditions (fig. B23D), with both experimental conditions suppressing neural activity (control compared to horizontal manipulation: $P = 0.018$; control compared to intensity manipulation: $P = 0.008$). In the polymorphic cell layers of the hippocampal dental gyrus, active neuron numbers differed extremely between all the three tested groups (fig. B23B). The control group showed extremely low activity rates and differed slightly from the activity displayed in the horizontal component group, whose numbers were also low ($P = 0.016$). Under intensity changes, neural activity increased markedly, resulting in significant differences between control and this experimental group ($P = 0.000005$) and between the two experimental groups ($P = 0.0001$).

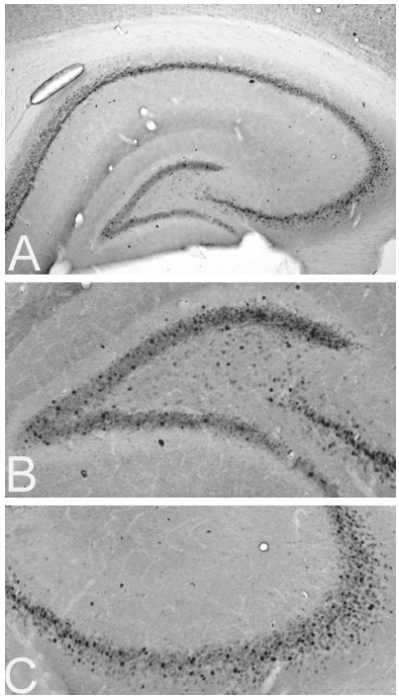

Fig. B22 Distribution patterns of c-Fos immunoreactive neurons in the Ansell's mole-rat hippocampus. (A) Photomicrograph of a section through the dorsal portion of the hippocampus. Higher power photomicrographs of the dentate gyrus (B) and CA3 (C). Picture taken by T. Burger and modified by the author.

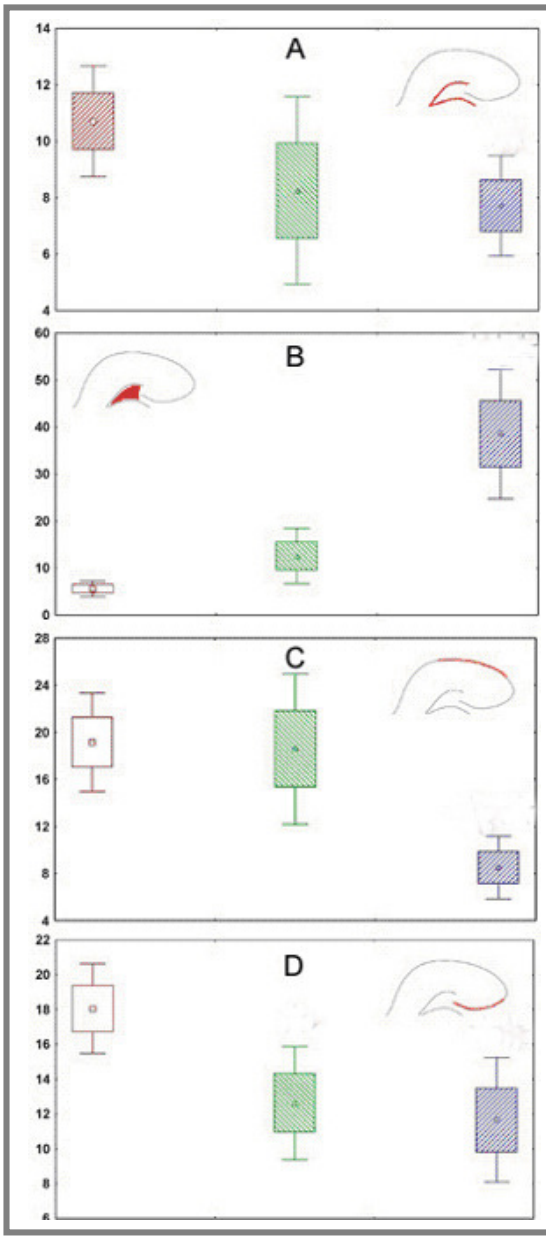

Fig. B23 Neurons immunoreactive to c-Fos in mole-rat hippocampal structures. Mean numbers of c-Fos immunoreactive neurons in the granular cell layer (A) and the polymorphic layers (B) of the dentate gyrus, in the CA1 (C) and CA3 (D) hippocampal fields of mole-rats subjected to different magnetic conditions. Control on the left side of the figures (red/white): natural, i.e. stationary MF; azimuth in the figures' middle (green): experimental MF with the horizontal component being manipulated every 30 seconds (i.e. mN shifted from 360° to 240° and back); intensity on the right side of the figures (blue): experimental MF with intensity being manipulated every 30 seconds (± 1000 nT). Figure created by T. Burger and modified by the author.

Figure B24 can be found on the next page. All mean values and standard deviations are comprised in tab. B10, on the second next page.

Differences in neural activity evoked by magnetic field manipulations could also be found in the dorsal subiculum (fig. B24A). The comparatively high activity numbers in the control group differed significantly from the intensity change group ($P = 0.000006$); and as activity in the group with the magnetic field's horizontal component manipulated was similarly high as the controls, there was also a strong difference between the two experimental groups ($P = 0.002$).

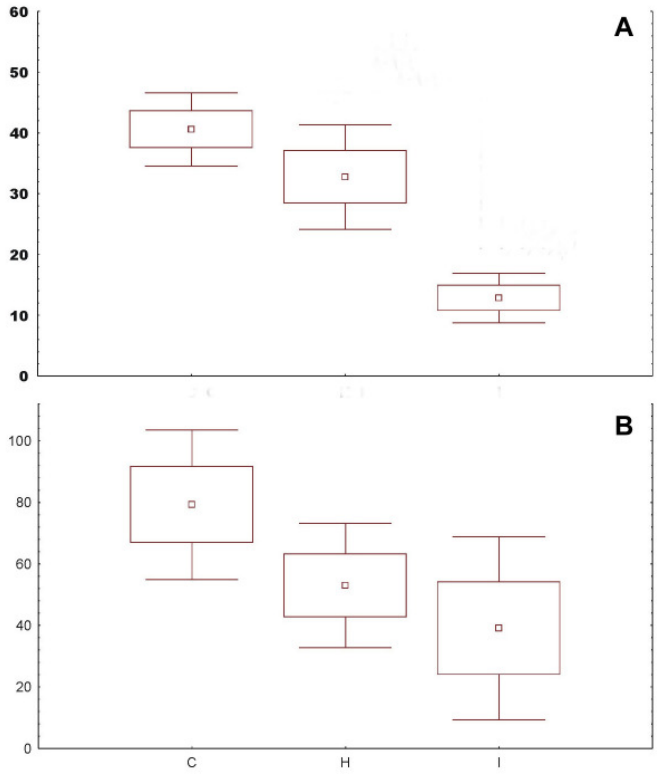

Fig. B24 Neurons immunoreactive to c-Fos in mole-rat subiculum and entorhinal cortex. Mean numbers of immunoreactive neurons in the dorsal part of the subiculum (A) and the entorhinal cortex (B) under different magnetic conditions: control (abscissa C) with a natural, i.e. stationary MF; experimental MF (H) with the horizontal component being manipulated every 30 seconds (magnetic North shifted from 360° to 240° and back); experimental MF (I) with the intensity being manipulated every 30 seconds (± 1000 nT). Figure created by T. Burger and modified by the author.

In the other brain structures examined, there were no significant differences in neural activity between control, horizontal component and intensity change group. No neural activity at all could be observed in the nucleus dorsalis tegmenti, the nucleus laterodorsalis thalami and the nucleus anterodorsalis thalami.

Table B10 Mean numbers of neurons immunoreactive to c-Fos in diverse brain structures of mole-rats under Magnetic Field manipulations. Nucleus dorsalis tegmenti and the nuclei laterodorsalis and anterodorsalis thalami were without neural activity. In the group column, (C) denominates control conditions, i.e. the natural, stationary MF; (H) gives the experimental MF with the horizontal component being manipulated every 30 seconds (magnetic North shifted from 360° to 240° and back); (I) gives the experimental MF with the intensity being manipulated every 30 seconds (± 1000 nT). Significance indicates differences between active neuron numbers of the different groups and is indicated by asterisks.

Structure	Substructure	Group	mean	SD	Significance
Hippocampus	CA1	C	19.14	12.45	C vs. I **
		H	18.57	16.61	H vs. I **
		I	8.51	6.83	
	CA3	C	18.07	7.55	C vs. H *
		H	12.65	8.3	C vs. I**
		I	11.67	9.49	
	Granular cell layer	C	9.63	7.21	
		H	8.26	8.64	
		I	7.72	4.72	
	Polymorphic cell layer	C	5.61	4.86	C vs. H*
		H	12.53	14.99	C vs. I***
		I	38.53	33.64	H vs. I***
Subiculum	Dorsal layer	C	39.14	15.34	C vs. H**
		H	32.73	16.98	C vs. I***
		I	13.18	7.45	
	Ventral layer	C	31.32	16.88	
		H	32.05	10.12	
		I	29.19	36.37	
Postsubiculum		C	8.41	6.09	
		H	6.77	5.65	
		I	7.13	5.31	
Retrosplenial cortex	Agranular cell layer	C	13.35	8.7	
		H	10.96	6.33	
		I	13.65	10.56	
	Granular cell layer	C	37.25	20.93	
		H	39.81	18.39	
		I	47.99	22.58	
Entorhinal cortex	Dorsomedial cell layer	C	79.24	37.24	C vs. I (*)
		H	52.95	30.9	(P = 0.057)
		I	39.06	30.34	
	Lateral cell layer	C	28.6	6.02	
		H	30	13.86	
		I	30.27	15.61	
Perirhinal cortex		C	14.19	6.56	
		H	19.18	12.9	
		I	14.48	5.95	
Nucleus lateralis mammilaris		C	9.51	12.12	
		H	3.97	3.65	
		I	2.79	2.46	

4 DISCUSSION

The second part of this thesis has shed light on some crucial aspects of magnetoreception in mammals. The results above introduced experiments on the nature of the underlying transduction mechanism, on the location and type of the respective sensory receptor as well as on the neuronal processing of magnetic information, and will be discussed separately in the following.

Ruling out Biochemical Processes

As expected in subterranean rodents, living and orientating in darkness, the hitherto determined characteristics of the magnetic compass in Ansell's mole-rats are consistent with the magnetite-based magnetoreception model. Evidence for this kind of sensation is supported by the following, above already mentioned findings. Compass orientation of Ansell's mole-rats is: 1) light-independent (Marhold et al. 1997a); 2) sensitive to the magnetic field's polarity (Marhold et al. 1997a); 3) disrupted by a brief strong magnetic pulse designed to alter (re-magnetize) single-domain magnetite or to affect superparamagnetic particles (Marhold et al. 1997b); 4) not disrupted by very weak oscillating high-frequency fields disturbing avian compass orientation (Chapter B2.2 & B3.1). While the latter experiment *per se* does not prove that the magnetic compass of mole-rats is magnetite-based, it indicates that it is not based on RPM. In contrast to birds, the mole-rats' orientation was not disrupted when a broad-band field of 0.1 to 10 MHz of 85 nT or a 1.315 MHz field of 480 nT was added to the static geomagnetic field. Even when increasing the intensity of the 1.315 MHz field to 4800 nT, more than a tenth of the static field, the mole-rats remained unaffected and continued to build their nests in the south. This behaviour differs greatly from the responses of European robins, *Erithacus rubecula*, in similar experiments: their orientation behaviour was strongly affected by weak high frequency fields, with a marked effect being observed at the frequency of 1.315 MHz that matches the energetic splitting induced by the local geomagnetic field (Thalau et al. 2005). These results indicate that in contrast to the magnetic compass of birds, that of the mole-rats does not involve radical pair processes. A magnetite-based mechanism seems to be indeed a better interpretation for their magnetic compass, since a magnetite-based sensor would not be affected by the high-frequency magnetic fields applied here. This conclusion is in agreement with the above mentioned earlier experimental findings on the functional characteristics of the mole-rats' magnetic compass.

It is not yet clear to what extent our support of magnetite as a putative transducer in mechanoreception in mole-rats is characteristic for mammals in general. In birds, a magnetic

compass has now been demonstrated in more than 20 species from 4 different orders. So far, the European robin is the only species where a radical pair mechanism has been identified; yet the inclination compass, which is to be expected if radical pair processes are involved, has been found in all avian species tested for it. In mammals, a magnetic compass was first indicated in woodmice, *Apodemus sylvaticus* (Mather & Baker 1981); in the following years, magnetic compass orientation was reported in other species of rodents (cf., Mather 1985; August et al. 1989; Burda et al. 1990b, 1991), horses (Baker 1989a) and humans (Baker 1989b). However, mole-rats are the only species so far where the functional mode has been analyzed and where the underlying physical processes are indicated (Marhold et al. 1997a,b; this study). It cannot be excluded that the mole-rats' magnetic compass is a special development adapted to their subterranean life style. On the other hand, many mammalian species are nocturnal or live in habitats with little light. This is also reflected in their sensory systems, with their optic sense inferior to that of day-active animals like birds, yet their auditory sense and in particular their sense of smell highly developed. In view of this, it would also seem possible that a general mammalian magnetic compass independent from light would have favoured mammals to occupy the subterranean niche.

Narrowing down the Receptor Site

Our findings of disrupted directional compass orientation after corneal anaesthesia show that the ocular region might accommodate the primary magnetic receptors in mole-rats. Contrary to the assumed association of magnetite-based receptors with the ophthalmic nerve, Cernuda-Cernuda et al. (2003) reported findings of crystalloid bodies in the inner segments of retinal photoreceptors of the Ansell's mole-rat. The authors interpreted these structures as potential magnetite grains, suggesting the retinal photoreceptors as the respective magnetite-based structure. However, the unperturbed ability of the mole-rats to discriminate between light and dark (Chapters A2.2 & A3.1) under corneal anaesthesia indirectly suggests that magnetic compass orientation in *Fukomys* is not photoreceptor-based because the application of anaesthetics did not influence visual performance or differential orientation behaviour *per se* in our study. Our results rather hint at a peripheral ophthalmic seat of the stimulus mediator in these mammals: our behavioural findings and their interpretation are consistent with the neuroanatomical findings of magneto-responsive neurons in *F. anselli* identified within the inner sublayer of the intermediate grey layer of the superior colliculus (Němec et al. 2001), i.e. in a layer dominated by trigeminal input in other mammals (Huerta & Harting 1984). Both approaches are consistent with the hypothesis that the cornea harbours the putative primary magnetoreceptors. We further assume that in Zambian mole-rats, the mechano-sensors mediating signals during magnetic orientation are magnetite-based. Next to the earlier

discussed findings, which had excluded retinal chemo-physical radical-pair reactions as the underlying signal mediating mechanism (Marhold et al. 1997b; this study), our results support innervated magnetite being the responsible sensory structure, because desensitisation of the cornea obviously affected mechano-sensibility and thus magnetic stimulus transmission.

Furthermore, our results of impaired directional nesting orientation after bilateral enucleation provide clear evidence for the ocular, possibly, corneal magneto-receptor location, though the impairment experiments involving specific bilateral section of the ophthalmic branch of the trigeminal nerve still need to be done to complete the picture. Although our results clearly suggest a difference between control and experimental post-enucleation data (see fig. B18), the statistical test refuses to support significance of the difference between controls and enucleation in the standard second order data set. The first order data set, however, comprising all taken data, confirms this difference. In our study, testing conditions seemed optimal, indicated by the similarity of both control groups, which had highly significant vector lengths, excluding any possible intra-group variablity. However, the single vector lengths of the tested mole-rat pairs were partly unexpectedly low, surprisingly both in the control and enucleation groups. However, the resulting mean vectors were significant (and that highly) in the controls. In the experimental enucleation group, the low vector length had the effect of resulting in a randomized pattern. The applied Watson's U^2 Test compares data sets using their mean square deviations. If the data set samples are from populations that differ in some way, the resulting *P*-value is low. As this difference may be in distribution, mean direction, or other parameters, one would expect a significant difference between two directional data sets with one data set basing on significant (control) and one on random mean directions (enucleation). Even if the resulting direction of the random mean directions resembled the control, the distribution patterns would differ starkly. The poor performance of the single mole-rat pairs and its effect on the weak results of the second data comparison maybe based on testing in the here firstly used new premise on the Essen campus. This new location might have been influenced by unknown external factors such as noise or odours. Magnetic disturbances could be, however, ruled out (S. Mayer, personal communication).

Our enucleation experiments nevertheless rule out the possibility that our findings of the anaesthesia experiments resulted from the affecting of the nose or the Harderian gland and refine the area of magneto-sensors to the mole-rat's eye.

Magnetic Orientation is Binocular

The here shown shift of nesting directions in mole-rats after monocular anaesthesia does not demonstrate an asymmetrical function of the magnetic sense, at least not at the receptor level in the eye. Both left and right eye anaesthesia resulted in the same directional shift, indicating no asymmetrical use of the eyes. If the magnetic sense had been lateralised in mole-rats, either magnetic orientation would have been disturbed with one of the eyes anaesthetised (i.e. resulting in a scattered nesting pattern, such as in European robins (Wiltschko et al. 2002)), or the two eyes would have shown a different task, thus a different resulting direction. For demonstrating lateralization, it is sufficient to show such behavioural effects in only some tested pairs, because the population, which the individuals under study derive from, is already regarded as lateralised if more than 50% of the tested individuals display the same direction (Denenberg 1981; Bisazza et al. 1998). In our study, six of eight pairs (75%) showed a directional shift and would thus fulfil the criterion of lateralization on the population-level. This shift, however, did not differ, i.e. was not displayed in an asymmetrical way, between the left and the right eye, indicating no functional division in magnetoreception.

The effect of monocular anaesthesia is, however, surprising. The eastward shift of nesting directions, both under left and right eye anaesthesia, suggests that for unambiguous position determination, incoming magnetic information from both eyes is needed. One explanation may be that the signal is simply weaker with only one eye in charge. This explanation does, however, not make clear why in both conditions, nesting direction is obviously shifted to the East; random nesting distribution due to the animals' uncertainty basing on a weak signal would rather be expected. One other explanation may be that monocular anaesthesia, e.g. via the lacrimal duct, also influenced the second eye, resulting in an even weaker stimulus. Interestingly, the shift of nesting directions from binocular (southern) to monocular (eastern) condition strongly resembled the nesting direction changes resulting from a strong, short magnetic pulse (0.5 T, 5 ms) (Marhold et al. 1997b). After the pulse, nesting directions were also shifted to the East and that on long-term. This effect was explained by a change of magnetization of magnetite as the substance assumedly underlying the magnetoreceptors. Whether the shift to the East under monocular conditions and under magnetization changes can be compared and/or explained by more than incidence, needs to be discussed.

Firstly, it is necessary to have a closer look at the monocular directional shift that might be explained by the following model (introduced by H. Burda): in the resting situation, both eyes are oriented in the same direction without any difference in strain or relaxation of the musculus rectus medialis or in the excitation of the oculomotor nerve, both of which are responsible for signal-dependent eye movement orientation. The importance of the eye-

moving structures is pictured by the well-developed and also large oculomotor nucleus in *Fukomys anselli* (Němec et al., 2004)[5]. The oculomotor nerve is discussed to innervate the M. retractor bulbi, a muscle responsible for retracting the eyeball. Simple eyeball retracting would however not need the apparent complex neuronal processing. One might speculate that the putative mechanoreceptors in the mole-rat's cornea, innervated by the ophthalmic nerve, report the incoming signal and entice the oculomotor nerve to rotate the animal's head until the signal is strongest or fades. One might call this procedure, comparing it to the human foveal orientation towards points of interest, a *magnetic fovea* orientation. Given magnetite particles located on the cornea acting as transducers during magnetic signal transduction, the mole-rat would be able to virtually detect the orientation of the magnetite relative to an imaginary North-South and East-West-axis. It would be possible for the animal to detect the North-South-axis horizontally and the East-West axis vertically. The area of magnetic particles (one might call it a "Macula magnetica") activity would be, in the resting state, directed symmetrically frontwards.

Assume that the magnetic stimulus is directly in front of the animal. When the animal moves and thus "shifts" the direction it faces to e.g. its left side, both muscle and nerve would undergo a stronger excitation in the right and a lesser excitation in the left eye; with the animal turning and thus "shifting" the faced direction to its right side, both muscle and nerve would undergo a lesser excitation in the right and a stronger excitation in the left eye. This model would explain why the mole-rats detect the North-South-axis solely with both eyes, i.e. in a binocular way, implying a necessary parallel signal inhibition from one eye and a signal enhancement from the other eye for unequivocal direction determination. With one eye being anaethetized, i.e. with monocular signal income only, the animal cannot react in a directional way, as it is impossible for the animal to detect the North-South-axis. It instead reacts to the continuously present, vertical East-West axis, which is the same in both eyes, explaining the similar outcome with either the right or the left eye anaethetized. The reason for the nesting preference in the eastern direction may be based on some yet unclear characteristics of the nervous processing or of the sensor, as does probably also the yet not understood south-eastern preference on the North-South-axis with both eyes active.

Bridging to the above mentioned coincidence with the shift in nesting directions of mole-rats after pulse re-magnetization towards East (Marhold et al. 1997b) and the monocular experimental data, this model might also supply an explanation and a base for comparison. Though it has been suggested that the very short pulse (5 ms) of 0.5 T may have shifted magnetization of the magnetic particles, the here presented model can explain the result also

[5] »The large oculomotor nucleus is perplexing.« (Němec et al., 2004)

by the idea that the pulse may have evoked a de-magnetization of the corneal magnetite resulting in a long-lasting functional loss of the animals' ocular ability to detect their virtual horizontal North-South-axis (such as was initiated by the local anaesthesia). The resulting directions need not resemble, as was the case here (significant direction deviation of 25°). The mole-rats would have thus been forced to rely on the information from their virtual vertical East-West-axis. Both directional preferences after pulsing and under monocular anaesthesia would then be based on the same underlying mechanism, yielding not as correct measurements as the binocular method. This weaker measuring ability could also explain the insignificant vector lengths of the right eye group and the pooled group, which, despite the obvious directional shift, indicate a high directional variance, possibly evoked by the animals' directional uncertainty.

Revealing Hippocampal Involvement

Here, we follow Witter & Amaral (2004) where the hippocampal region is described to comprise two sets of cortical structures, the hippocampal formation, and the parahippocampal region. These two regions differ mainly by their number of cortical layers and their overall connectivity. The hippocampal formation includes three regions which are cytoarchitectonically distinct, but comparable in their three-layered appearance and their largely uni-directional connectivity: the dentate gyrus, the hippocampus (proper) with its three fields CA3, CA2 and CA1, and the subiculum. The parahippocampal (or retrohippocampal) region comprises the entorhinal cortex, the perirhinal cortex, and the postrhinal cortex; these areas have more than three layers and show reciprocal connectivity. For an overview of these structures in the rat brain, please see Appendix AE.

Following this definition, our study shows that the areas apparently containing neurons that are responsive to magnetic stimuli are all of hippocampal character. This is of interest, as the hippocampus is generally considered to be the site of the cognitive map of the animal's environment (cf., O'Keefe and Nadel 1978; Sharp 2002; Jeffery 2003).

The profound neoplasmic activity sticks close to the acquisition of new memories (cf., Eichenbaum 2000). The pyramidal neurons of the hippocampus proper regions CA1 and CA3, where both intensity and horizontal component changes of the magnetic field evoked neuronal activity patterns significantly different from the control situation, serve as *place cells*, i.e. neurons that fire when the animal occupies a specific location in a particular environment (reviewed in e.g. Muller 1996). A change in place cell activity should particularly become clear under intensity change manipulation, as it supplies the animal with false information on its current position.

Our study shows that such changes in place cell activity under intensity changes occur predominantly in CA3 and in the dentate gyrus, and in a small amount also in CA1. Both CA1 and CA3 thus seem to play roles during location recognition, e.g. when trying to orient (and locate known places) in a magnetic field different from the static, familiar one. Cells with place correlates lie also in the dentate gyrus (Jung et al. 1994), where, at least in the polymorphic layer, neuronal activity was increased under increased magnetic field intensity.

Regarding the learning of known places as a prerequisite of their recognition by place cell firing, particularly the connection between CA1 and CA3 areas (the *Schaffer collateral*) seems predestined for harbouring the respective molecular process, as here, coincident release of the neurotransmitter glutamate and the strong depolarization of the postsynaptic membrane participate in long-time potentiation, LTP, a mechanism of prolonged excitatory synaptic potentation, inevitably connected with the storage of memory contents (Bear 1996; Kandel et al. 1995). However, the parahippocampal region is also of vital importance to the hippocampal memory system: it serves as a convergence site for cortical inputs and mediates the distribution of the cortical afferents further on to the hippocampus. The connections in the hippocampus itself could represent the base for a large network of associations, and these connections support plasticity mechanisms that could participate in the rapid coding of new information conjunctions (reviewed in Eichenbaum 2000), e.g. information on new or unknown locations.

Besides place cells, the hippocampal structures demonstrated in this study to harbour magnetoresponsive neurons, such as the dentate gyrus and CA1 and CA3, also comprise *head direction cells*. Complementary to place cell activity, head direction cells fire when the animal's head faces a particular direction (reviewed in e.g. Taube 1998; Sharp et al. 2001). A change in head direction cell activity should thus particularly become clear under horizontal component change manipulation, as it supplies the animal with false information on the direction that it faces, i.e. in this study with permanently changing directional information.

Significant increase in neuronal activity under such a permanent change of the horizontal component could be found in CA1 and in the dentate gyrus, and also, in a lesser amount, in CA3. These structures with the most frequent pyramidal cell type thus seem to participate in the interpretation of an animal's direction. Also in the subiculum with its demonstrated increased activity under horizontal component changes of the magnetic field, pyramidal cells make up for the principal cell layer. The major input that the subiculum receives from CA1, underlines its involvement in direction determination (Witter & Amaral 2004).

To sum up, place cells are the keystone of the neural machinery generating an abstract representation of the animal's spatial surroundings (a map), while head direction cells are

involved in the moment-by-moment representation of the animal's current heading (a compass). Our results of neuronal activity in the respective brain structures indicate that subterranean mole-rats may not only have a magnetic compass that derives directional information, as has been hitherto demonstrated by behavioural experiments, but that they also use magnetic cues to acquire magnetic map information.

Despite these highly interesting results, our knowledge about mammalian magnetoreception, i.e., what happens where in the rodent neuronal circuits, remains fragmentary and is far from complete.

IV RÉSUMÉ & OUTLOOK

This dissertation thesis has contributed to a better understanding of both light and magnetic reception in subterranean mole-rats of the genus *Fukomys*. Still, many open questions remain and might be the impulsion for future studies, some of which will now be shortly suggested. Note that the available number of mole-rats is always limited. Some standard procedures, e.g. using high numbers of sacrificed animals, are thus difficult to perform.

Already today, *Fukomys* mole-rats cannot be viewed as fully blind anymore. Vision in these subterranean rodents probably contributes more than marginally to optimising the crucial processes of temporal and spatial orientation underground. To provide further behavioural correlates for the present morphological data and to enlighten the biological sense of vision in *Fukomys*, retino- and neurophysiological studies would be surely of avail.

Furthermore, the surprisingly high cone share compared to the rod density, and particularly the relatively high proportion of cones reacting to the short wavelength spectrum of the light have given rise to the question whether Zambian mole-rats have colour vision. It will be certainly interesting to examine the spectral tuning of their photoreceptors. As the single cell recordings turned out to be difficult to perform and were scarce in results, the ultimate expression of the photon catch by the mole-rats' retina might be understood through future, visually mediated behaviour studies using operant colour light experiments. To better understand the origin and function of the involved opsins, they should be molecularly characterized, and their *in vitro* expression should be studied.

Vision and magnetoreception are interconnected and share a close coevolution; this view has for instance been supported in a recent study, which suggested that magnetic input originating in the photoreceptors of the bird's retina possibly shares neuronal pathways with the visual system (Möller 2006).

This close vicinity is, in mole-rats, expressed anatomically by the receptors of both senses, vision and magnetoreception, being located in the eye. To refine the picture that we have of mammalian magnetoreception, firstly, the neurotomy study should be performed to pin down the cornea as the receptive seat. The mole-rat cornea has further to be thoroughly histologically, histochemically, and ultra-microscopically examined. Here, staining methods for iron-containing particles, such as the Prussian Blue method, would be as advantageous as the new approach to visualize magnetic particles via so-called ferrofluids. An examination of the putative magnetite crystals *in situ* in the cornea with transmission electron microscopy (TEM) could give a detailed impression on the location and crystalloid characteristics of magnetite in the tissue and particularly on its relation to the surrounding cells, as well as on its innervation pattern. Another approach to locate small magnetite clusters in animals has been suggested by

Johnsen & Lohmann (2005). The authors recommend searching vertebrate genomic libraries for gene sequences involved in magnetite production. Such sequences might have been conserved during evolution. The approach might be successful, as magnetroreceptive magnetite crystals are probably formed through pathways involving molecular enzymes and transporters. These processes have been extensively studied in magnetotactic bacteria, and both transportes and chelators involved have been sequenced (Bazylinski & Frankel 2004).

Searching for magnetite crystals might, however, also be promising in the oculomotor muscles. As speculated above, magnetic orientation could be connected with eye movement. Anaesthesia of the ophthalmic nerve, which resulted in disturbed orientation, may have well also affected the oculomotor nerve and thus controlled eye movement. Assuming that magnetite may be located in muscle stretch receptors, it could be the stretch receptors of the oculomotor muscles that possess the magnetite crystals. Given the accessibility of the cornea, these studies may open new vistas for a further understanding of the primary transduction mechanisms of magnetite-based magneto-reception in mammals.

Using magnetic resonance tomography (MRT), the mole-rat brain could be systematically screened for neuronal activity under certain magnetic stimuli; the neuronal processing of magnetic information could be thus nearly optimally visualized, both spatially and temporally.

This dissertation thesis has, however, not touched the one crucial question arising in the second field of research presented here: the question of the biological sense and/or the adaptive meaning of magnetoreception. The following questions still need to be answered: What is the meaning of the use of magnetic information derived from the Earth's magnetic field? Why do these rodents prefer to build their nests in the South under laboratory conditions? Do the animals display the same preference also in the field? Are their burrows oriented in a certain direction, and if so, why? What use do the animals have from their magnetic compass? One explanation would be that maintaining a shallow inclination angle when digging requires less energy than digging steeper tunnels, as has been shown recently in the tuco-tuco, *Ctenomys talarum* (Luna & Antinuchi 2007). Measuring the inclination angle would then be of help for a digging animal, but a polarity compass is of no use for receiving inclination information. Magnetic cues could be, however, used for path integration within the burrow system, as has been shown in *Spalax ehrenbergi* (Kimchi et al. 2004).

In any case, conclusions on the light-independent magnetic compass in mole-rats as a representative of the mammalian magnetic compass must be drawn cautiously. The magnetite-based light-independent compass in mole-rats may alternatively display, along with the visual system, an adaptation to the dark subterranean environment. An interesting parallel may be drawn with blind salamanders inhabiting aphotic caves: they are not expected to have a light-

dependent magnetic compass although this type of mechanisms occurs in terrestrial salamanders like the eastern red-spotted newt (Phillips pers. comm.). It will be thus of high interest to study the mechanisms of magnetoreception also in surface-dwelling rodents.

V REFERENCES

Arendt D, Tessmar-Raible K, Snyman H, Dorresteijn AW & Wittbrodt J (2004) Ciliary photoreceptors with a vertebrate-type opsin in an invertebrate brain. *Science* 306: 869-871.

August PV, Ayvazian SG & Anderson JTG (1989) Magnetic orientation in a small mammal, *Peromyscus leucopus*. *J Mammal* 70: 1-9.

Bailey MJ, Chong NW, Xiong J & Cassone VM (2002) Chicken's Cry2: molecular analysis of an avian cryptochrome in retinal and pineal photoreceptors. *FEBS Letters* 513: 169-174.

Baker RR (1989a) Navigation and magnetoreception by horses and other non-human land mammals. In: *Orientation and Navigation - Birds, Humans and other Animals*. (Royal Institute of Navigation, Cardiff), paper 12.

Baker RR (1989b) Human navigation and magnetoreception. Manchester University Press, Manchester.

Banerjee SK & Moskowitz BM (1985) Ferrimagnetic properties of Magnetite. In: Kirschvink JL, Jones DS, MacFadden BJ, Magnetite Biomineralization and Magnetoreception in Organisms. Pp. 17-41, Plenum Press, New York.

Batschelet E (1981) Circular Statistics in Biology. Academic Press, London.

Bazylinski DA & Frankel RB (2004) Magnetosome formation in prokaryotes. *Nat Rev Microbiol* 2: 217–230.

Bear MF (1996) A synaptic basis for memory strorage in the cerebral cortex. *PNAS USA* 93: 13453-13459.

Beason RC & Semm P (1987) Magnetic responses of the trigeminal nerve system of the bobolink, *Dolichonyx oryzivorus*. *Neurosci Lett* 80: 229-234.

Beason RC & Semm P (1996) Does the avian ophthalmic nerve carry magnetic navigational information? *J Exp Biol* 199: 1241-1244.

Beason RC, Dussourd N & Deutschlander ME (1995) Behavioural evidence for the use of magnetic material in magnetoreception by a migratory bird. *J Exp Biol* 198: 141-146.

Beesley JE (1993) Immunocytochemistry. Oxford University Press, Oxford.

Begall S, Schleich C & Burda H (2007a). Sensory ecology. In: Begall S, Burda H & Schleich CE (eds), Subterranean rodents: News from underground. In press. Springer Verlag, Heidelberg.

Begall S, Lange S, Schleich C & Burda H (2007b). Acoustics, audition, and auditory system. In: Begall S, Burda H & Schleich CE (eds), Subterranean rodents: News from underground. In press. Springer Verlag, Heidelberg.

Benhamou S, Sauvé JP & Bovet P (1990) Spatial memory in large-scale movements – efficiency and limitations of the egocentric coding process. *J Theor Biol* 145: 1-12.

Berthold P (1990) Vogelzug: Eine kurze, aktuelle Gesamtübersicht. Wissenschaftliche Buchgesellschaft, Darmstadt.

Bingman VP & Cheng K (2005) Mechanisms of animal global navigation: comparative perspectives and enduring challenges. *Ethol Ecol Evol* 17: 295-318.

Bisazza A, Rogers LJ & Vallortigara G (1998) The origin of cerebral asymmetry: a review of evidence of behavioral brain lateralization in fishes, reptiles, and amphibians. *Neurosci Behav Rev* 22: 411-426.

Boles LC & Lohmann KJ (2003) True navigation and magnetic maps in spiny lobsters. *Nature* 412: 60-63.

Bradshaw J & Rogers LJ (1993) The evolution of lateral asymmetries, language, tool use and intellect. Academic Press, San Diego, California.

Brassart J, Kirschvink JL, Phillips JB & Borland SC (1999) A magnetite-based map component of homing in the eastern red-spotted newt. *J Exp Biol* 202: 3155-3160.

Brett RA (1991) The ecology of naked mole-rat colonies: burrowing, food and limiting factors. In: Sherman PW, Jarvis JUM & Alexander RD (eds), The biology of the naked mole-rat. Pp. 137-184. Princeton University Press, Princeton.

Burda H (1987) Magnetische Navigation bei den Graumullen, *Cryptomys hottentotus* (Bathyergidae)? *Z Säugetierk Suppl* 61:12.

Burda H (1989) Reproductive biology (behaviour, breeding, and postnatal development) in subterranean mole-rats, *Cryptomys hottentotus* (Bathyergidae). *Z Säugetierk* 54: 360-376.

Burda H (1990) Constraints of pregnancy and evolution of sociality in mole-rats. With special reference to reproductive and social patterns in *Cryptomys hottentotus* (Bathyergidae, Rodentia). *Z Zool System Evol* 28: 26-39.

Burda H & Begall S (2002) Sinnesökologie subterraner Säugetiere. *PdN – Biologie* 1 (51): 16-20.

Burda H, Bruns V & Müller M (1990a) Sensory adaptations in subterranean mammals. In: Nevo E & Reig O (eds.), Evolution subterranean mammals at the organismal and molecular levels. Pp. 269-293, Alan R. Liss, New York.

Burda H, Marhold S, Westenberger T, Wiltschko R & Wiltschko W (1990b) Magnetic compass orientation in the subterranean rodent *Cryptomys hottentotus* (Bathyergidae). *Experientia* 46: 528-530.

Burda H, Beiles A, Marhold S, Simson S, Nevo E & Wiltschko W (1991) Magnetic orientation in subterranean mole rats of the superspecies *Spalax ehrenbergi*: experiments, patterns and memory. *Isr J Zool* 37: 182-183.

Burda H, Honeycutt RL, Begall S, Grütjen O & Scharff A (2000) Are naked and common mole-rats eusocial and if so, why? *Behav Ecol Sociobiol* 47(5): 293-303.

Burda H, Sumbera R & Begall S (2007) Microclimate of subterranean burrows – revisited. In: Begall S, Burda H & Schleich CE (eds), Subterranean rodents: News from underground. In press. Springer Verlag, Heidelberg.

Byrne RA, Kuba MJ & Meisel DV (2004) Lateralised eye use in Octopus vulgaris shows antisymmetrical distribution. *Anim Behav* 68: 1107-1114.

Cain SD, Boles LC, Wang JH & Lohmann KJ (2005) Magnetic orientation and navigation in marine turtles, lobsters, and molluscs: concepts and conundrums. *Integr Comp Biol* 45: 539-546.

Cashmore A, Jarillo JA, Wu Y-J, Liu D (1999) Cryptochromes: Blue light receptors for Plants and Animals. *Science* 284: 760-765.

Cernuda-Cernuda R, DeGrip WJ, Cooper HM, Nevo E & Garcia-Fernandez JM (2002) The retina of *Spalax ehrenbergi*: novel histologic features supportive of a modified photosensory role. *Invest Ophthalmol Vis Sci* 43 (7): 2374-2383.

Cernuda-Cernuda R, Garcia-Fernandez JM, Gordijn MCM, Bovee-Geurts PHM & DeGrip WJ (2003) The eye of the african mole-rat *Cryptomys anselli*: to see or not to see? *Europ J Neurosci* 17: 709-720.

Chávez AE, Bozinovic F, Peichl L & Palacios AG (2003) Retinal spectral sensitivity, fur coloration, ad urine reflectance in the genus *Octodon* (Rodentia): implications for visual ecology. *Invest Ophthalmol Vis Sci* 44(5): 2290-2296.

Cooper HM, Herbin M & Nevo E (1993) Ocular regression conceals adaptive progression of the visual system in a blind subterranean mammal. *Nature* 361: 156-159.

Credle VR (1988) Magnetite and magnetoreception in stranded dwarf and pygmy sperm whales, Kogia simus and Kogia breviceps. Master thesis, University of Miami.

Czihak G, Langer H & Ziegler H (1990) Biologie. 4te Auflage. Springer Verlag Berlin, Heidelberg, New York.

Davila AF, Fleissner G, Winklhofer M & Petersen N (2003) A new model for a magnetoreceptor in homing pigeons based on interacting clusters of superparamagnetic magnetite. *Phys Chem Earth* 28: 647-652.

David-Gray ZK, Bellingham J, Munoz M, Avivi A, Nevo E & Foster RG (2002) Adaptive loss of ultraviolet-sensitive/violet-sensitive (UVS/VS) cone opsin in the blind mole rat (*Spalax ehrenbergi*). *Europ J Neurosci* 16: 1186-1194.

Denenberg VH (1981) Hemispheric laterality in animals and the effects of early experience. *Behav Brain Sci* 4: 1-49.

Deutschlander ME, Borland SC & Phillips JB (1999a) Extraocular magnetic compass in newts. *Nature* 400: 324-325.

Deutschlander ME, Phillips JB, Borland SC (1999b) The case for a light-dependent magnetoreception mechanism in animals. *J Exp Biol* 202: 891-908.

Deutschlander ME, Freake MJ, Borland SC, Phillips JB, Anderson LE & Wilson BW (2003) Learned magnetic compass orientation by the Siberian hamster, *Phodopus sungorus*. *Anim Behav* 65: 779-786.

Diebel CE, Proksch R, Green CR, Neilson P & Walker MM (2000) Magnetite defines a vertebrate magnetoreceptor. *Nature* 406: 299–302.

Dragunow M & Robertson HA (1987) Kindling stimulation induces c-fos protein(s) in granule cells of the rat dentate gyrus. *Nature* 329:441-442.

Dusenbery DB (1992) Sensory ecology: how organisms acquire and respond to information. W.H. Freeman and Co. Publishers, New York.

Eichenbaum H (2000) A cortical-hippocampal system for declarative memory. *Nat Rev Neurosci* 1: 41-50.

Eloff G (1951) Orientation in the mol-rat *Cryptomys*. *Brit J Psychol* 42: 134-145.

Eloff G (1958) The functional and structural degeneration of the eye of the South African rodent moles, *Cryptomys bigalkei* and *Bathyergus maritimus*. *S Afr J Sci* 54: 293-302.

Etienne AS & Jeffery KJ (2004) Path Integration in mammals. *Hippocampus* 14: 180-192.

Etienne AS, Maurer R & Saucy F (1988) Limitations in the assessment of path dependant information. *Behaviour* 106: 81-111.

Ewert JP (1973) Fortschritte der Zoologie, Band 21. Fischer Verlag, Jena.

Faulkes CG, Verheyen E, Verheyen W, Jarvis JUM & Bennett NC (2004) Phylogeographic patterns of speciation and genetic divergence in African mole-rats (Family Bathyergidae). *Mol Ecol* 13: 613-629.

Fischer JH, Freake MJ, Borland SC & Phillips JB (2001) Evidence for the use of magnetic map information by amphibian. *Anim Behav* 62: 1–10.

Fleissner G, Holtkamp-Rötzler E., Hanzlik, M, Winklhofer M, Fleissner Gü, Petersen N & Wiltschko W (2003) Ultrastructural analysis of a putative magnetoreceptor in the beak of homing pigeons. *J Comp Neurol* 458: 350-360.

Francescoli G (2000) Sensory capabilities and communication in subterranean mammals. In: Lacey EA, Patton JL & Cameron GN (eds), Life underground, the biology of subterranean rodents. Pp 111-144, University Chicago Press, Chicago.

Giovani B, Byrdin M, Ahmad M & Brettel K (2003) Light-induced electron transfer in a cryptochrome blue-light photoreceptor. *Nat Struct Biol* 6: 489-490.

Hanzlik M, Heunemann C, Holtkamp-Rötzler E, Winkelhofer M, Petersen N & Fleissner G (2000) Superparamagnetic magnetite in the upper beak tissue of homing pigeons. *BioMetals* 13: 325–331.

Haque R, Chaurasia SS, Wessel JH, Iuvone PM (2002) Dual regulation of cryptochrome 1 mRNA expression in chicken retina by light and circadian oscillators. *NeuroReport* 13: 2247-2251.

Hecht E (2001) Optics. 4th edition. Pearson Education, Upper Saddle River, NJ.

Herdegen T & Leah JD (1998) Inducible and constitutive transcription factors in the mammalian nervous system: control of gene expression by Jun, Fos and Krox, and CREB/ATF proteins. *Brain Res Rev* 28: 370-490.

Heth G, Nevo E & Beiles A (1987) Adaptive exploratory behaviour: Differential patterns in species and sexes of subterranean mole rats. *Mammalia* 51: 27-37.

Heth G, Todrank J, Begall S, Braude S, Koch R, Zilbiger Y, Nevo E & Burda H (2002) Odour-guided foraging: "Blind" subterranean rodents do not search "blindly*". Behav Ecol Sociobiol* 52: 53-58.

Heth G & Todrank J (2007) Using odors underground. In: Begall S, Burda H & Schleich CE (eds), Subterranean rodents: News from underground. In press. Springer Verlag, Heidelberg.

Hickman GC (1979) Burrow system structure of the Bathyergid *Cryptomys hottentotus* in Natal, South Africa. *Z Säugetierk* 44: 153-162.

Holland RA, Thorup K, Vonhof MJ, Cochran WW & Wikelski M (2006) Bat orientation using Earth's magnetic field. *Nature* 444: 702.

Huerta MF & Harting JK (1984) Connectional organization of the superior colliculus. *TINS* 7: 286-289.

Hunt DM, Wilkie SE, Bowmaker JK & Poopalasundaram S (2001) Vision in the ultraviolet. *Cell Mol Lif Sci* 58: 1583-1598.

Ingram CM, Burda H & Honeycutt RL (2004) Molecular phylogenetics and taxonomy of the African mole-rats, genus *Cryptomys* and the new genus *Coetomys* Gray, 1864. *Mol Phyl Evol* 31: 997-1014.

Jacobs GH (1993) The distribution and nature of colour vision among the mammals. *Biol Rev* 68: 413-471.

Jacobs GH, Neitz J & Deegan JF (1991) Retinal receptors in rodents maximally sensitive to ultraviolet light. *Nature* 353: 655-656.

Jeffery KJ (2003) The neurobiology of spatial behaviour. Oxford University Press, Oxford.

Johannesson-Gross K (1988) Lernversuche in einer Zweifachwahlapparatur zum Hell-Dunkel-Sehen des Maulwurfs (*Talpa europaea* L.). *Z Säugetierk* 53: 193-201.

Johnsen S & Lohmann KJ (2005) The physics and neurobiology of magnetoreception. *Nat Neurosci Rev* 6: 703-712.

Jung M, Wiener SI & McNaughton BL (1994) Comparison of spatial firing characteristics of units in dorsal and ventral hippocampus of the rat. *J Neurosci* 14: 7347-7356.

Kaernbach C & Scheibelhofer G (2006) Ein retinales Phänomen beim Betrachten eines Lichtpunkts. Poster presented at the 9th Wahrnehmungskonferenz, Tübingen.

Kalmijn AJ (1978) Electric and magnetic sensory world of sharks, skates and rays. In: Hodgson FS & Mathewson RF (eds), Sensory biology of sharks, skates and rays. Pp 507-528, Office Naval Res., Arlington, VA.

Kandel ER, Schwartz JH & Jessell TM (1995) Neurowissenschaften : eine Einführung. Kandel ER, Schwartz JH & Jessell TM (eds). Spektrum Akademischer Verlag, Heidelberg, Berlin, Oxford.

Keeton WT (1971) Magnets interfere with pigeon homing. *PNAS USA* 68: 102-106.

Kelber A & Roth LSV (2006) Nocturnal colour vision – not as rare as we might think. *J Exp Biol* 209: 781-788.

Kellie A, Dain SJ & Banks PB (2004) Ultraviolet properties of Australian mammal urine. *J Comp Physiol A* 190: 429-435.

Kimchi T& Terkel J (1999) Magnetic orientation by blind mole rats in a labyrinth. *Isr J Zool* 45: 318.

Kimchi T & Terkel J (2001) Magnetic compass orientation in the blind mole rat *Spalax ehrenbergi*. *J Exp Biol* 204: 751-758.

Kimchi T, Etienne AS & Terkel J (2004) A subterranean mammal uses the magnetic compass for path integration. *PNAS USA* 101: 1105-1109.

Kirschvink JL (1983) Biogenic ferrimagnetism: a new biomagnetism. In: Williamson SJ (ed), Biomagnetism. Pp 501-531. Plenum Press, New York.

Kirschvink JL & Gould JL (1981) Biogenic magnetite as a basis for magnetic field detection in animals. *BioSystems* 13: 181-201.

Kirschvink JL, Jones DS & MacFadden BJ, eds. (1985) Magnetite Biomineralization and Magnetoreception in Organisms. Plenum Press, New York.

Kirschvink JL, Walker MM & Diebel CE (2001) Magnetite-based magnetoreception. *Curr Op Neurobiol* 11: 462-467.

Klinowska M (1988) Catacean navigation and geomagnetic fields. *J Navigation* 41: 52-71.

Kock D, Ingram CM, Frabotta LJ, Honeycutt RL & Burda H (2006) On the nomenclature of Bathyergidae and *Fukomys* n. gen. (Mammalia: Rodentia). *Zootaxa* 1142: 51-55.

Koivula M, Koskela E & Viitala J (1999) Sex and age-specific differences in ultraviolet reflectance of scent marks of bank voles (*Clethrionomys glareolus*). *J Comp Physiol A* 185: 561-564.

Lanza R & Meloni A (2006) The Earth's magnetism. An introduction for geologists. Springer, Berlin, Heidelberg, New York.

Leask M (1977) A physicochemical mechanism for magnetic field detection by migratory birds and homing pigeons. *Nature* 267: 144-145.

Leask MJM (1978) Primitive models of magnetoreception. In: Schmidt-Koenig K, Keeton WT (eds), Animal migration, navigation and homing. Pp 318-322, Springer Verlag, Berlin, Heidelberg, New York.

Light P, Salmon M & Lohmann KJ (1993) Geomagnetic orientation of loggerhead turtles: evidence for a an inclination compass. *J Exp Biol* 182: 1-10.

Lipson SG, Lipson HS & Tannhauser DS (1997) Optik. Springer Verlag, Berlin, Heidelberg.

Lohmann KJ & Johnsen S (2000) The neurobiology of magnetoreception in vertebrate animals. *TINS* 23(4): 153-159.

Lohmann KJ & Lohmann CMF (1992) Orientation to oceanic waves by green turtle hatchlings. *J Exp Biol* 171: 1-13.

Lohmann KJ & Lohmann CMF (1996) Orientation and open-sea navigation in sea turtles. *J Exp Biol* 199: 73-81.

Lohmann KJ & Lohmann CMF (2006) Sea turtles, lobsters, and oceanic magnetic maps. *Mar Fresh Behav Physiol* 39: 49–64.

Lovegrove BG, Körtner Gü & Körtner Ge (1992) The magnetic compass orientation of the burrows of the Damara mole-rat *Cryptomys damarensis* (Bathyergidae). *J Zool Lond* 226: 631-633.

Lowenstam HA (1962) Magnetite in denticle capping in recent chitons (Polyplacophora). *Geol Soc Am Bull* 73: 435-438.

Luna F & Antinuchi CD (2007) Effect of tunnel inclination on digging energetics in the tuco-tuco, Ctenomys talarum (Rodentia: Ctenomyidae). *Naturwiss* 94: 100-106.

Madden RM & Phillips JB (1987) Failure to demonstrate magnetic field sensitivity in two species of small mammal. *Anim Learn Behav* 15: 130-134.

Marhold S, Wiltschko W & Burda H (1997a) A magnetic polarity compass for direction finding in a subterranean mammal. *Naturwiss* 84: 421-423.

Marhold S, Burda H, Kreilos I & Wiltschko W (1997b) Magnetic orientation in common molerats from Zambia. In: Orientation and Navigation: Birds, Humans and Other Animals. Paper No 5. Royal Institute of Navigation, Oxford.

Mason MJ & Narins PM (2001) Seismic signal by fossorial mammals. *Am Zool* 41: 1171-1184.

Mather JG (1985) Magnetoreception and the search for magnetic material in rodents. In: Kirschvink JL, Jones DS & MacFadden BJ (eds), Magnetite Biomineralization and Magnetoreception in Organisms. Pp. 509-533, Plenum Press, New York, London.

Mather JG & Baker RR (1981) Magnetic sense of direction in woodmice for route-based navigation. *Nature* 291: 152-155.

Mattis DC (1965) The theory of magnetism. An Introduction to the study of cooperative phenomena. Harper & Row Publishers, New York.

McCree KJ (1981) Photosynthetically active radiation. In: Lange OL, Nobel PS, Osmond CB & Ziegler H (eds.), Encyclopedia of Plant Physiology, Vol. 12 A. Pp. 41-55. Springer, Berlin.

Merkel FW (1980) Orientierung im Tierreich. Grundbegriffe der modernen Biologie, Bd. 15. Fischer, Stuttgart, New York.

Meyer CG, Holland KN & Papastamatiou YP (2005) Sharks can detect changes in the geomagnetic field. *J R Soc Interface* 2: 129-130.

Miyamoto Y & Sancar A (1998) Vitamin B2-based blue-light photoreceptors in the retinohypothalamic tract as the photoactive pigments for setting the circadian clock in mammals. *PNAS USA* 95: 6097-6102.

Middendorf A von (1859) Die Isepiptesen Russlands. Grundlagen zur Erforschung der Zugzeiten und Zugrichtungen der Vögel Russlands. *Mémoires de l'Académie Impériale des Sciences de Saint-Pétersbourg* 6ème série; Sciences Mathématiques, Physiques et Naturelles, Tome X et Dernier, 2nde partie: Sciences Naturelles, Tome VIII et dernier: 1-143.

Möller A (2006) Cryptochrom als potentielles Rezeptormolekül für die lichtabhängige Magnetkompassorientierung von Zugvögeln. Dissertationsschrift im Fachbereich Biowissenschaften, Johann Wolfgang Goethe-Universität, Frankfurt am Main.

Möller A, Sagasser S, Wiltschko W & Schierwater B (2004) Retinal cryptochrome in a migratory passerine bird: a possible transducer for the avian magnetic compass. *Naturwiss* 91: 585-588.

Mora CV, Davison M, Wild JM & Walker MM (2004) Magnetoreception and its trigeminal mediation in the homing pigeon. *Nature* 432: 508-511.

Mouritsen H, Janssen-Bienhold U, Liedvogel M, Feenders G, Stalleicken J, Dirks P & Weiler R (2004) Cryptochromes and neuronal-activity markers colocalize in the retina of migratory birds during magnetic orientation. *PNAS USA* 101: 14294-1429.

Muheim R, Edgar NM, Sloan KA & Phillips JB (2006) Magnetic compass orientation in C57BL/6 mice. *Learn Behav* 34(4): 366-373.

Muller R (1996) A quarter of a century of place cells. *Neuron* 17: 813-822

Munro U, Munro JA, Phillips JB, Wiltschko R & Wiltschko W (1997a) Evidence for a magnetite-based navigational 'map' in birds. *Naturwiss* 84: 26-28.

Munro U, Munro JA, Phillips JB & Wiltschko W (1997b) Effect of wavelength of light and pulse magnetization on different magnetoreception systems in a migratory bird. *Austr J Zool* 45: 189-198.

Narins PM, Lewis ER, Jarvis JUM & O'Riain J (1997) The use of seismic signals by fossorial southern African mammals: A neuroethological gold mine. *Brain Res Bull* 44: 641-646 .

Němec P, Altmann J, Marhold S, Burda H & Oelschläger HA (2001) Magnetotopic organization in the superior colliculus: involvement of a brain structure in magnetoreception. *Science* 294: 366-368.

Němec P, Burda H & Peichl L (2004) Subcortical visual system of the African mole-rat *Cryptomys anselli*: to see or not to see? *Europ J Neurosci* 20: 757-768.

Němec P, Burda H & Oelschläger HA (2005) Towards the neural nature of magnetoreception: A neuroanatomical approach. *Naturwiss* 92: 151-157.

Němec P, Cveková P, Burda H, Benada O & Peichl L (2007). Visual Systems and the role of vision in subterranean rodents: Diversity of retinal properties and visual system designs In: Begall S, Burda H & Schleich CE (eds), Subterranean rodents: News from underground. In press. Springer Verlag, Heidelberg.

Nevo E (1999) Mosaic evolution of subterranean mammals: regression, progression, and global convergence. Oxford University Press, Oxford.

Oakley TH (2003) The eye as a replicating and diverging, modular developmental unit. *TREE* 18 (12): 623-627.

Oelschläger HA & Northcutt RG (1992) Immunocytochemical localization of Luteinizing Hormone-Releasing Hormone (LHRH) in the nervus terminalis and brain of the big brown bat, *Eptesicus fuscus*. *J Comp Neurol* 315: 344-363.

Oelschläger HHA, Nakamura M, Herzog M & Burda H (2000) Visual system labeled by c-Fos immunohistochemistry after light exposure in the ‚blind' subterranean Zambian mole-rat (*Cryptomys anselli*). *Brain Behav Evol* 55: 209-220.

O'Keefe J & Nadel L (1978) The hippocampus as a cognitive map. Oxford University Press, Oxford.

Olcese J, Reuss J & Vollrath L (1985) Evidence for the involvement of the visual system in mediating magnetic field effects on pineal melatonin synthesis in the rat. *Brain Res* 333: 382-384.

Olcese J, Reuss S, Stehle J, Steinlechner S & Vollrath L (1988) Responses of the mammalian retina to experimental alteration of the ambient magnetic field. *Brain Res* 448: 325-330.

Park TJ, Catania KC, Samaan D & Comer CM (2007). Convergent notes from the underground: Somatosensory organization of naked mole-rats (and those similarly challenged) emphasizes the adaptability of brain and behavior. In: Begall S, Burda H & Schleich CE (eds), Subterranean rodents: News from underground. In press. Springer Verlag, Heidelberg.

Paxinos G & Watson C (1998) The rat brain in stereotaxis coordinates. 4th edition. Academic Press, San Diego.

Pedrotti FL & Pedrotti LS (1993) Introduction to optics. 2nd edition.Prentice-Hall International Limited, London.

Peichl L (2005) Diversity of mammalian photoreceptor properties: adaptations to habitat and lifestyle? *Anatom Rec A* 287: 1001-1012.

Peichl L, Němec P & Burda H (2004) Unusual cone and rod properties in subterranean African mole-rats (Rodentia, Bathyergidae). *Europ J Neurosci* 19: 1545-1558.

Phillips JB (1986) Two magnetoreception pathways in a migratory salamander. *Science* 233: 765-767.

Phillips JB & Borland SC (1992a) Behavioral evidence for the use of a light-dependent magnetoreception mechanism by a vertebrate. *Nature* 359: 142-144.

Phillips JB & Borland SC (1992b) Magnetic compass orientation is eliminated under near-infra-red light in the eastern red-spotted newt *Notophthalmus viridescens*. *Anim Behav* 44: 796-797.

Phillips JB & Borland SC (1992c) Wavelength specific effects of light on magnetic compass orientation of the eastern red-spotted newt *Notophthalmus viridescens*. *Ethol Ecol Evol* 4: 33-42.

Phillips JB, Deutschlander ME, Freake MJ & Borland SC (2001) The role of extraocular photoreceptors in newt magnetic compass orientation: evidence for parallels between light-dependent magnetoreception and polarized light detection in vertebrates. *J Exp Biol* 204: 2543-2552.

Phillips JB, Freake MJ, Fischer JH & Borland SC (2002) Behavioral titration of a magnetic map coordinate. *J Comp Physiol A* 188: 157-160.

Phillips JB, Schmidt-Koenig K & Muheim R (2006) True Navigation: Sensory Basis of Gradient Maps. In: Brown MF & Cook RG (eds), Animal Spatial Cognition: Comparative, Neural and Computational Approaches. [On-line]. Available: www.pigeon.psy.tufts.edu/asc/phillips/.

Poduschka W (1978) Zur Frage der Wahrnehmung von Lichtreizen durch die Mullratte, *Cryptomys hottentotus* (Lesson, 1826). *Säugetierk Mitt* 26: 269-274.

Press F & Siever R (2003) Allgemeine Geologie. 3rd edition. Spektrum Akademischer Verlag, Heidelberg, Berlin, Oxford.

Presti D & Pettigrew JD (1980) Ferromagnetic coupling to muscle receptors as a basis for geomagnetic field sensitivity in animals. *Nature* 285: 99-101.

Quinn TP, Merrill RT & Brannon EL (1981) Magnetic field detection in sockeye salmon. *J Exp Zool* 217: 137-142.

Rado R, Terkel J & Wollberg Z (1998) Seismic communication signals in the blind mole-rat (*Spalax ehrenbergi*): electrophysiological and behavioural evidence for their processing by the auditory system. *J Comp Physiol A* 183: 503-511.

Reuss S, Semm P & Vollrath L (1983) Different types of magnetically sensitive cells in the rat pineal gland. *Neurosci Lett* 40: 23-26.

Reuss S & Olcese J (1986) Magnetic field effects on rat pineal gland: role of retinal activation by light. *Neurosci Lett* 64: 97-101.

Riccio AP & Goldman BD (2000a) Circadian rhythms of locomotor activity in naked mole-rats (*Heterocephalus glaber*). *Physiol Behav* 71: 1-13.

Riccio AP & Goldman BD (2000b) Circadian rhythms of body temperature and metabolic rate in naked mole-rats. *Physiol Behav* 71: 15-22.

Ritz T, Adem, S & Schulten K (2000) A model for photoreceptor-based magnetoreception in birds. *Biophys J* 78: 707-718.

Ritz T, Phillips JB & Dommer DH (2002) Shedding light on vertebrate magnetoreception. *Neuron* 34: 503-506.

Ritz T, Thalau P, Phillips J, Wiltschko R & Wiltschko W (2004) Resonance effects indicate a radical-pair mechanism for avian magnetic compass. *Nature* 429: 177-180.

Rogers L & Andrew RJ (2002) Comparative Vertebrate Lateralization. Rogers L & Andrew RJ (eds). Cambridge University Press, Cambridge.

Sancar A (1994) Structure and function of DNA photolyase. *Biochemistry* 33: 2-9.

Sancar A (2003) Structure and Function of DNA Photolyase und Cryptochrome Blue-Light Photoreceptors. *Chem Rev* 103: 2203-2337.

Sanyal S, Jansen HG, De Grip WJ, Nevo E & De Jong WW (1990) The eye of the blind mole rat, *Spalax ehrenbergi*: rudiment with hidden function? *Invest Ophthalmol Vis Sci* 31: 1398–1404.

Sauvé JP (1988) Analyse de l'orientation initiale dans une expérience de retour au gîte chez le mulot, *Apodemus sylvaticus*. *Sci Tech Anim Lab* 13: 9-91.

Scharff A & Grütjen O (1997) Evidence for above ground activity of Zambian mole-rats (*Cryptomys*, Bathyergidae, Rodentia). *Z Säugetierk* 62: 253-254.

Scharff A, Locker-Grütjen O, Kawalika M & Burda H (2001) Natural history of the giant mole-rat, *Cryptomys mechowi* (Rodentia: Bathyergidae), from Zambia. *J Mammal* 82: 1003-1015.

Schleich C & Antinuchi CD (2004) Testing Magnetic Orientation in a Solitary Subterranean Rodent *Ctenomys talarum* (Rodentia: Octodontidae). *Ethology* 110: 485-495.

Schulten K & Windemuth A (1986) Model for a physiological magnetic compass. In: Maret G, Boccara N & Kiepenheuer J (eds), Biophysical effects of steady magnetic fields. Pp 99-106, Springer Verlag, Berlin, Heidelberg, New York.

Schwartz J & Begley S (2003) The Mind and the Brain: Neuroplasticity and the Power of Mental Force. ReganBooks from Harper Collins Publishers, New York.

Semm P, Schneider T & Vollrath L (1980) Effects of an earth-strength magnetic field on electrical activity in pineal cells. *Nature* 288: 607-608.

Semm P & Demaine C (1986) Neurophysiological properties of magnetic cells in the pigeon's visual system. *J Comp Physiol A* 159: 619-625.

Semm P, Nohr D, Demaine C & Wiltschko W (1984) Neural basis of the magnetic compass: interaction of visual, magnetic and vetsibular inputs in the pigeons brain. *J Comp Physiol A* 155: 283-288.

Semm P & Beason C (1990) Responses to small magnetic variations by the trigeminal system of the bobolink. *Brain Res Bull* 25: 735-740.

Sharp PE (2002) The neural basis of navigation. Evidence from single cell recording. Kluver Academic Publishers, Boston.

Sharp PE, Blair HT & Cho JW (2001) The anatomical and computational basis of the rat head-direction cell signal. *TINS* 24: 289-294.

Shcherbakov VP & Winklhofer M (1999) The osmotic magnetometer: a new model for magnetite-based magnetoreceptors in animals. *Eur Biophys J* 28: 380–392.

Skiles DD (1985) The geomagnetic field: its nature, history, and biological relevance. In: Kirschvink JL, Jones DS & MacFadden BJ (eds), Magnetite Biomineralization and Magnetoreception in Organisms. Pp 43-102, Plenum Press, New York, London.

Stehle J, Reuss S, Schroeder H, Henschel M & Vollrath L (1988) Magnetic field effects on pineal N-acetyltransferase activity and melatonin content in the gerbil—the role of pigmentation and sex. *Physiol Behav* 44: 91-94.

Šumbera R, Burda H, Chitaukali WN & Kubova J (2003) How adaptive is the pattern of burrowing in subterranean rodents? The case of the solitary silvery mole-rat *Heliophobius argenteocinereus*, Bathyergidae. *Naturwiss* 90: 370-373.

Šumbera R, Chitaukali WN & Burda H (2007) Biology of the silvery mole-rat (*Heliophobius argenteocinereus*).Why study a neglected subterranean rodent species? In: Begall S, Burda H & Schleich CE (eds), Subterranean rodents: News from underground. In press. Springer Verlag, Heidelberg.

Sun Q, Yoda K, Suzuki M & Suzuki H (2003) Vascular tissue in the stem and roots of woody plants can conduct light. *J Exp Bot* 54 (387): 1627-1635.

Szél Á, Lukáts Á, Fekete T, Szepessy Z & Röhlich P (2000) Photoreceptor distribution in the retinas of subprimate mammals. *J Opt Soc Am A* 17: 568-579.

Taube JS (1998) Head direction cells and the neurophysiological basis for a sense of direction. *Progr Neurobiol* 55: 225-256.

Thalau P, Ritz T, Stapput K, Wiltschko R & Wiltschko W (2005) Magnetic compass orientation of migratory birds in the presence of a 1.315 MHz oscillating field. *Naturwiss* 92: 86-90.

Tipler P (2004) Physics for Scientists and Engineers: Electricity, Magnetism, Light, and Elementary Modern Physics. 5th edition. W.H. Freeman and Co. Publishers, New York.

Vallortigara G (2000) Comparative neuropsychology of the dual brain: a stroll through animals' left and right perceptual worlds. *Brain Lang* 73: 189–219.

Van Daele PAAG, Dammann P, Kawalika M, Meier J-L, Van De Woestijne C & Burda H (2004) Cromosomal diversity in *Cryptomys* mole-rats (Rodentia: Bathyergidae) in Zambia with the description of new karyotypes. *J Zool Lond* 264: 317-326.

Vasicek CA, Malpaux B, Fleming TA & Bennett NC (2005) Melatonin secretion in the Mashona mole-rat, *Cryptomys darlingi* – influence of light on rhythmicity. *Physiol Behav* 83, 689-697.

Viguier C (1882) Le sens de l'orientation et ses organs chez les animaux et chez l'homme. *Rev Phil France et Etranger* 14: 1-36.

Viitala J, Korpimäki E, Palokangas P & Kolvula M (1995) Attraction of kestrels to vole scent marks visible in ultraviolet light. *Nature* 373: 425-427.

Walcott CF, Gould JL & Kirschvink JL (1979) Pigeons have magnets. *Science* 205:1027-1029.

Walker MM, Diebel CE, Haugh CV, Pankhurst PM, Montogomery JC & Green CR (1997) Structure and function of the vertebrate magnetic sense. *Nature* 390: 371-376.

Walker MM, Dennis TE & Kirschvink JL (2002) The magnetic sense and its use in long-distance navigation by animals. *Curr Op Neurobiol* 12: 735-744.

Welker H, Semm P, Willig R, Commentz J, Wiltschko W & Vollrath L (1983) Effects of an artificial magnetic field on serotonin N-acetyltranferase activity and melatonin content of the rat pineal gland. *Exp Brain Res* 50: 426-432.

Werner SJ, Nolte DL & Provenza FD (2005) Proximal cues of pocket gopher burrow plugging behavior: Influence of light, burrow openings, and temperature. *Physiol Behav* 85, 340-345. doi: 10.1016/j.physbeh.2005.04.024.

Williams MN & Wild JM (2001) Trigeminally innervated iron-containing structures in the beak of homing pigeons and other birds. *Brain Res* 889: 243–246.

Wiltschko R & Wiltschko W (1995) Magnetic Orientation in Animals. Springer, Berlin, Heidelberg, New York.

Wiltschko R & Wiltschko W (2006) Magnetoreception. *BioEssays* 28: 157–168.

Wiltschko R, Ritz T, Stapput K, Thalau P & Wiltschko W (2005) Two different types of light-dependent responses to magnetic fields in birds. *Curr Biol* 15: 1518-1523.

Wiltschko W & Gwinner E (1974) Evidence for an innate magnetic compass in Garden Warblers. *Naturwiss* 61: 406.

Wiltschko W & Merkel FW (1966) Orientierung zugunruhiger Rotkehlchen im statischen Magnetfeld. *Verhandl Dtsch Zool Ges* 59: 362-367.

Wiltschko W & Wiltschko R (1972) Magnetic compass of European Robins. *Science* 176: 62-64.

Wiltschko W & Wiltschko R (1995) Migratory orientation of European Robins is affected by the wavelength of light as well as by a magnetic pulse. *J Comp Physiol A* 177: 363-369.

Wiltschko W & Wiltschko R (2001) Light dependent magnetoreception in birds: the behavior of European robins, *Erithacus rubecula*, under monochromatic light of various wavelengths. *J Exp Biol* 204: 3295-3302.

Wiltschko W & Wiltschko R (2002) Magnetic compass orientation on birds and its physiological basis. *Naturwiss* 89: 445-452.

Wiltschko W & Wiltschko R (2005) Magnetic orientation and magnetoreception in birds and other animals. *J Comp Physiol A* 191: 675-693.

Wiltschko W, Munro U, Ford H & Wiltschko R (1993) Magnetic inclination compass: A basis for the migratory orientation of birds in the northern and southern hemisphere. *Experientia* 49: 167-170.

Wiltschko W, Traudt J, Güntürkün O, Prior H & Wiltschko R. (2002) Lateralization of magnetic compass orientation in a migratory bird. *Nature* 419: 467-470.

Wiltschko W, Munro U, Ford H & Wiltschko R (2003) Lateralisation of magnetic compass orientation in silvereyes, *Zosterops lateralis*. *Austr J Zool* 51: 597-602.

Winklhofer M, Holtkamp-Rötzler E, Hanzlik M, Fleissner G & Petersen N (2001) Clusters of superparamagnetic particles in the upper-beak skin of homing pigeons: evidence of a magnetoreceptor? *Eur J Mineral* 13: 659-669.

Winter Y, López J & von Herlversen O (2003) Ultraviolet vision in a bat. *Nature* 425: 612-614.

Witter MP & Amaral DG (2004) Hippocampal formation. In: Paxinos G (ed), The Rat Nervous System, 3rd edition. Pp 443-493. Academic Press, New York.

Yorke E (1979) A possible magnetic transducer in birds. *J Theor Biol* 77: 101-105.

Zeki SM (1994) Das geistige Abbild der Welt. In: Physiologie der Sinne. Pp 104-113. Spektrum Akademischer Verlag, Heidelberg, berlin.

Zwahr A (1993): Der Brockhaus, F.A. Brockhaus, Mannheim.

Zhu H & Green CB (2001) Three cryptochromes are rhythmically expressed in *Xenopus laevis* retinal photoreceptors. *Mol Vis* 7: 210-215.

VI APPENDIX

A Abbreviations

Physics & Mathematics

nm	nanometre
cm	centimetre
m	metre
nT	nanotesla
µT	microtesla
T	tesla
s	second
h	hour
ml	millilitre
µmol	micro mol
°	degree
°C	degree Celsius
λ	wave length in nanometre
Δ	deviation/difference
%	percentage
>	bigger than
<	smaller than
=	equals
E	East
F	MF vector = MF direction
H	Magnetic Field
J_i	induced Magnetization
J_r	resulting Magnetization
N	North
S	South
W	West

Statistics

X^2	Chi-square value
P	*P*-value of probability of error
*	$P<0.05$, probability of error lower than 5%
**	$P<0.01$, probability of error lower than 1%
***	$P<0.001$, probability of error lower than 0.1%
med.	median
ns	not significant; $P>0.05$, probability of error higher than 5%
t	*t*-value for paired *t*-test
r_A	length of mean vector of mean direction of all tested mole-rat pairs after one experiment
α_A	mean direction of all tested mole-rat pairs after one experiment
α_P	mean direction of six tested mole-rat pairs after four experiments
r_P	length of mean vector of mean direction of six tested mole-rat pairs after four experiments

ICC

AB	antibody
1°AB	primary antibody (analogous: 2°, 3° AB)
ABC	Avidin-biotin complex
BSA	Bovine serum albumin
c-fos	an immediate early gene, second messenger
DAB	3,3-diaminobenzidine tetrahydrochloride
Fos	antigene/product of the gene c-fos; its expression can be visualized by application of the right antibody
H_2O_2	hydrogen peroxide
ICC	immunocytochemistry (Immunohistochemistry)
IEG	immediate early gene, e.g. c-*fos*
ITF	Inducible Transcription Factor
PB	phosphate buffer
PBS	phosphate-buffered saline solution
PFA	paraformaldehyde: 4% paraformaldehyde in 0.1 M PB, pH 7.4
"SAPJE"	PBS with 0.1% BSA and 0.5% Triton

Others

C	control
e.g.	*exempli gratia* (for instance)
EM	electromagnetic
fig.	figure
i.e.	*id est* (that is)
IR	infrared (Light)
L-cone	cone with visual pigment (opsin) sensitive to long wavelengths
L-opsin	visual pigment sensitive to long wavelengths
MF	magnetic field
MHz	megahertz
MSP	Micro-Spectro-Photometry (MSP)
N	number of tested animals
NRM	Natural Remanent Magnetization
PNA	peanut agglutinin; a cone-specific marker
TF	transcription factor
RPM	Radical Pair Model
SD	single domain
S-cone	Cone with visual pigment (opsin) sensitive to short wavelengths
S-opsin	visual pigment sensitive to short wavelengths
SP	superparamagnetic
tab.	table
TM	transduction mechanism

B Figure legends

C Table legends

D Wavelength spectra

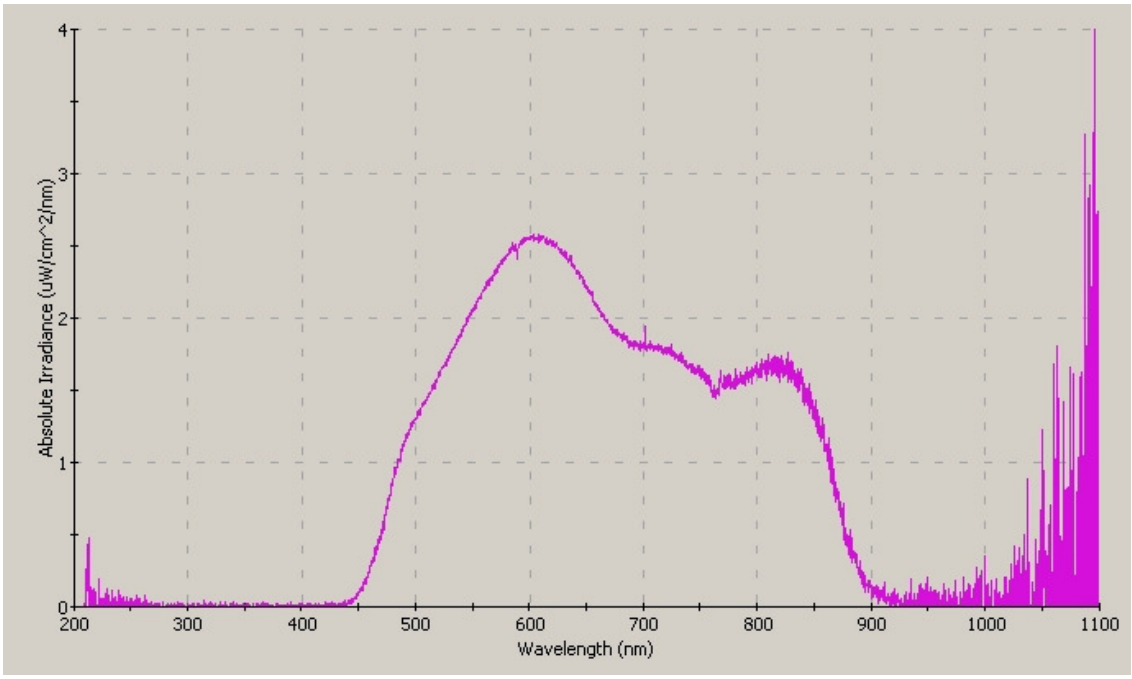

Fig. D1 Wavelength spectrum of white light in a tunnel opening (lamp height 60 cm).

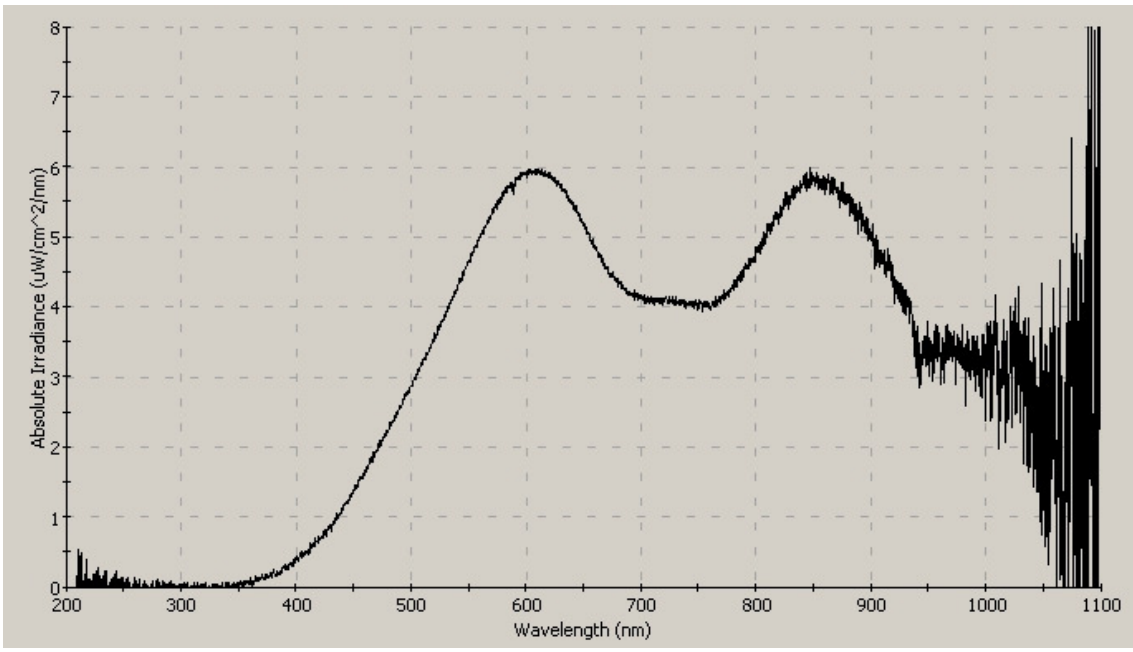

Fig. D2 Wavelength spectrum of white light in a tunnel opening (lamp height 40 cm).

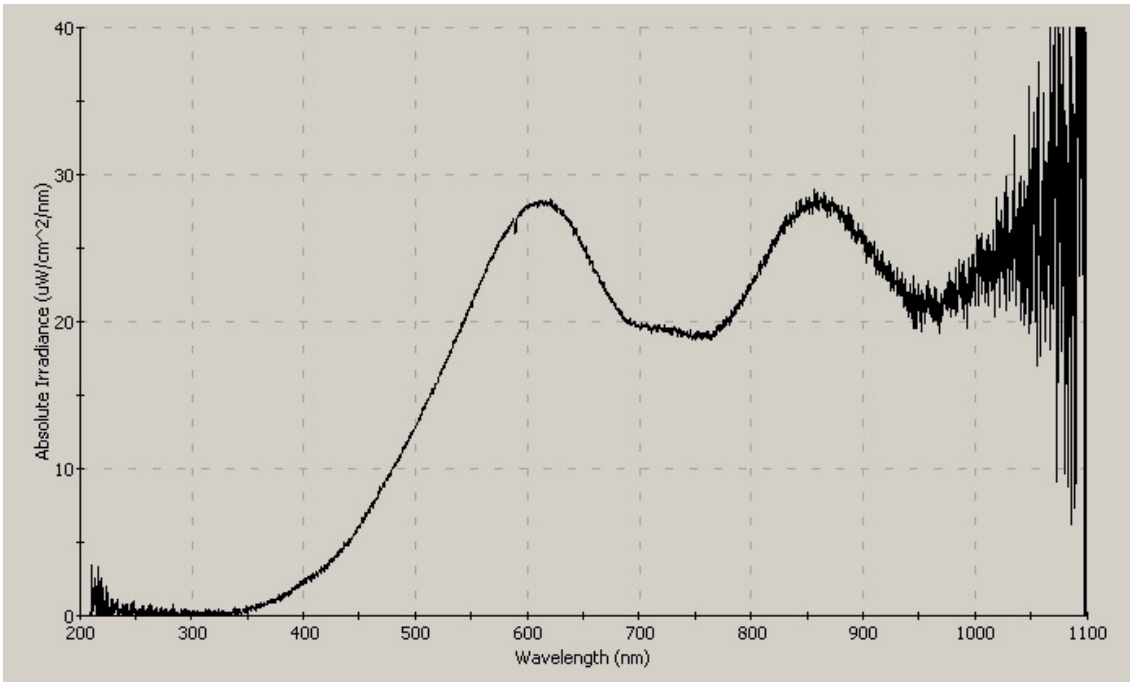

Fig. D3 Wavelength spectrum of white light in a tunnel opening (lamp height 20 cm).

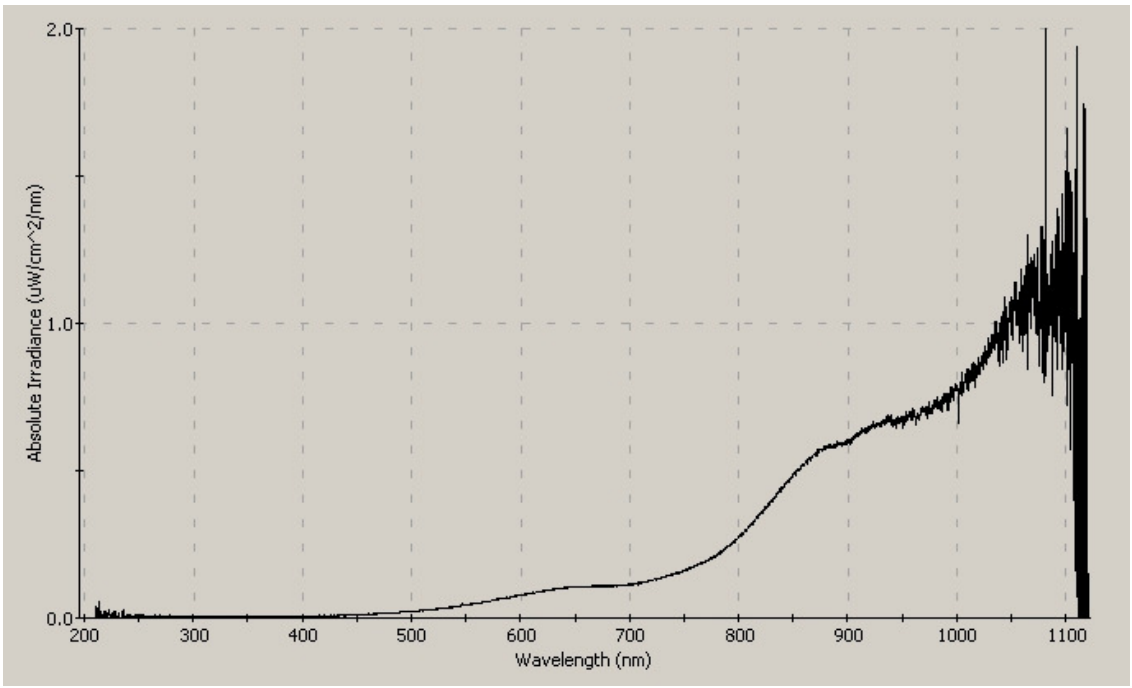

Fig. D4 Spectral attenuation of white light in a tunnel (10 cm distance).

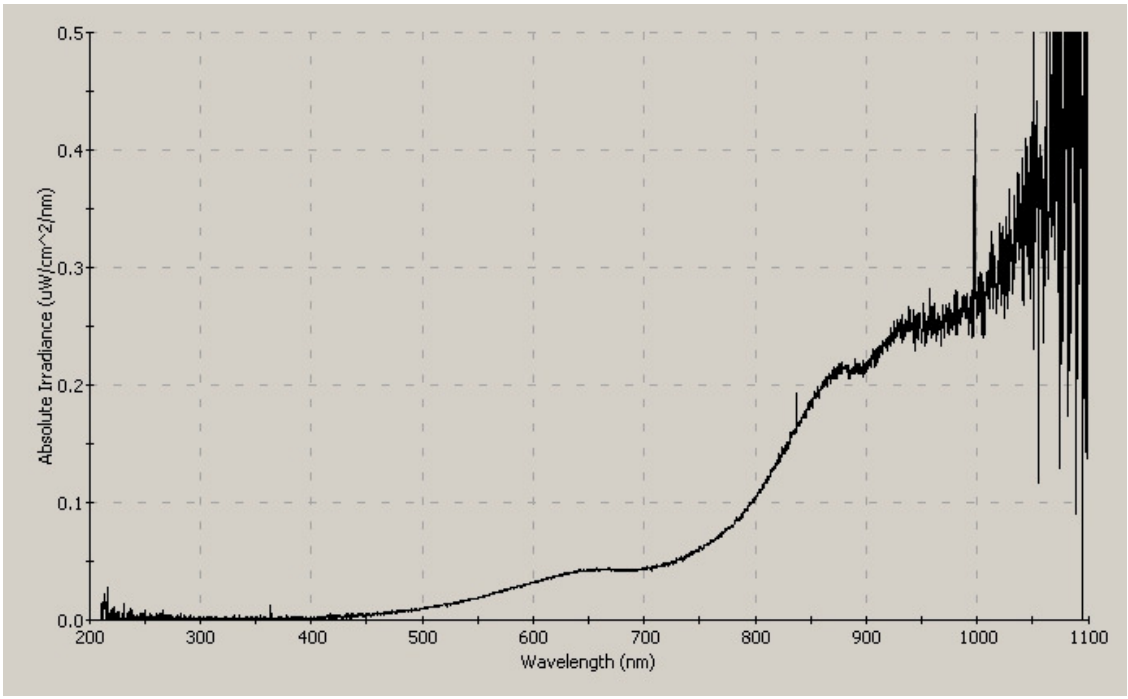

Fig. D5 Spectral attenuation of white light in a tunnel (20 cm distance).

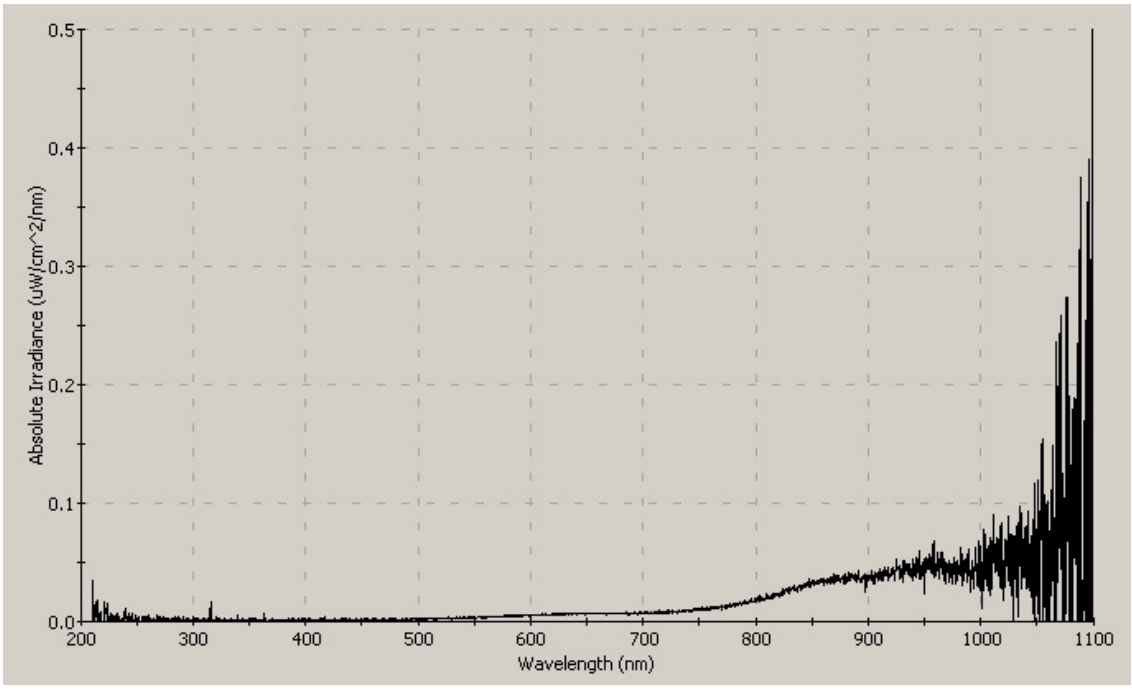

Fig. D6 Spectral attenuation of white light in a tunnel (50 cm distance).

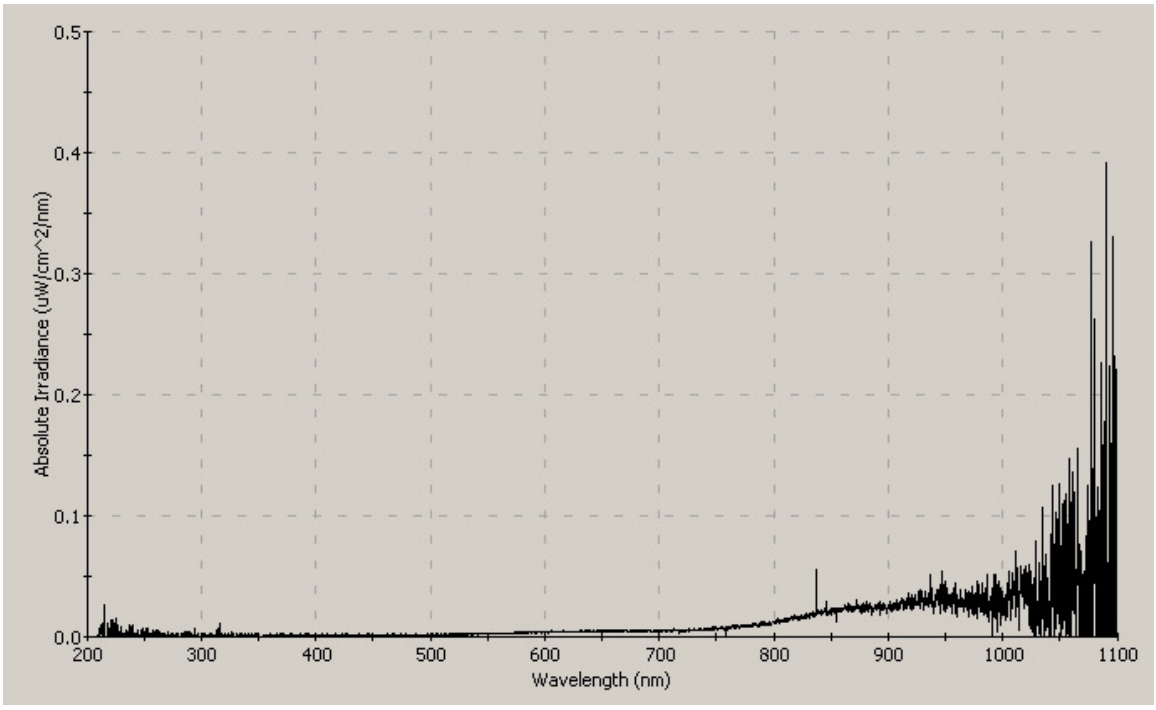

Fig. D7 Spectral attenuation of white light in a tunnel (60 cm distance).

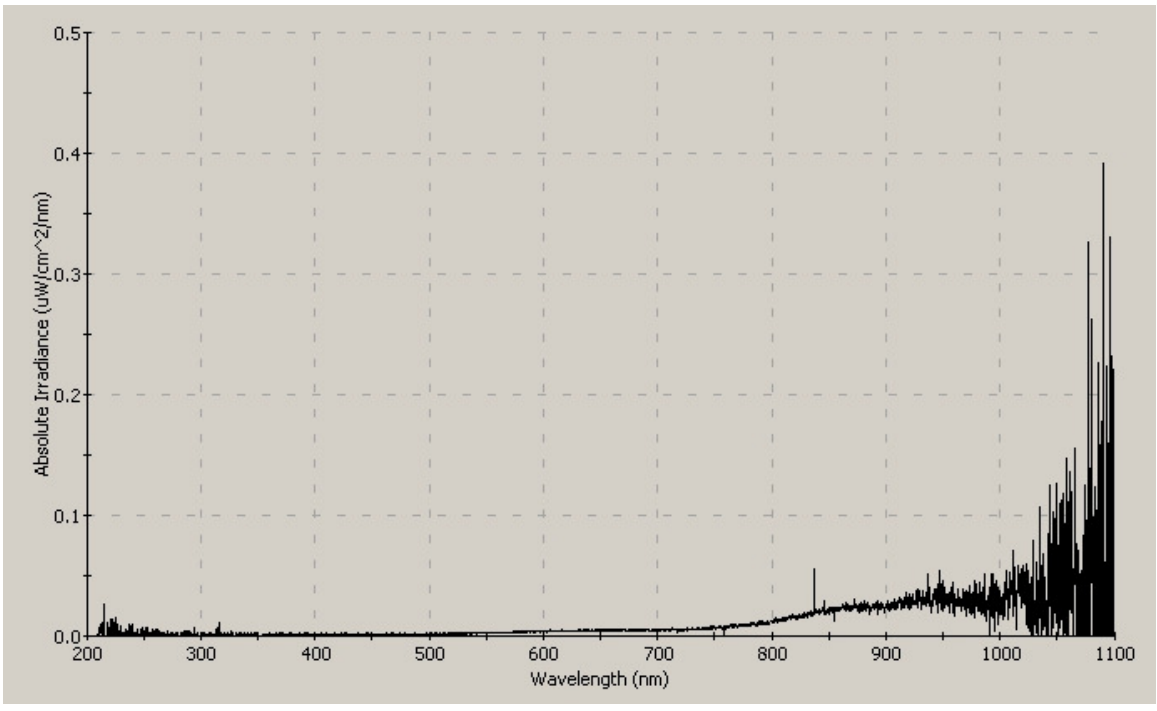

Fig. D8 Spectral attenuation of white light in a tunnel (65 cm distance).

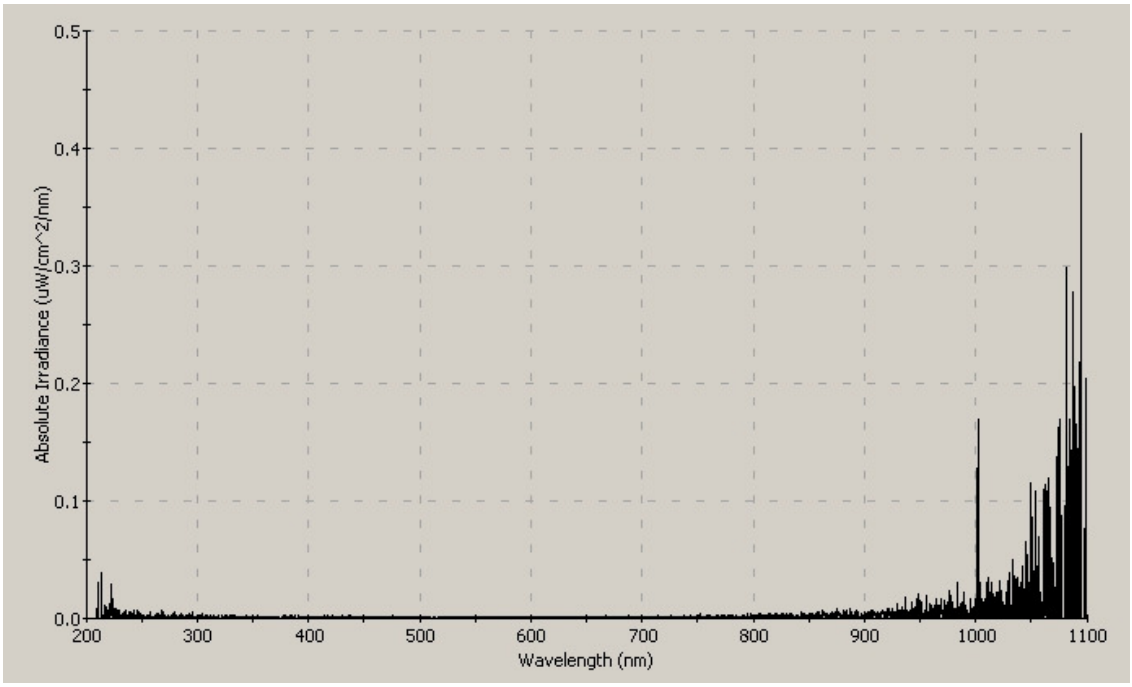

Fig. D9 Spectral attenuation of white light in a tunnel (70 cm distance).

E The rat brain hippocampus

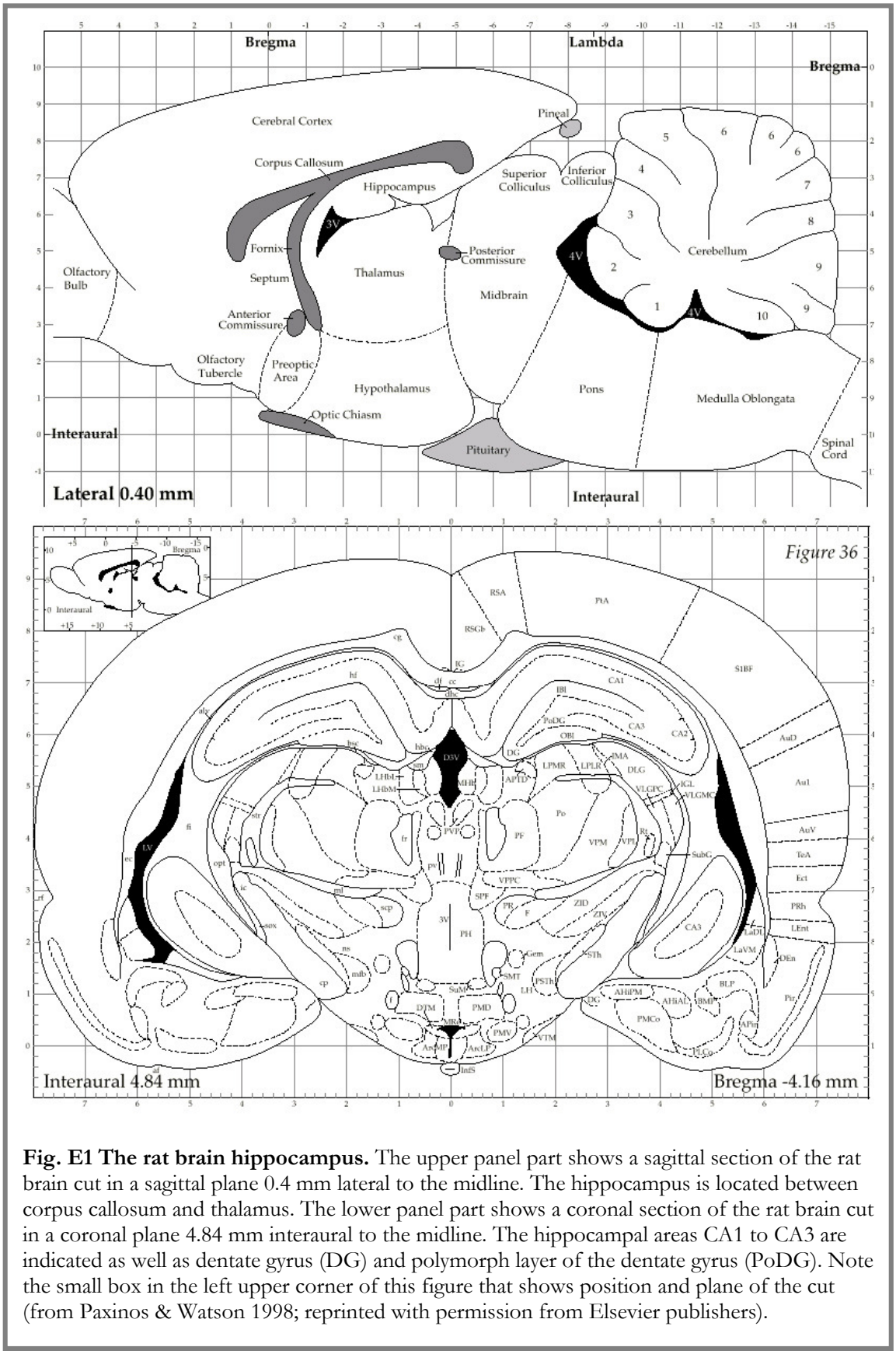

Fig. E1 The rat brain hippocampus. The upper panel part shows a sagittal section of the rat brain cut in a sagittal plane 0.4 mm lateral to the midline. The hippocampus is located between corpus callosum and thalamus. The lower panel part shows a coronal section of the rat brain cut in a coronal plane 4.84 mm interaural to the midline. The hippocampal areas CA1 to CA3 are indicated as well as dentate gyrus (DG) and polymorph layer of the dentate gyrus (PoDG). Note the small box in the left upper corner of this figure that shows position and plane of the cut (from Paxinos & Watson 1998; reprinted with permission from Elsevier publishers).

F ICC protocol

A) PERFUSION

i) PREPARATION

a) phosphate buffer saline (PBS)
b) paraformaldehyde-phosphate buffer (PFA)

Recipe for 2l phosphate buffer (PB):

2 l dH_2O + 4.32g KH_2PO_4 (Riedel-de Haen, Seelze, Netherlands) + 23.12g Na_2HPO_4 (Merck, Darmstadt, Germany).

1. Stir dH_2O.
2. Add salts.
3. Let dissolve completely; store in fridge (4°C); pH=7.3

Recipe for 2l phosphate buffer saline (0.9%) (PBS):

Dito; add 18g NaCl.

Recipe for phosphate buffer/paraformaldehyde solution (PB/PFA – fixative for perfusions):

1l **HOT** PB (0.1M) + 40g paraformaldehyde (0.1M; Serva, Heidelberg, Germany)); filtrate freshly, store at 4°C.

c) Work at stereomicroscope/binocular. 2 perfusion facilities (charge with PBS and PFA in advance); additional bottle with spare-buffer and spare-PFA; PBS+0.5 ml heparin ≈ 2500 IU heparin; tripod; large hook; trays (large and small); folding boxes; gloves (thick and thin); jar for blood & syringe for extraction by suction; catgut; jar with instruments (scissors, tweezers, tweezer scissors, clamps); canulas (needles) in several sizes (blunt and sharp); PB-bottle for rinsing; adhesive tape for animal fixation; anaesthetic (ether); jars for head and body; garbage bags; jar for lethal ether dose; first aid box.

ii) IMPLEMENTATION

a) Install perfusion equipment; rinse system with PB.
b) Thoracotomy/laparotomy; taxidermy of *Aorta ascendens*; broach the left ventricle (cardiac apex) with sharp canula of the appropriate size, protrude until marking, then insert blunt identical canula (drippy at end of hose) until in Aorta ascendes. Open up right atrium. Attach canula with clamp, pin and tape down.
c) Open hose clip → rinse (possible indicators: eye, tongue, nose)
d) Add PFA directly after rinsing. **Cave - Bubbles!**
e) Finish latest after muscles at neck become inflexible (lower jaw fixed?)
f) Close hose clip, remove canula.

iii) OPEN SKULL-ROOF *in situ*

Decapitation; store body (PFA). Total removal of meninges (imperative for gelatine embedding!) and advisably of bone (prevents from add. decalcification).

(iv) POST-FIXATION: ~12H IN FRIDGE OVERNIGHT

B) GELATINE EMBEDDING

i) DECALCIFICATION / SKULL REMOVAL

In *decal*.
Alternative: remove brain carefully from skull by breaking off small pieces of skull-bone.

ii) TRANSFER

Transfer brain into PB (exchange twice), then into PB-sucrose until subsiding.

Recipe: Dissolve 30g sucrose (Merck, Darmstadt, Germany) in 100ml PB; add 100µl NaN_3 (1% stock solution; Ferak, Berlin, Germany). = AZIDE

iii) MARKING

For subsequent orientation of sections, mark brain by small cut.

Transversal series: longitudinal notch into bulb, hemisphere & cerebellum (1 side!).
Sagittal/horizontal series: cut in cortex of one hemisphere from *sulcus interhemisphaericus* to base of temporal lobe (transversal notch).

iv) GELATINE EMBEDDING

Iced bath, spoon spatula for transfer, paraffine mould (shape and size according to sample), sucrose-gelatine (300 bloom).
Put mould into iced bath, heat gelatine in microwave for about 1 min. Dry sample well on cellulose tissue. Fill mould bottom with gelatine (let cool down, then fill up). Insert sample, position with tweezers, wait, until position is fixed; let harden.

Recipe for 200ml sucrose-gelatine:
200ml dH_2O + 20g gelatine (Type A, 300 bloom; Lot 21H0580; Sigma, St. Louis, U.S.A.). Intersperse into cold *Aqua bidest.*, let well until subsiding, heat, stir until clearly dissolved. Then add 60g sucrose (saccharose), stir; add 200 µl azide (NaN_3 – 1% stock solution - fridge). Store sucrose-gelatine in fridge.

Fixative solution PFA-Sucrose: Add 4g PFA and 30g sucrose to 100ml hot PB (always prepare freshly).

v) FIXING THE BLOCK

PFA-sucrose for 12-24h (Block subsided?)

NOTA BENE: Quality of gelatine appears MUCH better, if tissue is allowed post-fixation for 48h!

vi) TRIMMING THE BLOCK

Trim gelatine brain-block with moist, warm blade to subsequently be able to optimally orient the sample on the microtome holder. CAVE: Risk of mistaking brains!

vii) TRANSFER/STORAGE INTO PB-SUCROSE

For storage, transfer into PB-sucrose (see B-ii). Block subsided?

C) FREEZE-CUTTING

i) PREPARATION

Freeze sample in advance at –70°C if applicable (label the contact area prior to freezing!). Prepare jars for sections (24-wells or sorting boxes with 12 compartments), label wells! C-knives, 1 pair of crude tweezers, 1 pair of fine tweezers, 1 scalpel, 2 brushes no. 4, PB, azide, Tissue-Tec®, filter paper, adhesive tape, marker, scissors, spatula spoons, protocol copies; if necessary, roster of jars (wells), which harbours sections until further treatment.

Bring microtome-holder into backward position. Saturate small piece of filter paper (*Aqua bidest.*), set onto microtome-holder without bubbles. Apply the readily trimmed, *en bloc* embedded sample with Tissue-Tec® (according to designated cutting direction).

Freeze with maximal cooling capacity, isolate sample in the meantime by styrofoam-coating; fill PB into prepared jars, store in fridge.

ii) CUTTING

a) sagittal/horizontal series
b) transversal series (rostral → caudal)

Adjust plane, unspoilt position of knife, label/record positins. While cutting, optimize temperature. **Too cold**: sections will roll up. **Optimal**: sections unroll on knife like jalousie. **Too warm**: sections appear sludgy.

Chosen thickness of sections	
Number of well-plates	
Number of sections per well	
Σ of sections	

Cool well-plates with sections at around 4°C; treat sections preferably in fresh condition, otherwise add azide (1 drop per well), or store in buffer beforehand (0.05-0.1%). → Select sections for diverse AB and label with colour stickers.

D) PRIMARY INCUBATION

i) Removal of endogenous peroxidase

Removal of endogenous peroxidase through incubation of sections in H_2O_2-solution (30min).

- H_2O_2 conc. bottle (30%)
- dilute H_2O_2 with bidest. 1:100 (0.3%)

ii) Pre-incubation/pre-adsorption

Addition of homologous antigen (c-Fos) into serum of primary incubation in order to adsorb c-Fos-AB (anti-c-Fos).

iii) Adsorption control

Omit primary AB (anti-c-Fos) and subsequently treat sections identically.

- -

Chosen 1° antibodies:_____ (see aliquotation-protocol)

CAVE! Aliquote free of bubbles; dismiss pipette tip, if necessary! Use micro-litre syringes at best.

iv) Preparation and first wash

Select sections, prepare protocol.
Prepare: chilled PBS (pH 7.4); shaker, netted jars, dishes (tube cylinder), 6-well-plates, hockey-sticks. Use hockey-sticks for transferring sections from well-plates into netted jars located within dishes (short tube cylinder, filled with PBS).

Wash (3x, 10 min. each); PBS 1.5cm high in dishes on the shaker.

v) Preparation of 1°AB

In the meantime, mix 1° AB.

Example: c-Fos-aliquots
Pre-dilution 1:10 with 25 µl/aliquot (is serum pre-diluted?)

Entire dilution factor: 1:_____

Calculation for dilution (example 1:2,000, 1:10 pre-diluted); aliquots à 25µl
1 aliquot yields: 25µl x 200 = 5000µl = 5ml

►1 aliquot (25µl) → 5ml solution
►1 aliquot for 5ml equivalent to 1 compartment à appr. 10-12 sections

vi) Further washing procedure

1 wash with fresh "SAPJE" (30 min.).

***Recipe for „SAPJE"*:** 200ml PBS + 0.2g BSA + 1ml tritone; **NO** azide!

1 rinse with PBS (5 min.).

Avidin-blocking (15 min.).

1 wash with PBS (max. 5 min.).

Biotin-blocking (15 min.).

3 washes with PBS (10 min. each).

vii) Application of 1°AB

Application of primary antibody (1° AB) and overnight incubation (appr. 12h) at room temperature: Fill up compartments of well-plates with 5ml of 1°AB each directly after mixing. Use 5ml Eppendorf Combitip-syringes designated solely for the used AB (e.g. c-Fos). Seal well-plates witch adhesive tape (e.g. Scotch tape®, TESA®), put into small freezer bags and tape onto shaker.

When re-using 1°AB, freeze the latter or add azide!

E) SECONDARY INCUBATION

Chosen 2° antibodies:_____

i) First washing

3 washes (10 min. each) in PBS.

ii) Application of 2°AB

During preceding PBS-washings, prepare 2° AB (e.g. Goat-anti-rabbit [Gar]).

Dilution factor 1: _____ (e.g. [Gar] from ABC-Kit 1:200)

Example: (adapt for respective task)

Add 3 drops (150µl) of normal blocking serum stock (yellow label) to 10ml of buffer in mixing bottle and add one drop (50µl) of biotinylated antibody stock (blue label).

[Gar] needed for 10 ml solution (2 compartments): 1 x 50 µl Gar in 10 ml SAPJE.

Fill up each well (solely using a Combitip-syringe designated for the chosen 2°AB, e.g. [Gar]) with 5ml of diluted/mixed serum.

Transfer sections in net-jars into the 2°AB (e.g. [Gar]), incubate for 90min on the shaker at room temperature.

Note: Prepare ABC-complex prior to this incubation (see F), let rest for 30min.

iii) Further washing

3 washes with PBS (10 min. each)

F) ABC INCUBATION

Prepare avidin-biotin-complex (Vectastain® Elite® ABC-Kit, Vector Laboratories Inc., Burlingham, U.S.A.).
(cf., data sheet 1:100, i.e. 1 drop A and 1 B each (=1 drop ABC-complex) in 10 ml [1 drop = 50 µl]); other dilution: 1 drop (=100 µl) ABC-complex in 40 ml SAPJE, i.e. 1:800). Use fresh Combitip-syringes and fill 5ml/compartment into well-plates. Incubate for 2 hours on the shaker.

Dilution factor 1: _____

Note: Prepare DAB during 2nd hour of incubation (see G)!

G) DAB PREPARATION

i) First washing

3 washes with PBS (10 min. each)

From now on use again PB instead of PBS!

ii) Preparation

Work under fume-hood! Take respective amount of DAB (frozen aliquot) out of freezer (use thick gloves!!!), warm up DAB under luke-warm running water.
Prepare also well-plates, 5ml-Combitip-syringes, transfer-pipette, $(NH_4)_2Ni(SO_4)_2$-solution (1%), $CoCl_2$-solution (1%); both recipes see below; beakers, filter paper and funnels, DAB-measuring cylinder, stop-watch, dishes with 0.1 ml PB (stop-bath).
Prepare also H_2O_2-bottle (30%), 1ml tuberculine-syringe and pipette 200-1000 µl.

Recipe for heavy metal solutions: (each 1%)
(1) 1g $(NH_4)_2Ni(SO_4)_2$ + 100ml dH_2O (stir until diluted)
(2) 1g $CoCl_2$ + 100ml dH_2O
Both to be stored in tight glass bottles!

iii) Mixing the reagents

Add reagents in prescribed order (see Recipe box below); filtrate!
1 aliquot DAB (5ml) + 92.75ml PB + 1ml $(NH_4)_2Ni(SO_4)_2$-solution + 1.25ml $CoCl_2$ (prepare enough solution, filter will absorb much!) → prepare 10ml pre-incubation solution per compartment (5ml for pre-incubation, 5ml for DAB-reaction).

Recipe for DAB & heavy metal mixture calculation (per 100 ml):
1 aliquot DAB (ca. 5 ml)
1ml $(NH_4)_2Ni(SO_4)_2$ (1%)
1.25ml $CoCl_2$ (1%)

iv) Preparing the incubation solution

Process in steps per well-plate dish/box (keep strictly to order; use gloves!).
Prepare incubation solution (see recipe box below); filtrate; incubate in delayed steps (15-30 sec.).

Recipe for DAB-incubation solution:
660 µl H_2O_2(3%) / 100 ml DAB-reaction solution
33 µl H_2O_2 / 5 ml (per compartment) → 200 µl per well-plate per 30ml reaction solution

v) Reaction

Add 5 ml incubation solution per compartment. Move the reaction tubes slightly to and fro. Incubation time is determined until optimal marking is achieved (check under light microscope). Do not let sections get too dark (particularly c-Fos). Test small amounts first and check those; add H_2O_2 to DAB only when needed!

vi) Stop reaction

Stop the reaction by washing twice in PB on the shaker, each 10 min (Add azide if necessary; cover with parafilm).

vii) Storage before mounting onto slides

Transfer the sections within the reaction jars into PB and store them until mounting onto glass slides in the fridge.

Authors: C. Helpert et al.
Modified Translation: R. E. Wegner

G Glass slide gelatine cover recipe

COVERING GLASS SLIDES WITH CHROME-ALAUN-GELATINE SOLUTION

Materials ad 1000ml *Aqua bidest.*:
5g Gelatine-powder, Merck (Darmstadt, Germany), Art. 4078, 60 Bloom
0.5g Chrome-Alaun (Potassic chrome (III) sulphate), Merck (Darmstadt, Germany), Art. 1036

Heat *Aqua bidest.* until luke-warm. Add chemicals while stirring and heat solution up to 60°C.
Take jar off heating plate and let cool down (stir!).
Let solution cool down (room temperature); filtrate shortly prior to use.
Only use thoroughly cleaned glass (mild detergent; *Aqua bidest.*; only touch at edges).
Bath in gelatine twice; let dry in cabinet drier.

Authors: C. Helpert et al.
Modified Translation: R. E. Wegner

H Nissl-staining recipe

CRESYL-VIOLET SOLUTION FOR SUBSEQUENT NISSL-STAINING

Cresyl violet solution:
5 g Cresyl Violet (BDH, Poole, UK)
60 ml Sodium acetate solution (Merck, Darmstadt, Germany)
340 ml Acetic Acid (Roth, Karlsruhe, Germany)
600 ml *Aqua bidest.*

Mix and stir for approximately one week. Filtrate. Stir prior to use approximately two other days. Filtrate. Protect from light. Store at 4°C.

Nissl-staining:
Transfer mounted, well-dried sections through descending ethanol series :
1) 5 min. each in ethanol 100%, 96%, 80%, and 70%
2) 30 sec. in *Aqua bidest.*
3) 15 min. in cresyl violet solution (0.5%, 39°C; for sections of 60 µm thickness)
4) 30 sec. in mixture of concentrated acetic acid (0.1 ml in 0.1 l *Aqua bidest.*)
5) 5 min. in ethanol 70%
6) 5 min. in ethanol 96%
7) differentiate into mixture of 0.1 ml concentrated acetic acid in 0.1 l ethanol (96%)
8) 5 min. in isopropanol (100%)
9) repeat step 8
10) 5 minutes in xylol
11) repeat step 10
12) close by coverslipping with Eukitt (Kindler, Freiburg).
60 ml Sodium acetate solution (Merck, Darmstadt, Germany)

I Technorama Forum Lecture: 2000 years of magnetism

Technorama Forum Lecture

2000 years of magnetism in 40 minutes

Presented by Paul Doherty, 18 October 2001
http://www.exo.net/~pauld/technorama/technoramaforum.html

The legend has it that before 1 AD a Greek shepherd boy named Magnus from the Greek region of Magnesia noted that certain stones attracted iron nails. These stones we now call magnetite, they are made of iron and oxygen with the chemical equation, Fe_3O_4. Lucretius wrote that these stones attracted and repelled each other. Then an amazing thing happened for the next 1000 years, at least amazing viewed from our modern perspective, nothing. After all that time in China it was found that if loadstone were carved into a spoon shape the handle of the spoon when placed on a smooth surface would point south.
Chinese refer to compasses as "south pointers." South was an important direction in the Chinese practice of Geomancy. It is now still important in Feng Sui. It is hard to tell when the compass was invented because there is another "south pointer" in Chinese, the emperor's chariot. The chariot was geared so that as it twisted and turned in its progress through a city the emperors throne always pointed in the same direction, south. It is difficult to determine when the words "south pointer" stopped meaning the emperor's chair and started meaning a compass but it was sometime before 1100 AD.)
Meanwhile back in Europe...In 1265 a warrior scientist named Peter Peregrinus wrote about his experiments with magnets. He noted that they had two special ends which he named "polus" or poles, and that when the magnets were floated on water the poles lined up so that one pointed to the north star. The Europeans used the compass to navigate and so gave great importance to the north pointing end, the end that showed them the location of the north pole star during the day. The end that pointed to the north pole star was named the "north seeking pole." Later this was shortened to the north pole.
Aside: Since navigators were lead by the stones they were called leadstones which has become lodestones in modern English. (By the way, the name of magnetite stones in French is appropriately "loving stones," since the stones attract and "kiss.")
It was known that like poles repelled and opposite poles attracted. For example, north poles repelled north poles and attracted south poles.

Why did the north seeking pole point north? 300 years later William Gilbert discovered why the stones pointed north, the earth itself was a magnet. Unfortunately, this meant that the names that Peter Peregrinus had chosen were confusing. The north pole of a magnet pointed to the north geographic pole of the earth because it was attracted to the north geographic pole which meant that the north geographic pole was a south magnetic pole, the confusion this caused has remained until the present day. On all maps the south pole of the earth magnet is named the "north magnetic pole."

The Curie Point Gilbert thought that the earth was an iron magnet. While the core of the earth is made of iron, it cannot be magnetic because it is so hot. What Gilbert didn't know is that when iron is heated up hot enough it loses all of its magnetism, the temperature of a material where it loses its ferromagnetism is known as its curie point. For iron the curie point is 770 °C. The iron inside the earth is much hotter than 770 °C and so cannot be an iron magnet. I have several rods with a curie point of -5 °C. I can attract these out of the ice using ferrite magnets. When the rods warm up they lose their magnetism and drop off the magnet. When rods start above the Curie point and are cooled below it in the presence of a magnetic field such as that of the earth they become magnetized. The Chinese used this to make compasses out of iron. Lava includes hot, iron-containing minerals such as basalt, which can be magnetized. As the lava cools it locks in the direction of the magnetic field of the earth. This locks in the latitude at which the lava cooled. On

Aneroid peak in eastern Oregon there are lava layers which preserve horizontal magnetic fields. This means that those lavas cooled near the equator. Continental drift has moved them far north to where they are today in Oregon.

Magnetic Bacteria There are bacteria which use the magnetic field of the earth. Inside these bacteria are grains of magnetite. The bacteria are anaerobic, i.e. killed by oxygen. They use the magnetic field to sense "down" which is the direction away from oxygen and toward life. In the northern hemisphere these bacteria swim towards a south magnetic pole, in the southern hemisphere they swim toward north poles.

Life on Mars Grains similar to those made by bacteria have been found in a meteorite from Mars. This meteorite was found in the Allan Hills region of Antarctica and is called ALH 840001. It is one bit of evidence that there were at one time bacteria on Mars.

The Connection between Electricity and Magnetism In 1820 a physics lecturer, Hans Christian Oersted, was passing an electric current from a voltaic pile through a wire in an experiment which showed that the wire became hot.(I will repeat this experiment soon.) Nearby was a compass. When the current started to flow through the wire, Oersted noted that the compass needle moved. This was the first time electricity and magnetism were shown to be connected. An electric current creates magnetism.

The Magnetic Field In England, Michael Faraday made a great advance in magnetism by using field lines to understand magnetic experiments. Perhaps you have sprinkled iron filings over a magnet, they line up around the magnet in a pattern. Faraday hypothesized that they lined up with a force field made by the magnet.

The Magnetic field of Sunspots The sun also has a magnetic field. Indeed sunspots are magnetic and come in pairs one north pole spot paired with a south pole spot.

A simple Experiment A simple experiment can be done which cannot be understood without the concept of field lines. This is a dangerous experiment, I'm going to use magnets which are so big and strong that they can leap several inches and crush the bones of my fingers between them as they smash together. I start with a pile of three large flat magnets, one on top of the other. The north pole of one next to the south pole of its neighbor attracting the two together. When I pull the top magnet to the side it is pushed up in the air by the same magnet that had been pulling it down! I work hard to pull the top magnet to the side to emphasize the danger. The field lines from the central magnet point up above the magnet and then point down on the sides of the magnet. This changes the direction of the force on the other magnets from a downward attraction when one magnet is above the other to upward repulsion when one magnet is pulled to the side. It is incongruous to see a magnet leaning on the air. It is even more interesting to give the leaning magnet a downward push and watch it bob up and down for a long time. Put one magnet to either side and start one oscillating. The magnetic fields will push on the distant magnet and start it oscillating too. Tune the oscillations so that they have the same frequency and the magnet you started will come to rest while the other magnet steals all of its motion. The process then continues as all the motion is returned.

Light is Electromagnetic Radiation Faraday's discoveries provided the basis from which James Clerk Maxwell created the theory of electromagnetism and discovered that light was electromagnetic radiation.

Motion from Magnetism Faraday also discovered that magnets could push on current carrying wires. This led to the invention of the electric motor which has revolutionized our lives. Think of all the electric motors that surround you: powering refrigerator compressors, blowing air in hair dryers, rolling down car windows and many many more.

Ferrofluid One great modern material is ferrofluid, an oil full of suspended magnetic particles. You can see some great ferrofluid demonstrations here at Technorama.
I have some homemade ferrofluid here. Ferrofluid in a bottle rises against gravity and jumps up the

the neodymium magnet above. Notice that when I hold a strong magnet above it the fluid begins to bulge upward and then leaps up against gravity to reach the magnet. This ferrofluid is made by burning steel wool to make iron oxide, and then grinding the iron oxide to a fine powder with a mortar and pestle. It is then mixed with cooking oil.

Magnetic Levitation To see a fluid leap upward against gravity makes most people laugh, but it would be even better to suspend material in mid air. To make matter fly. Unfortunately, a scientist named Earnshaw once showed that there was no stable levitation possible using static electric and magnetic fields. After Earnshaw, physicists didn't even try to make levitated object using static magnets. However, other experimenters found a way around Earnshaw's theorem. For example I can use electrostatics to levitate a shredded plastic ribbon. I get around Earnshaw's theorem by using a time varying, i.e. non-static feedback system, me. Earnshaw's theorem doesn't apply if other stabilizing forces are present such as those from a pencil. Slide two donut magnets onto a pencil and one will levitate above another. It pays to watch children. They will do things that physics professors would never think of doing. I did this pencil levitation trick for 40 years before a 7'th grade boy showed me a neat trick. Using a pencil with a steel eraser band you can hold the pencil point between two fingers and the lower magnet will stay on the pencil as it is attracted to the steel. Raise up the top magnet and drop it. The upper magnet falls and seems to pass through the lower magnet. This is an illusion resulting from an elastic collision in which the upper magnet collides with the lower one. The upper magnet stops and is caught by the eraser band while the lower one pops off at the same speed as the upper one. Earnshaw's theorem can also be bypassed by using spinning magnets which are stabilized by their gyroscopic action. This was used in the toy known as a Levitron. Martin Simon of Los Angeles and Ortwin Schenker of Germany have recently built the spin stabilized magnetic levitator with the highest levitation ever achieved.

Diamagnetism Earnshaw's theorem also disallowed levitation using a weak form of repulsive magnetism known as diamagnetism. In the 1980's very strong magnets were invented by a team at General Motors Research Laboratory that included a student of mine. These magnets are made of neodymium, iron, and boron. They are strong enough to reveal the weak magnetism of everyday objects, called diamagnetism, which causes some materials to be repelled by both poles of a magnet.
With even stronger magnetic fields from electromagnets wound from superconducting wire an entire frog can be suspended in air against gravity. No harm comes to the frog. At the moment no one can conceive of a magnet strong enough to levitate a person. However it would certainly be a great feeling to be able to fly.

AC Levitation A pulse of AC magnetic field can be used to accelerate a conducting ring of aluminum and so shoot it into the air. This is shown by the exhibit, "Magnetic cannon," at Technorama. Aluminum is not magnetic yet the AC magnetic field induces an alternating electric current in the aluminum this current is then repelled by the AC magnetic field. This is what is happening inside the grapes, except that the electric current is inside the atoms and molecules of water and sugar inside the grapes. This behavior is described by Lenz's law which says that when a magnetic field through a conductor changes, currents will flow in the conductor that make a magnetic field which opposes the change. If we can increase the electric current in the aluminum ring we can increase the magnetic force on the ring and increase the height to which it is shot. I can do this by making the aluminum a better conductor. This is done by cooling the aluminum in liquid nitrogen. Cold aluminum conducts electricity better than room temperature aluminum. Besides the cold aluminum condenses a trailing cloud from the humid air of the room and looks cool. Chill the aluminum ring in liquid nitrogen and shoot it out of the magnetic cannon. It goes twice as high. It's a good thing that I tested this experiment earlier. Materials also shrink when they get cold. When the aluminum ring was chilled it shrank so much that it would not fit over the glass tube of the magnetic cannon any more. (We removed an inner ring of Teflon from the aluminum before it would fit.)

Superconducting Levitation In 1911 Kammerlinge Onnes in Norway discovered that some materials lost all resistance to electrical current when cooled. These materials are called superconductors. In the 1980's superconductors were found which worked at temperatures of 70 K, below the boiling point of liquid nitrogen. I have a disk of this material known as 1,2,3

compound because it is made from Yttrium barium cupric oxide with an equation $Y_1Ba_2Cu_3O_8$. This material will levitate against gravity when placed over neodymium magnets. And, in accordance with Newton's third law of action and reaction, neodymium magnets will also levitate above the superconductor. Recently very pure graphite crystallized in the right orientation has been found to show enough diamagnetism to levitate above a track made of neodymium magnets. I'd like to show you the first demonstration of this discovery tonight.

And so I've taken you across 2000 years of magnetic history, but I've left out the most important part of the story. It turns out magnetism can be used to record music on a magnetic tape recorder and to create music in what I think is the pinnacle of magnetic technology...

The electric guitar The electric guitar is made from a 2 meter long dowel, steel piano wire stretched between eye bolts, a magnetic coil, and neodymium magnets. In this my privately designed "Bender" electric guitar, so named because by bending it I bend the notes, you can see how the magnets magnetize the music wire. The wire moves and makes a changing magnetic field in the coil of wire. This makes an electric current which is amplified. The current changes in the same way that the wire moves, musically. A steel wire stretched tight over a Radio Shack pickup coil. Neodymium magnets hold the pickup to the wood dowel and magnetize the wire. And thus magnetism reaches its highest form helping us to make music.

And so ends my tale of human progress in understanding magnetism.
Who knows what will come next?

J Acknowledgements

My first and deepest thanks belongs to Prof. Dr. Hynek Burda, who gave me the wonderful opportunity for writing my PhD-thesis in his working-group; with a challenging topic (two topics, to be honest), time for substantial talks, the encouragement to think and work self-responsibly, and always an endless pool of inspiring ideas combined with a motivating smile.

My colleagues, particularly my room-mate and dear friend Dr. Sabine Begall, were a constant source of both scientific and private feedback, helping more than was to be hoped for and sharing with me wonderful times on the large scale at numerous conference journeys, but also on the small scale during our daily coffee breaks. Technically, I would have been lost without Gerd Hamann and his a-maze-ing help and without Dr. Wittmann and her spectrometer.

I am also deeply indebted to my hard-working, persistent, brave, active and motivated students. Without them, many project parts would have not been pushed past the threshold of the "Material & Methods" chapter. In order of appearance: Tanja Pletz (Visual performance), Sandra Bootsmann & Beate Timpert (Lateralization experiments).

I am thankful to Prof. Dr. Helmut Oelschläger and to Dr. Pavel Němec, who made it possible for me to dare a little step into the neuroanatomical laboratory world, and who were always incredibly encouraging. Thanks also to Dr. Stephan Marhold for quick supply of original data from his scientific work. Some other colleagues and dear friends need to be mentioned who have always supplied me with the feeling that I could make it: Jo & Giora, Rafita & Claude.

With love I think of some special people, who made the past years more colourful, sharing the event of "getting promoted" in the same timely frame, but in different academic fields: Christiane, Jasmin, Gerrit & Stefanie in Essen, Mülheim, Marburg, Würzburg; Andrea, Katrin & Clemens in Frankfurt (you saved me from going nuts in the W. lab); Louis in San Francisco/Paris; Zita in Oldenburg; Philipp in Hamburg; and last not least my weekly writing workshop mates Daniela, Kirsten & Minty in Duisburg.

My Mischpoke has not always exactly understood what I was doing, but they never stopped supporting me. You're wonderful. As is my husband Patrick. Thank you.

My work was funded by DFG BU 717/10-3, a graduate grant (GraFöG) & travel grants from the University of Duisburg-Essen, and an [i]-lab travel award.

K Curriculum Vitae

Regina E. Moritz
Dipl.-Umweltwissenschaftlerin

Steinzeitweg 18 – 44805 Bochum
0234-2981957
regina.moritz@uni-due.de

PERSONALIA

Geboren	22. November 1976 in Bottrop/NRW
Familienstand	verheiratet

THEORIE

11.03 - 02.07	Wissensch. Mitarbeiterin Abt. Allg. Zoologie Universität Duisburg-Essen/NRW
11.02 - 11.03	Graduiertenförderung Universität Duisburg-Essen
seit 06.02	Promotion Abt. Allgemeine Zoologie – Universität Duisburg-Essen
1996 -2002	Studium der Ökologie Universität Duisburg-Essen
1995 -1996	Archäologisches Studium WWU Münster/NRW
1995	Allgemeine Hochschulreife Gymnasium Petrinum, Dorsten/NRW

PRAXIS

06.06 - 12.06	Koordinatorin der Doktorandinnenförderung des FB Biologie & Geographie Universität Duisburg-Essen
08.03	Veranstaltungen: Bundesweite Sommeruniversität für Frauen in Naturwissenschaften und Technik, Universität Duisburg-Essen
06.03	Workshop „Evolutionary Biology“ in Guarda/Schweiz Organisator: Universität Fribourg
05 - 06.03	Gestaltung einer zoologischen Unterrichtsreihe für hochbegabte Kinder: „Leben in der Tiefe – Tiere im Wasser und ‚unter Tage‘“ [Zusammenarbeit mit www.dreistein.net]
07.02	Tutorinnen-Tätigkeit: Bundesweite Sommeruniversität für Frauen in Naturwissenschaften und Technik, Universität Essen
01.02 - 02.02	Redaktionelles Praktikum bei NATURE, München
07.99 - 12.01	Studentische Hilfskraft in der Abt. Allgemeine Zoologie
07.97 - 08.97	Praktikum im Umweltamt der Stadt Dorsten

VORTRÄGE

06.06	Vortrag Université Pierre et Marie Curie, Paris 6 „Quo vadis? The magnetic compass in animal orientation"
09.05	Jahrestagung der Deutschen Gesellschaft für Säugetierkunde in Essen „Narrowing down the magnetic compass mechanism in a rodent (*Cryptomys anselli*)"
08.05	Gastredner bei der Summer School Ethologie der Südböhmischen Universität Budweis, Tschechien „Magnetic Compass Orientation – What Behaviour tells us"
08.05	International Mammalogical Congress IX in Sapporo, Japan Doppelpräsentation mit Dr. S. Begall „Sensory Ecology of subterranean rodents: news in a nutshell"
10.04	International Postgraduate Course „Sensory Ecology" in Lund, Schweden „The enigma of seeing in the subterranean mole-rat *Coetomys anselli* (Bathyergidae): behavioural approach", unterstützt durch einen [i]lab travel award
07.04	Kongress ‚Rodens et Spatium' in Lublin, Polen „The enigma of seeing in the subterranean mole-rat *Coetomys anselli* (Bathyergidae): behavioural approach"
07.02	Kongress ‚Rodens et Spatium' in Louvain-la-Neuve, Belgien „Effect of trap barrier systems on populations of ricefield rats (*Rattus argentiventer*) in Indonesian ricefields"

AUSLANDSAUFENTHALTE

03.03	Forschungsaufenthalt in Zambia
06.01 - 09.01	Forschungsaufenthalt in Australien und Indonesien
1990	Sprachaufenthalt in Irland

ZUSÄTZLICHE...

Sprachen	Englisch und Französisch fließend in Wort und Schrift
Kenntnisse	Latinum; EDV: SPSS, Photoshop, ORIANA
	Imperia 8 (Prozessorientiertes Content Management)
Interessen	Kryptozoologie, Bewusstseinsforschung
	Deutsche Dichter, Oper, Kochen, Glossen

Essen, den 30. Januar 2007

L List of Publications

[Regina E. Moritz, geb. Wegner]

published

15 Lange S, Burda H, Wegner RE, Dammann P & Kawalika M (2007) Living in a stethoscope: Burrow-acoustics promotes auditory specializations in subterranean rodents. *Naturwissenschaften* 94: 134-138.

14 Wegner RE, Begall S & Burda H (2006) Magnetic compass in the cornea: local anaesthesia impairs orientation in a mammal. *The Journal of Experimental Biology* 209: 4747-4750.

13 Wegner RE, Begall S & Burda H (2006) Light perception in 'blind' subterranean Zambian mole-rats. *Animal Behaviour* 72: 1021-1024.

12 Thalau P, Ritz T, Burda H, Wegner RE & Wiltschko R (2006) The magnetic compass mechanisms of mammals and birds are based on different physical principles. *Journal of the Royal Society Interface* 3: 583-587.

11 Wegner RE (2006) Graumull. In: Faszination Natur; Tiere: Säugetiere I. Brockhaus, Mannheim. p. 359.

10 Wegner RE (2006) Kap-Strandgäber. In: Faszination Natur; Tiere: Säugetiere I. Brockhaus, Mannheim. pp. 357-358

9 Jacob J & Wegner RE (2005) Does continuous removal of individuals separate high and low quality ricefield rats? *Journal of Wildlife Management* 69(2): 821-826.

8 Wegner RE & Burda H (2005) The enigma of seeing in the subterranean mole-rat *Cryptomys anselli* (Bathyergidae): behavioural approach. *Proceedings of the RIN-05 Conference on Orientation and Navigation - Birds, Humans and Other Animals*; Royal Institute of Navigation, London.

7 Heth G, Todrank J, Begall S, Wegner RE & Burda H (2004) Genetic relatedness discrimination in eusocial *Cryptomys anselli* mole-rats. *Folia Zoologica* 53(3): 269-278.

6 Wegner R & Schiermeier Q (2002) Conservationists under fire in the Philippines. *Nature* 416: 669.

5 Schiermeier Q & Wegner R (2002) Foreign researchers turn their backs on Germany. *Nature* 415: 945.

in press

4 Moritz RE, Burda H, Begall S & Němec P (2007) Magnetic compass: A useful tool underground. In: Begall S, Burda H & Schleich CE (eds), Subterranean rodents: News from underground. Springer Verlag, Heidelberg.

in preparation

3 Dammann P, Van Daele P, Lange S, Moritz RE, Nova P, Ingram C & Burda H (in prep.) On the karyotype and taxonomic status of Cryptomys "Monze" (Rodentia, Bathyergidae).

2 Frieling S, Begall S, Moritz RE & Burda H (in prep.) Behavioral evidence for distant heat sensing in the Zambian subterranean mole-rat *Cryptomys anselli*.

1 Němec P, Burger T, Lucova M, Moritz RE, Burda H & Oelschläger HHA (in prep.) The hippocampus involved in magnetic orientation in a subterranean mammal.

Erklärung Hiermit erkläre ich, gem. §6 Abs 2, Nr. 8 der Promotionsordnung der Math.-Nat.-Fachbereiche zur Erlangung des Dr. rer. nat., dass ich das Arbeitsgebiet, dem das Thema „Sensory Ecology of Electromagnetic Radiation Perception in Subterranean Mole-Rats (*Fukomys anselli & Fukomys kafuensis)*" zuzuordnen ist, in Forschung und Lehre vertrete und den Antrag von Frau Moritz befürworte.

Essen, 30. Januar 2007

- (Hynek Burda) -

Erklärung Hiermit erkläre ich, gem. §6 Abs 2, Nr. 6 der Promotionsordnung der Math.-Nat.-Fachbereiche zur Erlangung des Dr. rer. nat., dass ich die vorliegende Dissertation selbstständig verfasst habe und mich keiner anderen als der angegebenen Hilfsmittel bedient habe.

Essen, 30. Januar 2007

- (Regina E. Moritz) -

Erklärung Hiermit erkläre ich, gem. §6 Abs 2, Nr. 7 der Promotionsordnung der Math.-Nat.-Fachbereiche zur Erlangung des Dr. rer. nat., dass ich keine anderen Promotionen bzw. Promotionsversuche in der Vergangenheit durchgeführt habe und dass diese Arbeit von keiner anderen Fakultät abgelehnt worden ist.

Essen, 30. Januar 2007

- (Regina E. Moritz) -